



Review Paper

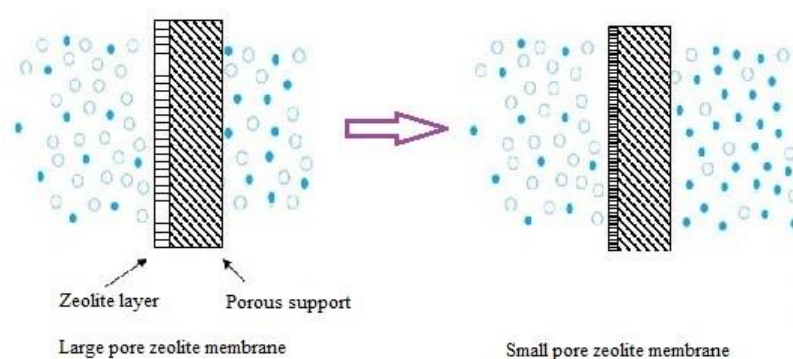
Recent Progress in Zeolite/Zeotype Membranes

C. Feng^{1,2}, K.C. Khulbe^{*2}, T. Matsuura², R. Farnood¹, A.F. Ismail³¹ Chemical Engineering and Applied Chemistry Department, University of Toronto, On., M5S 3E5, Canada² Industrial Membrane Research Laboratory, Department of Chemical and Biological Engineering, University of Ottawa, On. K1N 6N5, Canada³ Advanced Membrane Technology Center (AMTEC), Universiti Teknologi Malaysia, 81310 Skudai, Johor Bahru, Malaysia

HIGHLIGHTS

- Widely discussed recent progress in different zeolite/zeotype membranes and ceramic, inorganic membranes.
- Recent progress of using zeolite/zeotype membrane.

GRAPHICAL ABSTRACT



ARTICLE INFO

Article history:

Received 27-06-2014

Revised 08-10-2014

Accepted 08-10-2014

Available online 09-10-2014

Keywords:

Inorganic membrane
Zeolite
Membrane preparation
Membrane application

ABSTRACT

This is a comprehensive review of the recent progresses made in the field of zeolite membranes. It describes zeolitic materials and methods of membrane fabrication, followed by a summary of applications for gas separation, pervaporation and separation of liquid mixtures. Special attention is called to polymer mixed matrix membranes (MMMs) and membranes based on metal organic frame works (MOFs). In this comprehensive survey, the following trends were observed during the past 5 – 10 years. New zeolitic materials and new synthesis methods, such as hydrothermal synthesis, seeding and microwave heating, have been continuously reported in the literature. Many efforts have been devoted to the synthesis of hybrid or mixed matrix membranes (MMMs) since MMMs clearly outperformed polymeric membranes. MOFs also showed improved performance in gas separation. Many attempts have been made to develop thin (1 μ m) supported zeolite layers on a variety of carriers such as capillaries, fibers, tubes, etc. The assembly of nanozeolite building blocks and nanosheets is the starting point for the synthesis of thin defect free zeolite membranes. The present review presents the recent progresses made in the field of zeolite/zeotype membranes. Different types of zeolite membranes, methods of preparation and application aspects especially for separation of gases have been focused on, including the individual zeolites which are in use or are to be used as inorganic fillers in mixed matrix membranes (MMMs). Despite the enormous efforts of researchers, the commercialization of zeolite membranes has been achieved only in a limited area. The future works necessary to change the current situation are hence suggested.

© 2014 MPRL. All rights reserved.

1. Introduction

The exact definition of the term “Zeolite” is still the subject of discussion [1]. The naming of zeolites in the literature seldom follows a scientific

system. If natural analogs exist, the synthetic zeolites are often named after the minerals (e.g. faujasite, mordenite, ferrierite, and offretite). Alternatively, the names given by the discoverers are used. Zeolites are natural minerals that are mined in many parts of the world; most zeolites used commercially are

* Corresponding author at: Tel/fax: +1-613-562-5800 ext.6114
E-mail address: khulbe@eng.uottawa.ca (K.C. Khulbe)

produced synthetically. When developing applications for zeolites, it is important to remember that not all of these minerals are the same. Synthetic zeolites are widely common.

There are some differences between natural and synthetic zeolites; including 1) Synthetics are manufactured from energy consuming chemicals and naturals are processed from natural ore bodies, 2) Synthetic zeolites have a silica to alumina ratio of 1 to 1 and natural clinoptilolite (clino) zeolites have a 5 to 1 ratio, 3) Clino natural zeolites do not break down in a mildly acid environment, whereas synthetic zeolites do. The natural zeolite structure has more acid resistant silica to hold its structure together.

The early synthetic materials discovered by Milton and Breck and his coworkers at Union Carbide used the modern Latin alphabet, for example, zeolites A, B, X, Y, L. The use of the Greek alphabet was initiated by Mobil and Union Carbide with the zeolites alpha, beta, and omega [2]. Zeolites with identical framework structures can therefore appear in the literature under different names. Some order has been imposed by the introduction of a classification system in the *Atlas of Zeolite Structure Types*. The *Atlas of Zeolite Structure Types* [3] published and frequently updated by the IZA (International Zeolite Association) Structure Commission assigns a three - letter code to be used for a known framework topology irrespective of composition. Illustrative codes are LTA for Linde zeolite A, FAU for molecular sieves with a faujasite topology (e.g., zeolites X, Y), MOR for the mordenite topology, MFI for the ZSM - 5 and silicalite topologies and AFI for the aluminophosphate AIPO topology. The acceptance of a newly determined structure of a zeolite or molecular sieve for inclusion in the official Atlas is reviewed and must be approved by the IZA Structure Commission. The IZA Structure Commission was given authority at the Seventh International Zeolite Conference (Tokyo, 1986) to approve and/or assign the three - letter structure code for new framework topologies. The definition and usage of the term “zeolite” has evolved and changed, especially over the past decade, to include non - aluminosilicate compositions and structures. Beginning with the second revised edition of the *Atlas* [4], the term “zeolite and zeolite - like materials” are introduced to try and capture the range of materials of interest. The inclusion of a structure in the *Atlas* is limited to three - dimensional, tetrahedral oxide networks with a framework density less than about 21 T atoms per 1000 Å³ irrespective of the framework composition. Similarly, the term zeolite has been broadened in the mineralogy literature to include tetrahedral framework compositions with T - elements other than Al and Si but where classic zeolite properties are exhibited (e.g., structures containing open cavities in the form of channels and cages, reversible hydration - dehydration characteristics [5]. Very recently as a sign of the times, the term “nanoporous” materials has been applied to zeolites and related molecular sieves [6]. In general, zeolites can be classified into three categories which are as follows [7].

- i) Small pore structures have pore apertures consisting of six, eight or nine tetrahedral (6-, 8-, and 9-membered rings).
- ii) Medium pore frameworks have 10 membered rings.
- iii) Large pore zeolites have 1- membered rings and ultra large structure

In the entire world, there are about 150 types of zeolite, a compound of silicon, aluminium and oxygen, but there could be more types of zeolites. Zeolites are characterized by having pore openings of uniform dimensions, having a significant ion exchange capacity, and being capable of desorbing an adsorbed phase which is dispersed throughout the internal voids of the crystal without significantly displacing any atoms which make up the permanent zeolite crystal structure. Zeolites are distinguished from each other on the basis of their composition, crystal structure and adsorption properties. A project at Rice University came up with a list that shows the structures of more than 2.7 million zeolite-like materials (www.internetchemie.info/news/2009/zeolites.html). Since 2000, over 430 patents have been issued pertaining to advances in the hydrogen selectivity membrane [8]. In an effort to develop zeolite membranes more suitable for H₂ separation, various types of zeolite membranes are modified. The aim of the modification is to tune the size of zeolite pores and/or to decrease the number of defects within as synthesized zeolite membranes. The modification attempts include silylation on different zeolites.

Due to the presence of alumina, zeolite exhibits a negatively charged framework, which is counterbalanced by positive cations resulting in a strong electrostatic field on the internal surface. These cations can be exchanged to fine- tune the pore size or the adsorbent characteristics. For instance, the sodium form of zeolite A has pore opening of approximately 4 Å, called molecular sieve. If the sodium ion is exchanged with the larger potassium ion, the pore opening is reduced to approximately 3 Å (3A molecular sieve). The Si/Al ratio in the crystal framework is between 0.7-1.2.

Zeotype is any crystalline material (e.g. aluminophosphates, titanosilicates) with a 3D framework in which one of the tetrahedral sites occupied by Si is replaced with another element. Many zeotypes have the same structure as the known zeolite. Zeolites have a porous structure that can

accommodate a wide variety of cations, such as Na⁺, K⁺, Ca²⁺, Mg²⁺ and others. These positive ions are rather loosely held and can readily be exchanged for others in a contact solution. Zeolites have pores of molecular dimensions (2-20 Å) and narrow pore size distribution. These properties plus their high thermal, chemical, and mechanical stabilities make them ideal membranes. They possess molecular sieving, selective adsorption properties and catalytic abilities. Zeolite structures are formed by combining tetrahedra that consist of a central cation surrounded by four oxygen atoms. They are usually aluminosilicates, but the central cation can be Si, Al, P, Ga, Ge, B, etc.

In general, zeolites are crystalline aluminosilicate materials having microporous (zeolite pore) in their structure. They are built up by various connections of TO₄ (T = Si or Al) tetrahedral which result in the various zeolite pore sizes and structures. Small gas permeation and separation data evaluated for a wide temperature range in small and intermediate zeolites, i.e. A-type, DDR type, and MFI type will provide improved understanding of gas diffusion and permeation properties of these materials.

The assembly of nanozeolite building blocks and nanosheets is also the starting point for the synthesis of thin defect free zeolite membranes. The ultrafast synthesis of zeolites in a microwave has contributed to prevent the dissolution of the support. These new synthesis methods and new materials have been reported in the last ten years. The preparation of a ‘defect free’ zeolite layer, for gas separation, was the first and is still a matter of study. The control of the orientation of the zeolite crystals was accomplished by secondary growth and the use of organic structure-directing agents.

Zeolite membranes are used for dehydration, H₂ and CO₂ separation, but they can be used as catalyst reactors, as sensors for detection and/or controlling, and as devices for the separation of gas, and/or liquid separation [7].

One of the main challenges in zeolite membrane development is to minimize the intercrystal pores formed inherently in polycrystalline zeolite membranes. The existence of intercrystal pores is the major cause for decline in molecular separation efficiency [9].

Ceramic membranes are a type of artificial membranes made from inorganic materials (such as alumina, Titania, zirconia oxides or some glassy materials). They are used in membrane operations. By contrast with polymeric membranes, they can be used in separations where aggressive media (acids, strong solvents) are present. They also have excellent thermal stability which makes them usable in high-temperature membrane operations and are inert to microbiological degradations. Furthermore, zeolite membranes are easy to clean and also have catalytic activity’. Like polymeric membranes, they are either dense or porous. Defect formation during preparation is a major problem in ceramic membrane technology. The nature of the pore structure is one of the most important factors along with molecular properties and the interaction with the pore walls of gaseous species during their transport through the porous membrane. It is important to precisely control the membrane pore size uniformity in nanometer scale without pinholes or cracks [10]. Zeolite membranes can be grown, either as individual crystals or as intergrown layers on a wide variety of supports including metal surfaces, ceramic and polymeric plates, metallic wires, organic or inorganic fibers and even surfaces with special characteristics, such as electronic circuits or medical prostheses. These zeolite membranes constitute a special type of nanostructured interface capable of very specific interactions with individual molecules [11].

Polymeric membranes are widely used for hydrogen recovery. Due to their limitation of temperature when used for the separation of hydrogen, zeolite membranes may be the alternative. Crystalline zeolites have much better thermal and hydrothermal stability. Gas permeation results including hydrogen separation for silicate-1 membranes have been reported in many studies. In these cases the separation effect is based on the interplay of adsorption and diffusion effects.

Despite much progress in the development of zeolite molecular sieve membranes, there has so far been no industrial gas separation by zeolite membranes, with the exception of the de-watering of bio-ethanol by steam permeation using LTA membranes [12]. During the last ten years, metal-organic framework (MOF) membranes have been developed and tested in gas separation and achieved some success for their potential application in the future.

2. Structure of different zeolites

There are approximately 150 different structures reported by the International Zeolite Association (IZA). Among them, only 15 structures have been experimented to fabricate membranes [13]. Table 1 shows a brief description of the structure and pore sizes of a few different zeolites used for membranes.

Table 1
Brief description of structure and pore sizes of different zeolites used for membranes etc.

Zeolites	Structure etc.	Pore sizes, channels	Ref.
NaX, Faujasite (FAU) T	Comprised of 12 membered rings. The inner cavity has a diameter of 12 Å and is surrounded by 10 sodalite cages Intergrowth type zeolite of erionite and offertite	$d_p = 7.4$ Å	[14,15]
W	Same framework topology as the mineral merlinoite (MER), eight membered ring	$d_p = 0.36$ nm x 0.51 nm, $d_p = 0.41$ nm	[16]
B-substituted β-zeolite	Three dimensional, 12 ring, interconnected channel	Channel dimension 0.31 nm x 0.35 nm	[16]
SAPO-5	Microporous, non-intersecting tubular channels circumscribed by 12-membered rings Chabazite type structure	$d_p = 0.53$ x 0.57 and 0.71 x 0.73 nm $d_p = 7.3$ - 8.0 Å	[17] [18]
SAPO-44		$d_p = \sim 0.43$ nm diameter	[19]
SAPO-34		$d_p = \sim 0.38$ nm diameter	[20]
NA	Crystalline aluminosilicate	Channel opening size 0.41 nm	[21]
ZIF-8	Sodalite type structure	Large pores of 11.6 Å which are accessible through small apertures of 3.4 Å	[22]
L	The channels contain cationic sites, which can interact with negatively charged or polarized molecules*	One dimensional pore with an opening 0.71 nm which runs along its c-axis	[23]
AIPO-18	Built of AlO_4 and PO_4 tetrahedral building units. Three dimensional framework possessing eight membered intersecting channels	$d_p = 3.8$ Å	[24]
Isorecticular zeolite Imidazole SUZ-4	Metal atoms such as Zn linked through N atoms by ditopic imidazole ($C_3N_2H_4$) or functionalized Im links to form neutral frameworks Framework topology is related to zeolites ferrierite and ZSM-57 and contains straight channels having apertures defined by rings of ten (Si, Al)-O species; a novel cage may be the site for non-exchangeable potassium ions.	$d_p = 17.3$ - 7.1 Å	[25]
MOF-5	Face centered cubic crystal structure. Each corner is formed by $(ZnO)_4$ metal cluster, while each edge is linked by 1,4-benzenedicarboxylate (BDC)	Narrow pore size distribution with 97 nm mean diameter and 760 nm long of needle crystal shape	[26]
MFI	Intra-crystal	Narrow pore size distribution centered at 1.56 nm	[27]
ZIFs	Ordered porous structures with hybrid frameworks consisting of inorganic metal ion or metal clusters coordinated with organic imidazole/imidazole ligands	$d_p = 0.8$ - 1.0 nm $d_p = 0.02$ to 30.1 Å	[28] [29]
DDR	Comprised of silicon and oxygen atoms, eight membered ring, clathrasil type (Clathrasil are porous framework silicates with cage like voids)	Aperture of 0.36 x 0.44 nm	[30,31,32]
MER	Comprised double-eight-rings and Y-cage	$d_p = 0.27$ - 0.52 nm	[33]

* Pore diameter.

3. Preparation of zeolite membranes

3.1. Synthetic zeolite membranes by crystallization and seeding

Zeolitic membranes and membranes are completely different from simple crystalline zeolite powders and their preparation requires new strategies. One of the most challenging problems in the preparation of zeolitic membranes is the complete exclusion of the pinholes from the membranes, particularly under conditions of severe thermal cycling.

Synthetic zeolites are generally made by mixing solutions of aluminates and silicates, often with the formation of a gel, and by maintaining the mixture at a temperature of 100 °C or more for selected periods. The synthesis of zeolites involves several steps as shown below:

Reactant → Reactant mixtures → Nucleation → Crystal growth

However, the mechanisms of zeolite formation are very complex due to the plethora of chemical reactions, equilibria, and solubility variations that occur through the heterogeneous synthesis during the crystallization period.

There are many methods for the synthesis of zeolites, such as in-situ (without seeding) hydrothermal synthesis, secondary (seeded) growth, vapor phase transport and post treatments of zeolite membranes [34]. Widely-used synthesis methods are in-situ synthesis and secondary growth. In the case of in-situ synthesis, a simultaneous and abundant heterogeneous nucleation is the prerequisite for the formation of a good quality zeolite membrane. Thus, in-situ synthesis generally requires stringent synthesis conditions.

Zeolite membrane synthesis is more commonly carried out by the *in situ*-crystallization technique which involves placing a porous support in contact with a synthesis solution or gel under hydrothermal conditions. For successful membrane formation, proper conditions are necessary to allow for preferential nucleation and growth of zeolite crystals on the support surface (possibly competing with solution events) in an interlocking fashion with minimal non-selective interzeolitic porosity.

The process is thermally activated and usually takes place at elevated temperatures in order to achieve a high yield of crystals in an acceptable period of time. The variables in the synthesis of zeolites are temperature, alkalinity (pH), and chemical composition of the reactant mixtures. These variables do not necessarily determine the products obtained in hydrothermal reactions, because nucleation appears to be kinetically rather than thermodynamically determined and controlled. The kinetic variables include the treatment of reactants prior to crystallization, their chemical and physical nature.

The other approach for zeolite membrane formation is a technique called secondary (seeded) growth, which involves attaching a closely packed layer of zeolite seed crystals on the surface of a support. The first paper on seeding

was demonstrated by Horii et al. [35]. The use of seed crystals facilitates the formation of zeolite membranes since a seeded support grows to a pure-phase zeolite membrane more easily even when the crystallization conditions and the chemical batch composition are not optimum. Seeded growth has significant advantages such as better control over membrane microstructure (thickness, orientation), higher reproducibility, and a wider range of hydrothermal synthesis conditions leading to continuous membrane formation. Elimination of the constraints imposed by the need for crystal nucleation, due to the pre-existence of nuclei on the support surface, renders crystal growth as the main membrane formation mechanism and thus adds improved flexibility in the zeolite membrane and membrane preparation [36]. There are four main ways to attach the seeds to the support [37].

1. Charging the support surface by pH control to achieve opposite surface charges of seeds and support for an electrostatic attachment.
2. Charging the support surface by adsorption of positively charged cationic polymers like poly-DADMAC (diallyl dimethyl ammonium chloride) or Redifloc (Trade name of EKA Chemicals, a polyamine) to adjust the difference in zeta potentials between the ceramic support and the zeolite Nanocrystals to be attached as seeds. The counter ions of the ammonium polymer, usually chlorides, go in the solution and negatively charged silica nano-particles are attached. The use of seeded supports usually results in a c-orientation of the MFI layer (MFI zeolite membrane is composed of zeolite crystals where b-axes are all uniformly oriented perpendicular to a substrate) but under certain conditions also for secondary growth the desired b-orientation can be obtained.
3. Electrophoresis deposition of nanosized seeds on solid supports.
4. Immersion of the dried support into a seed solution followed by thermal treatment of the seeded support to burn organic additives and to fix the seeds via de-hydroxylation to the support.

Heating and driving chemical reactions by microwave energy has been an increasingly popular theme in the scientific community, and also in the fields of zeolites and zeolite membranes. As compared with conventional hydrothermal synthesis, microwave synthesis of zeolites has the advantages of a very short time, small zeolite particle size, narrow particle size distribution and high purity. All these characteristics make it a promising method for rapid preparation of high performance zeolite membranes [37].

Tompsett et al. [38] dedicated a comprehensive review on the microwave synthesis of nanoporous materials and summarized the preparation of zeolites, mixed oxides and mesoporous molecular sieves by employing microwave energy. Articles written by Li and Yang [39] are worth reading.

Articles written by Cundy [40] and Li et al. [34] are recommended for more general information on the subject of synthesis of microwave zeolites and microwave chemistry. Figure 1 illustrates a comparative synthesis of a zeolite membrane by microwave heating and conventional heating.

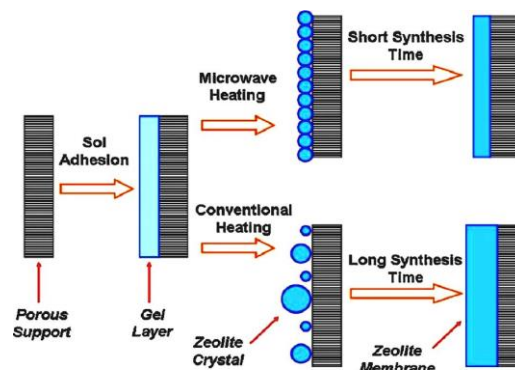


Fig. 1. Comparative synthesis model of zeolite membrane by microwave heating and conventional heating [39].

Cheng et al. [41] synthesized NaA zeolite using microwave heating. The method involved two steps, prior seeding of 120 nm of LTA crystals on the substrate and then employing a secondary hydrothermal synthesis. The effects of seeding times and synthesis time on the performance etc. were studied. The ideal H_2/N_2 selectivity was increased from 1.90 of the substrate to 6.37 of the three stage synthesized membrane, which was distinctly higher than the corresponding Knudsen diffusion selectivity of 3.74 .

Li et al. [34] developed a method called, "*in-situ* aging-microwave synthesis" of zeolitic membranes without seeding. It decouples two successive steps in the formation of zeolite membranes. The first step is the rearrangement of synthesis mixture and formation of germ nuclei on the support surface which can be obtained by *in-situ* aging. The second step is the nucleation and crystal growth on the support which can be achieved by *in-situ*

crystallization under fast and homogeneous heating. Choi et al. [42] demonstrated that rapid thermal processing in the preparation of zeolitic membranes can improve the separation performance of thick columnar membranes of a certain zeolite (silicate-1) by eliminating grain boundary defects, possibly by strengthening grain bonding at a grain boundary.

Naskar et al. [43] prepared silicate-1 zeolite membranes hydrothermally on the porous ceramic supports, both unmodified and modified with 3-aminopropyl triethoxysilane (APTES) as coupling agents, following the *ex situ* (secondary) crystal growth process. The membrane developed on surface modified support rendered lower permeance value, i.e. $9 \times 10^{-7} \text{ mol/m}^2 \text{ sPa}$ of N_2 compared to that formed on the unmodified support which gave permeance value of $20 \times 10^{-7} \text{ mol/m}^2 \text{ sPa}$ of N_2 .

Au et al. [44] demonstrated that the synthesis composition and conditions directly influence the size and shape of the zeolite crystal grains that make up the membrane microstructure. It was also shown that the growth behavior of zeolites within the confinements of the membrane environment is not necessarily similar to that of the free-floating zeolite crystal in the solution. The zeolite structure and chemistry dictate the transport properties through the crystalline zeolite channels, whereas the membrane microstructure governs the number and types of non-zeolite pathways. The micro-scale structural properties in the zeolite membrane have a direct effect on the separation performance.

Wong et al. [45] studied the effects of synthesis parameters (i.e. tetraethylorthosilicate (TEOS), 2,5-tetrapropylammonium ion, (TPA^+) , (OH^-)), dilution and temperature on the membrane thickness and orientation for MFI zeolite membranes grown onto seeded supports (i.e. porous glass and alumina). The zeolite crystals grew preferentially with its *c*-axis aligned normal to the support surface. This gave the membrane a preferred orientation of (101) at temperatures below 433 K and an orientation of (002) at higher temperatures. An empirical model for zeolite membrane growth as a function of synthesis variables was derived based on the experimental data. The model gave an adequate description of the membrane growth and provided an excellent guide for the synthesis of zeolite membranes with an engineered microstructure.

Chau et al. [46] discussed the chemistry of the surface of zeolite for direct manipulation of zeolite membrane microstructure by controlling the number and types of nucleation sites available on the support surface membrane during the zeolite membrane formation. The chemical nature of the support surface influences zeolite nucleation, crystal growth and membrane adhesion. Surface roughness and pore size define the optimum zeolite crystal size and the membrane thickness. Surface coating with a thin metal or metal oxide layer provides a simple technique for direct manipulation of the zeolite membrane microstructure by controlling the number and types of nucleation sites available on the support surface. The attachment of the zeolite seeds onto the support is dependent on the affinity of the seeds to the surface and usually requires significant modification of the support surface.

Varoon et al. [47] demonstrated the synthesis and structure determination of highly crystalline nanosheets of zeolite frameworks MWW (MWW structure zeolites such as MCM-22 possess two independent pore systems. One system consists of two dimensional sinusoidal 10-member ring (MR) channels with an elliptical ring cross section of $4.1 \text{ \AA} \times 5.1 \text{ \AA}$. The other is composed of large 12-MR super-cage connected by 10-MR windows [48] and MFI (mordenite framework inverted). It was reported that the purity and morphological integrity of those nanosheets allow them to pack well on porous supports, facilitating the fabrication of molecular sieve membranes.

Aoki et al. [49] fabricated a highly hydrophilic polycrystalline membrane on the outer surface of a porous α -alumina tube via the hydrothermal process. Permeation tests with a variety of permeate showed that the membrane possessed two types of pores: zeolitic pores of $0.4 - 0.43 \text{ nm}$ diameter and nonzeolitic pores. The coexisting nonzeolitic pores, through which large molecules were able to diffuse, complicated the permeation properties of the membrane. For binary mixed-feed systems, the separation factors were dependent on the size of the permeants, the absorptivity of molecules to the pore walls, and the hydrophobicity of permeants. The A-type zeolite membrane showed a strong affinity for H_2O molecules.

Shqau et al. [50] applied for a patent on supported zeolite Y membranes exhibiting high CO_2 selectivities when used in CO_2/N_2 gas separations. The membranes were produced by the seeding/secondary (hypothermal) growth approach in which a structure directing agent such as tetramethyl-ammonium hydroxide was included in the aqueous crystal growing composition used for membrane formation.

First et al. [51] developed and demonstrated an automated method which can fully characterize the three dimensional porous network of zeolites and other microporous materials. This method can be used to provide insights about postulated modifications that can improve the effectiveness of the structure. It can also be adapted to uniform molecular simulation tools.

3.2. MOFs (Metal-organic framework) zeolite membrane

Metal-organic frameworks (MOFs) are hybrid organic-inorganic nanoporous materials that exhibit regular crystalline lattices with well-defined pore structures. Chemical functionalization of the organic linkers in the structures MOFs affords facile control over pore size and chemical/physical properties making MOFs attractive for membrane based gas separation. MOFs possess a combination of organic and inorganic building blocks that give them enormous flexibility in pore size, shape, and structure when compared with the zeolite. The porosity in MOFs is 90% higher than in zeolites and research has shown that some of them are thermally stable, even in the presence of steam, up to $400 \text{ }^\circ\text{C}$ [52]. However, there are some challenges associated with fabricating membranes of MOF materials, including poor-substrate-membrane interactions, moisture sensitivity, and thermal/mechanical instability, since even nanometer-scale cracks and defects can affect the performance of a membrane for gas separation.

1. An application of MOFs is predicted in so-called mixed matrix membranes (MMMs) which show improved performance in comparison with the pure polymer membrane. Different from zeolite as organic-inorganic material, the MOF nanoparticles can be easily embedded into organic polymers, and standard shaping technologies to hollow fibers or spiral wound geometries can be applied [11]. Traditionally, MMMs are comprised of zeolite particles dispersed in a polymer matrix. Zeolites often exhibit relatively high penetrant sorption capacities and penetrant size-based selectivities compared to polymers due to their large micropore volumes and well defined, rigid structures. There are several drawbacks to the use of zeolites in MMMs [53]; such as to get defect free zeolite membrane, surface chemistry, non-economical, to get reproducible data, adhesion between polymer matrix and zeolite surface etc.

These reasons demand for new filler materials for MMMs. Metal organic frameworks (MOFs) are a relatively new class of microporous materials comprised of transition metals and transitional metal oxides connected by organic linkage to create one-, two-, and three-dimensional microporous structure. MOF particles are an attractive alternative to zeolite particles in MMM applications. Many MOFs can be synthesized easily and quickly. Further, a variation of MOF compositions and structures, including high ratio MOFs, may be particularly unlimited and the organic linkages provide a useful platform for chemistries that may improve adhesion to the polymer matrix.

The layer by layer liquid-phase deposition of the building blocks of a MOF on a support by repeated dip coating potentially allows the automatized preparation of ultra-thin high-flux MOF membranes. Immersing a substrate alternatively in a metal salt solution and in a linker solution produces homogeneous and well oriented membranes of about 40-100 nm thickness. Bétard et al. [54] fabricated a metal-organic framework (MOF) membrane by step by step MOFs with the general formula $[\text{Cu}_2\text{L}_2\text{P}]_n$ (L= dicarboxylate linker, P = pillaring ligand). Fine tailoring for adsorption affinity and pore size is possible by variation or functionalization of the L and P linkers. Two compounds were chosen: i) non polar A [L=1,4-naphthalenedicarboxylate (ndc), P = 1,4-diazabicyclo(2,2,2) octane (dabco)], and ii) polar B [linker L with two conformationally flexible either side chains (L=2,5-bis(2-methoxyethoxy)-1,4-benzene-dicarboxylate=BME-bdc, P=dabco). The framework structure of "A" is shown in Figure 2 and "B" may be derived by simple substitution of the ndc linker by BME-bdc (see Figure 2). The step-by-step, liquid phase deposition A and B resulted in pore-plugging of macroporous ceramic supports. Functionalization of linkers can induce CO_2 membrane selectivity: CO_2/CH_4 mixtures were separated with an anti-Knudsen separation factor of 4-5 in favor of CO_2 . The isoreticular concept of MOFs can be used to derive membranes that show adsorption-based separation rather than molecular sieve separation of gas mixtures.

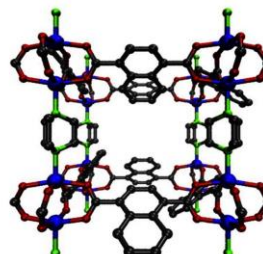


Fig. 2. Structure of $[\text{Cu}_2\text{L}_2\text{P}]_n$ MOFs (here $[\text{Cu}_2(\text{ndc})_2(\text{dabco})]_n$) (A) with linker L = ndc(1,4-naphthalenedicarboxylate) and ligand P = dabco(1,4-diazabicyclo(2,2,2)octane) seen in [1 0 0] direction. Structure B is quite similar to A but just replacing ndc by BME-bdc (see Fig. 3) [54].

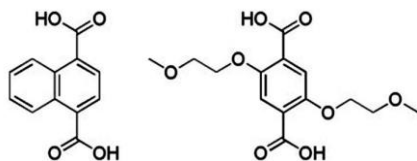


Fig. 3. Dicarboxylic acid linkers used in this work; left, H₂ndc (ndc: 1,4-naphthalene dicarboxylate) and right, H₂BME-bdc (BME-bdc: 2,5-bis(2-methoxyethoxy)-1,4-benzene dicarboxylate) [54].

Zeolite membranes with their advantageous separation and catalytic properties can be coated on traditional catalysts to achieve highly effective performance. Jin et al. [55] developed a boehmite gel modified seeded method to synthesize the MFI-type zeolite membrane encapsulated activated carbon particles (AC). By using the spray-coating process, the boehmite sol precursor was introduced in a gel layer on the AC surface to provide a smooth surface for seed dispersion and a binder for seed fixation. The obtained seed layer was dense and firm even without calcination. After 6 hrs of rotary hydrothermal synthesis, continuous zeolite membrane encapsulated AC particles were obtained. The technique provides an efficient way to prepare zeolite membranes on different supports.

4. Application of Zeolite membranes

4.1 Natural zeolite membranes

In 2003, Ackley et al. [56] wrote a review covering the application of natural zeolites in the purification and separation of gases and Sand and Mumpton [57], and Tsitsishvili et al. [58] wrote another reviews covering both the properties and the applications of natural zeolites.

4.1.1. Clinoptilolite

Natural zeolite membranes which have been compacted by time and nature have recently been shown to demonstrate apparent molecular sieving of H₂ from the H₂/CO₂ mixture by An et al. Very dense clinoptilolite has been identified as a structure which has been compressed by time and nature in the form of masses with essentially no microporosity. These geomorphic natural zeolites do not have the fragile crystal grain boundaries found in synthetic zeolite analogs and, therefore, have the molecular robustness to be considered for large-scale industrial processes. Natural zeolite membranes are already showing promises in the separation of hydrogen from syngas at elevated temperature [59].

Clinoptilolite has a two-dimensional (2D) micropore/channel structure. The framework of clinoptilolite contains three sets of intersecting channels (A, B, C). The channels A and B are parallel to the c-axis and channels C are parallel to the a-axis. A channels are formed by strongly compressed 10-membered rings (aperture 4.4×7.6 Å), and the B channels are confined by 8 membered rings (aperture 4.7×4.1 Å). The C channels are also formed by eight-member rings (aperture 5.5×4.0 Å). Dimensions of the largest channel of the clinoptilolite-framework are 0.44×0.72 nm which is smaller than most hydrated cations, an indication that it has a potential for desalination applications [8]. Swenson et al. [60] used the clinoptilolite membrane for the desalination via pervaporation technique. Complete rejection of Mg²⁺ and Ca²⁺ (99.99% and 98.52%) and high levels of rejection of Na⁺ and K⁺ (over 97.5%) were observed when using a synthetic seawater feed at 75 °C and 1 atm feed-side pressure. Water flux through the natural zeolite membranes was dependent on the ion concentration in the feed, the operating temperature and the feed sanity. At 93 °C, water fluxes of 2.5 kg/m²h and 0.39 kg/m²h were obtained for feed concentrations of 100 mg/L Na⁺ and 5500 mg/L Na⁺, respectively.

Hejazi et al. [61] described the characterization of natural clinoptilolite membranes made from dense mineral deposits by single gas H₂ and CO₂ permeation. Permeability values as a function of temperature and pressure were analyzed on the basis of mass transport fundamentals of gas permeation through zeolite and nonzeolite pathways. H₂ and CO₂ fluxes through the membranes were fitted with a model based on a combination of zeolitic, Knudsen, and viscous transports so that the selective and nonselective flux fractions could be quantified. An increase in feed pressure increased the total permeance especially at low temperatures.

Moreno et al. [62] evaluated the potentiality of a natural Mexican zeolite from the northern state of Sonora as microfiltration membranes. The main components of the Mexican zeolites were clinoptilolite and heulandite. Two steps were used to prepare the membranes from this zeolite pressing and sintering. It was necessary to use lubricants and agglomerates with a different

particle size of the zeolites. The best properties of the porous membranes were obtained using zinc stearate (4 wt%) as lubricant, boehmite (15 wt%) as agglomerate and the best particle size ranged from 63 to 300 μm. The thermal treatment of the porous membrane was carried out at several temperatures (500-1000 °C). The porous membranes obtained were studied by x-ray diffraction, SEM and nitrogen physisorption (to find the porosity), phase transformation and pore size distribution. A loss of crystallinity, decreased porosity and a lower surface area were found when the sintering temperature was increased. The results of pore distribution suggest that these materials are porous membranes for microfiltration.

Ajenifuja et al. [63] fabricated microporous ceramic matrix membranes with complementary proportions of naturally available zeolitic aluminosilicate materials (obtained from a quarry site near Jalingo, Taraba State, Nigeria) and abundant lateritic clay minerals (obtained from a construction site in Obafemi Awolowo University Campus, Ile-Ife, Nigeria). The clay material being sourced from laterite was richer in iron oxide than the zeolite raw material. The membranes cast as circular disks (22.78 mm diameter and 2.11 mm thickness) were treated with silver nitrate solution to avoid microbial growth on their surface and then sintered at 900 ± 5 °C for about 20 h. With pore size down to a range between 0.05 to 0.1 μm, the ceramic membranes were efficient at retaining bacteria and cysts through size exclusion mechanism and adsorption. Thus, between 82% and 100% of the bacterial population in water can be removed by the composite ceramic membrane filter; and most rust and suspension can be removed almost entirely. The other results showed its promising adsorption characteristics for the removal of heavy metals from water.

4.2 Synthetic zeolites

4.2.1. DDR zeolites

The all-silica zeolite deca-dodecasil 3R (DD3R) is a clathrasil (8-ring) and was first synthesized by Gies [64]. Its crystal structure consists of three dimensional arrangements of building units. The highly siliceous DDR (Deca-Dodecasil 3R)-type zeolite contains pores formed by a polyhedron with an oxygen eight-membered ring. This zeolite has a high thermal stability allowing a study of gas permeation (or diffusion) at high temperatures at which adsorption is negligible. This avoids the necessity to measure equilibrium of gas adsorption in the supported, thin zeolite membrane. Furthermore, this zeolite has a small pore opening (0.36×0.44 nm²) making it an ideal candidate to study the effects of size or molecular weight of gases on permeation or diffusion properties for zeolites and zeolite membranes. The DDR critical diameter with eight-membered-ring windows closely matches the diameters of light hydrocarbons and carbon dioxide.

Nakayama et al. [65] patented the method for the preparation of DDR zeolites. They reported that the DDR type zeolite membrane separates at least one type of a gas component from a mixed gas containing at least two types of gases selected from a group consisting of carbon dioxide, hydrogen, oxygen, nitrogen, methane, propane, propylene, carbon monoxide and nitrogen oxide. Each single gas permeance at room temperature and 100 °C were different, respectively, enabling the separation of at least one selected gas component from the mixed gas.

Tomita et al. [30] coated molecular-sieve type zeolite (DDR) with an aperture of 0.36×0.44 nm on a porous alumina substrate by the hydrothermal process. The permeation through the membrane in the single gas feed of helium, hydrogen, carbon dioxide, oxygen, nitrogen, methane, n-butane, i-butane and sulfur hexafluoride were measured at 301 and 373 K up to 0.5 MPa. Figure 4 shows the permeation of each gas plotted against the kinetic diameter of various gases. The permeance decreased by more than three orders of magnitude between 0.35 and 0.40 nm of the kinetic diameter of permeated gas at both 301 and 373 K. The separation factor of CO₂ to CH₄ in 50% CO₂ and 50% CH₄ mixed gas feed was 220 and 100 at 301 and 373 K, respectively at 0.5 MPa total gas feed pressure. It was concluded that the DDR type membranes have few defects and work as a molecular-sieving membrane.

Kanezashi et al. [66] prepared DDR type zeolite membranes by the secondary method on a porous α-Al₂O₃ disk. To eliminate the crystalline micropores, the surface was modified by the on-stream counter diffusion chemical vapor deposition (CVD) technique. Following Table 2 shows the permeance for four gases for the CVD-modified DDR-type zeolite membranes before and after exposure to steam at 500 °C. From Table 2, it is clear that there is irrelevant change in gas permeation before and after exposure to steam. Similar results were also observed for activation energy. It proved that the CVD-modified DDR type membrane is hydrothermally stable. It is also indicated by Table 2 that single gas permeance (or diffusivity) decreases as H₂>He>CO, which is determined by both molecular size and weight of

permeating gases. This indicates the presence of intercrystalline pores in the as-synthesized DDR-type zeolite membranes.

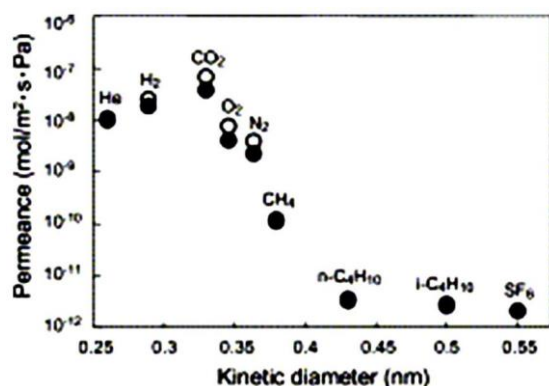


Fig. 4. Permeance in the single gas feed through DDR type zeolite membrane at 301 K (○) and 373 K (●) against kinetic diameter of gas [30].

Table 2

Permeance of gases for CVD-Modified DDR-Type Zeolite Membrane before and after exposure to steam at 500 °C (Partial Pressure of Steam: 50 kPa) [66].

Gases	Permeance at 500 °C ($10^{-8} \text{ mol m}^{-2} \text{ s}^{-1} \text{ Pa}^{-1}$)	
	Before exposure to steam	After exposure to steam
He	2.79	2.74
H	2.34	2.18
CO ₂	0.38	0.39
CO	0.20	0.18

Himeno et al. [31] coated a porous α -alumina tube with a highly hydrophobic DDR zeolite membrane. At pressures up to 5 and 2 MPa, permeation of single gas CO₂, CH₄, He, H₂, O₂ and N₂, and, CO₂/CH₄ selectivity was studied. The permeances were in the following order: CO₂>H₂>He>O₂>N₂>CH₄. Single-gas permeance was dependent on the relative molecular size of the DDR pore diameter. However, CO₂ permeance was dominated by the adsorption affinity to the pore wall of DDR zeolite. The respective single-gas permeances of CO₂ and CH₄ at 298 K at a feed pressure of 0.2 MPa and a permeate pressure of 0.1 MPa were 4.2×10^{-7} and $1.2 \times 10^{-9} \text{ mol m}^{-2} \text{ s}^{-1} \text{ Pa}^{-1}$; the ideal selectivity for CO₂/CH₄ being 340. The DDR zeolite membranes were compared to other zeolite membranes for evaluation of their CO₂/CH₄ selectivity, and CO₂ permeance. The DDR-type zeolite membranes showed better CO₂/CH₄ separation and CO₂ permeance.

Himeno et al. [67] developed a membrane separation process for biogas using the DDR-type zeolite membrane with high CO₂/CH₄ selectivity. Biogas produced in a sewage plant was separated by using a DDR-type zeolite membrane, and the performance and durability of the membrane was estimated. It was reported by Himeno et al. that the developed membrane separation process was fully applicable to the separation and purification of biogas. They also believed that membrane performance was reduced by long periods of ventilation and high boiling compounds such as higher hydrocarbons and siloxane, which are present as impurities in the biogas.

Bergh et al. [68] studied the permeation of CO₂, N₂ and CH₄ and their mixtures through a DDR membrane over a wide range of temperatures and pressures. The synthesized DDR membrane showed a very high selectivity for CO₂ and a moderate selectivity for N₂ over CH₄ with good permeance. At a total pressure of 101 kPa and temperature of 225 K, the selectivity for CO₂ was found to be over 3000 and 40 for N₂ in a 50/50 feed mixture with CH₄, which both decreased with temperature. The N₂/CH₄ selectivity remained constant with pressure, while that of CO₂/CH₄ decreased. An engineering model, based on the generalised Maxwell-Stefen equation was used to interpret the transport phenomena in the membrane.

4.2.1.1. Hydrogen separation by using DDR zeolite

Zeolite membranes are more successful for the separation of hydrogen in comparison with polymeric and other inorganic membranes in many respects. Following Figure 5-a shows the permeance of hydrogen, He, CO, CO₂ and SF₆ through the silicate membranes in a large temperature range [37]. The kinetic diameter increases as He (2.6 Å) < H₂ (2.89 Å) < CO₂ (3.3 Å) < CO (3.76 Å) < SF₆ (5.5 Å). As shown, SF₆ has much lower gas permeation with activation energy larger than zero. At room temperature, H₂/SF₆ permselectivity is 90, much larger than Knudsen selectivity (8.5). Figure 5-b shows permeance of various gases through small pore DDR zeolite membranes. For carbon dioxide, the permeance decreases drastically with increasing temperature. Carbon dioxide can be strongly adsorbed by DDR

zeolite. The decrease in permeance with increasing temperature of carbon dioxide is mainly due to the decrease in the equilibrium sorption constant with increasing temperature. Different from of the silicate membrane, the permeance for hydrogen and helium in the DDR zeolite membrane increases with increasing temperature exhibiting a large activation energy. Thus, diffusion of hydrogen and helium in the DDR zeolite has a larger activation energy than in silicate. At high temperature (>300 °C) and for small gas molecules, the adsorption effect can be neglected and the gas permeance is determined by diffusivity. The experimental data show that at high temperatures the molecules of these gases in the zeolite retain their gas characteristics. For silicate membranes, the permeance decreases with increasing temperature and is determined by the molecular weight, not the kinetic diameter of the molecules. Diffusion of small molecules in the small pore DDR zeolite and amorphous silica membrane exhibits an activated process, with decreasing permeance as the molecular size increases [37].

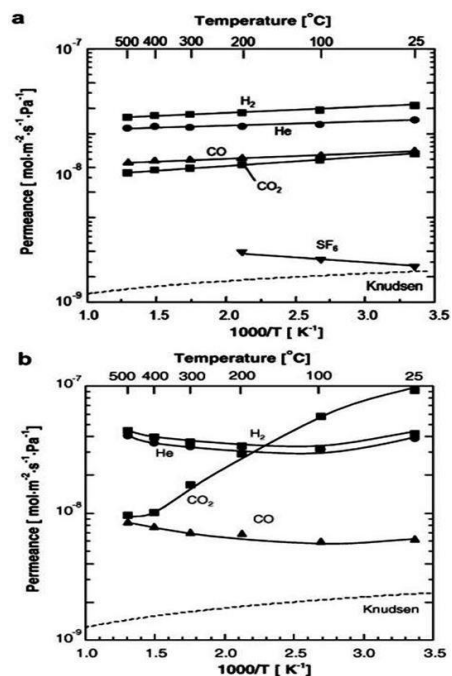


Fig. 5. Single gas permeance for silicalite membrane (a) prepared by template-free secondary growth method and for DDR-type zeolite membrane made by NGK Insulators Ltd Japan (b). Data reported in literature [37].

Kanezashi et al. [69] fabricated homogeneous polyhedral oligomeric silsesquioxane (HOMO-POSS) derived silica membranes by the sol-gel method. HOMO-POSS-derived membranes showed a CO₂ permeance of $1.1 \times 10^{-7} \text{ mol m}^{-2} \text{ s}^{-1} \text{ Pa}^{-1}$ with a CO₂/CH₄ permeance ratio of 131 at 100 °C, which was superior to CO₂/CH₄ separation performance in comparison with tetraethoxysilane (TEOS)-derived silica membranes. From the activation energy data with respect to the kinetic diameter of the gases it was noticed that HOMO-POSS-derived silica membranes were similar to that of DDR-type zeolite membranes.

4.2.1.2. Carbon dioxide separation by DDR zeolite

Separation of CO₂ from CH₄ is an important problem because of the large volume of natural gas that are known to contain high levels of CO₂. The efficient separation of CO₂ and CH₄ is challenging because of the similar size of these two molecules. Glassy polymers are used for natural gas purification (removal of CO₂, H₂O, H₂S), but they suffer from swelling – plasticization induced by CO₂ and hydrocarbon incorporation. This kind of effect is not in zeolite membranes [37]. There exist polymer membranes with a high performance for CO₂/CH₄, but these membranes have only a rather low separation performance in the CO₂/N₂ separation because of low diffusivity and solubility selectivities due to the similar size of CO₂ and N₂ (kinetic diameter CO₂, 0.33 nm, CH₄, 0.38 nm and N₂, 0.36 nm). A few zeolite membranes have already shown promising results in the separation of CO₂ from N₂ and CH₄. As the separation of these membranes is based on competitive adsorption, the selectivities were found to be low. It is well known that CO₂ adsorbs preferentially in DDR relative to CH₄ [37].

Jee and Sholl [70] used molecular simulations to describe diffusion of CO₂ and CH₄ inside DDR pores and suggested that DDR membranes are favorable for CO₂/CH₄ separations. DDR membranes exhibit very high

selectivities for CO₂/CH₄ separations with good permeance. At a total pressure of 101 kPa and at -50 °C, selectivity of an equimolar mixture was reported to be >3000. The CO₂ selectivity drops with increasing temperature and pressure, but it is still above 100 at 100 °C and 10 bar total feed pressure. The selectivity drop with increasing pressure is attributed to the dependency of the diffusivity on the total loading. The high selectivity is caused by the molecular sieving effect of CH₄ and to some extent by the preferential adsorption of CO₂. A variety of mixture gas permeation results were reported in the literature with an all-silica DDR membrane, illustrating its separation and permeation characteristics. Figure 6 shows the selectivities of equimolar mixture through the DDR membranes as a function of the temperature.

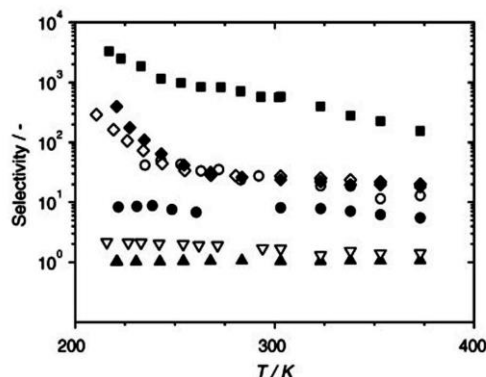


Fig. 6. Selectivities of equimolar mixtures through the DDR membrane as a function of the temperature at constant total feed pressure of 101 kPa, with sweep gas He at 101 kPa. Legend: CO₂/CH₄ (■), N₂/CH₄ (○), CO₂/Air (●), N₂O/A (◇), Air/Kr (▲), O₂/N₂ (▽), N₂O/CO₂ (▲). [70].

4.3. Silicoaluminophosphate (SAPO) Zeolites

SAPO zeolites are a series of microporous silicoaluminophosphate. Due to their special characteristics, these zeolites can be used as advanced materials for catalyst or adsorbent in petroleum refining, petroleum industry or other fields. Its linear formula is (SiO₂)_x(Al₂O₃)_y(PO₅)_z and it is a microporous zeolite.

SAPO-34 membranes have been shown to be highly selective for CO₂/CH₄ separation even at high feed pressures, because CO₂ preferentially adsorbs in the SAPO-34 pores and CH₄ (0.38 nm kinetic diameter) diffuses more slowly than CO₂ (0.34 nm kinetic diameter and similar in size to the SAPO-34 pore (0.34 nm)) [71]. Ping et al. [71] synthesized SAPO-34 zeolite membranes on seven-channel-alumina monolith supports and reported that the membranes had high CO₂/CH₄ selectivities even at high pressures. SAPO-34 seeds were added to the synthesis gel instead of seeding the support surface. It was noticed that seeding the gel simplified synthesis and improved reproducibility.

The values for SAPO-34 membranes prepared via in-situ crystallization (Si/Al gel ratio = 0.15) (M3), and via seeding (containing one layer of seed zeolite) (S1) were significantly above the upper bound for the polymeric membrane for CO₂/CH₄ separation selectivities versus CO₂ permeabilities (Figure 7) as Robenson discussed [72].

Li et al. [20,73] synthesized SAPO-34 by in situ-crystallization on a porous tubular stainless steel support. The SAPO-34 is a silico-aluminophosphate having the composition Si_xAl_yP_zO₂ where x = 0.01-0.98, y = 0.01-0.60, z = 0.01-0.52 and x + z = y. These membranes were used to separate a 50:50 CO₂/CH₄ mixture at 295 K at a feed pressure of 222 kPa and a permeate pressure of 84 kPa. For a SAPO-34 membrane with a Si/Al gel ratio of 0.15, a CO₂/CH₄ mixture selectivity of α = 170 with a CO₂ permeance of P = 1.2 × 10⁻⁷ mol m⁻²s⁻¹Pa⁻¹ was found at 295 K.

Carreon et al. [74] studied the CO₂/CH₄ separation by using alumina supported SAPO-34. The crystal size of the SAPO-34 seeds was controlled in the 0.7 to 8.5 μm range. And all crystals had the chabazite structure. It was revealed that the CO₂/CH₄ separation performance of SAPO-34 membranes was a function of average size of the seed crystals. Seeds less than 1 μm produced membranes with superior separation performance. Smaller seeds with a narrow size distribution have the potential to closely pack more homogeneously than larger crystals, so that the inter-crystalline regions that need to intergrow are smaller, and a thinner membrane can be prepared. The membranes had CO₂/CH₄ separation selectivities higher than 170, with CO₂ permeances as high as ~ 2.0 × 10⁻⁶ mol m⁻²s⁻¹Pa⁻¹ at 295 K and a feed pressure of 224 kPa. The membranes effectively separated CO₂/CH₄ mixtures up to 1.7 MPa.

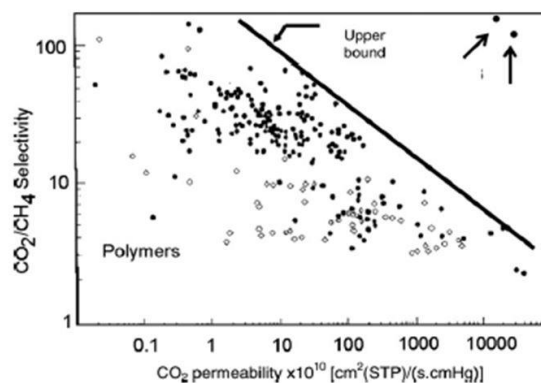


Fig. 7. Comparison of CO₂/CH₄ separation selectivity versus CO₂ permeability (Robson plot) for polymeric membranes and two SAPO-34 membranes at room temperature and feed and permeate pressures of 22 and 84 kPa respectively. The two arrows indicate the experimental results on two SAPO-34 membranes [37].

Poshusta et al. [75] revealed that SAPO-34 membranes coated on porous alumina tubular supports can be used for light gas separations at low and high temperatures. Single gas permeances of CO₂, N₂, and CH₄ decreased with increasing kinetic diameter. For the best membrane at 300 K, the He and H₂ permeances were less than that of CO₂, because He, H₂ and CO₂ were small compared to the SAPO-34 pore, and differences in the heat of adsorption determined the permeance order. The permeation of smaller components was faster in CO₂/CH₄, CO₂/N₂, N₂/CH₄, H₂/CH₄ and H₂/N₂ mixtures between 300 and 470 K. The CO₂/CH₄ selectivity at room temperature was 36 and decreased with temperature. The H₂/CH₄ mixture selectivity was 8 and remained constant at temperatures up to 480 K.

Hong et al. [76] studied the SAPO-34 membrane for the separation of CO₂/H₂ and H₂/CH₄ mixtures at feed pressure up to 1.7 MPa. Strong CO₂ adsorption inhibited H₂ adsorption and decreased H₂ permeances significantly, especially at low temperature, so that CO₂ preferentially permeated and CO₂/H₂ selectivities were higher at low temperatures. At 253 K, CO₂/H₂ separation selectivities were greater than 100 with CO₂ permeances of 3 × 10⁻⁸ mol m⁻²s⁻¹Pa⁻¹. The CO₂/H₂ ideal selectivity was around 2, and it decreased at a lower temperature, as shown in Figure 8.

The CO₂/H₂ separation exceeded the upper bounds (selectivity-permeability plot for polymer membranes) (Figure 9).

Liu and Cheng [19] synthesized SAPO-44 by the sol-gel method and a defect-free zeolite membrane was coated on the porous α-Al₂O₃ plate. The permeating results showed that the H₂/N₂ and H₂/CO permeabilities were 5.78 and 7.15, respectively. These values were higher than theoretical Knudsen diffusion and substrate values. H₂ permeation was 1.40 × 10⁻⁷ mol m⁻²s⁻¹Pa⁻¹.

Das et al. [77] prepared SAPO-34 zeolite membranes on a tubular mullite support. The support surfaces were coated with seed crystals. Before seeding, the substrate was treated with polyvinylpyrrolidone (PVP) to orient the seeds. Both the treated and untreated supports were seeded, and membranes were synthesized on those support tubes by the in-situ hydrothermal method. The PVP molecule existed in the two resonance structures. Hence the acylamino bond -N⁺=C-O⁻ acts as an intermediate linker between the support surface and seed surface. Due to charge interaction, the seed crystals were anchored strongly to support the surface. The single-gas permeation with CO₂ and H₂ was investigated. Up to 5 bar of feed pressure, the permselectivity of CO₂ and H₂ was as high as 4.2.

Chew et al. [78] studied the effect of cation exchanged H-SAPO-34 on the separation of CO₂/CH₄ gas separation. It was reported that the CO₂ permeance reduced with cation-exchanged membranes in the order of Ca(II) > Mg(II) > Sr(II) > Ba(II). The maximum CO₂/CH₄ separation selectivity of 103 with CO₂ permeance of 37 × 10⁻⁸ mol/m²sPa was obtained for equimolar of CO₂ and CH₄ at 303K and 100 kPa pressure difference across the Ba-SAPO-34 membrane.

In the catalytic cracking of methyl-diethoxysilane (MDES) using boron-substituted ZSM-5 and SAPO-34 membranes, the selectivity of H₂ separation from light gases increased [79]. The MDES reacted in the B-ZSM-5 pores and reduced the effective pore diameter, so that silylation significantly increased their H₂ selectivity. The H₂/CO₂ separation selectivity at 473 K increased from 1.4 to 37, whereas the H₂/CH₄ separation selectivity increased from 1.6 to 33.

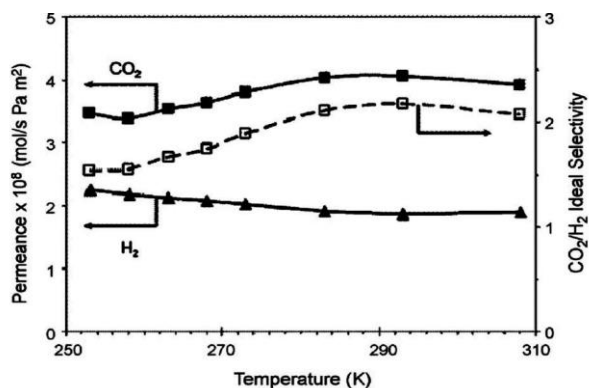


Fig. 8. CO₂ permeance and CO₂/CH₄ separation selectivity at 295 K versus feed pressure for a 7-channel SAPO-34 monolith membrane that was prepared using a seeded gel. The feed was a 50/50 CO₂/CH₄ mixture at flow rate of 20 standard L/min [76].

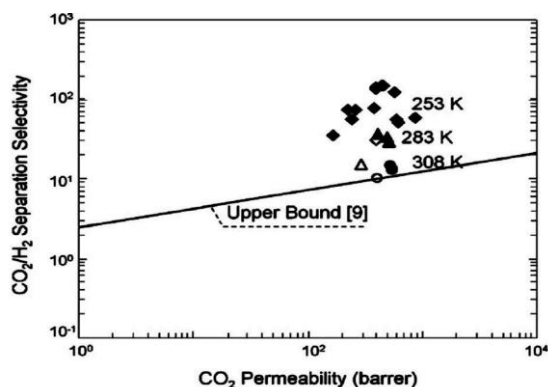


Fig. 9. CO₂/H₂ separation selectivity vs. CO₂ permeability for the SAPO-34 membrane (closed symbols) at 308 K (●), 283 K (▲), and 253 K (◆) and a cross-linked poly(ethylene glycol) copolymer membrane at 308 K (○), 283 K (△), and 253 K (◇). The data points at 253 K for the SAPO-34 membrane were obtained at different feed pressures and compositions [76].

4.4. Beta zeolite or ZSM zeolite (MFI Zeolite membranes (ZSM -5))

Beta zeolite is an old zeolite discovered before Mobil began the "ZSM" naming sequence. As the name implies, it was the second in an earlier sequence. The structure of zeolite beta was only recently determined because the structure is very complex and interest was not high until the material became important for some dewaxing operations. Zeolite beta consists of an intergrowth of two distinct structures termed Polymorphs A and B. The polymorphs grow as two-dimensional sheets and the sheets randomly alternate between the two. Both polymorphs have a three dimensional network of 12-ring pores. The intergrowth of the polymorphs does not significantly affect the pores in two of the dimensions, but in the direction of the faulting, the pore becomes tortuous, but not blocked.

Among the different types of zeolites available, zeolite MFI (ZSM-5 and its Al-free analog, silicate-1) has been more commonly used in zeolite membrane synthesis, because of its pore size (~5.5 Å) suitable for several industrially important separations and the relatively easy synthesis from a variety of silica sources and structure directing agents. ZSM-5 is composed of several pentasil units linked together by oxygen bridges to form pentasil chains. A pentasil unit consists of eight five-membered rings. In these rings, the vertices are Al or Si and an O is assumed to be bonded between the vertices. The pentasil chains are interconnected by oxygen bridges to be corrugated with 10-ring holes. Its chemical formula is Na_nAl_nSi_{96-n}O₁₉₂·16H₂O (0 < n < 27) (http://helios.princeton.edu/zeomics/cgi-bin/view_structure.pl?src=iza&id=MFI).

MFI zeolite membranes were prepared by Takata et al. [80] via secondary growth on α -alumina microfiltration membranes. Colloidal silicate (size around 100 nm) was used as seed crystals. An MFI membrane, in which the zeolite layer was oriented to the (1 0 1) plane showed an n-C₄H₁₀ permeance of 1.5×10^{-5} m³ (STP) m⁻²s⁻¹kPa⁻¹ and an n-C₄H₁₀/iso-C₄H₁₀ selectivity of 15 at 150 °C. N₂ permeated faster than He at temperatures lower than 150 °C. It was reported by them that at high temperature (300 °C) the permeation mechanism obeys the Knudsen mechanism, irrespective of molecular size in the experimental range.

ZSM-5 membrane was prepared by Kwon et al. [81] on the porous alumina support using the in-situ seeding technique in hydrothermal conditions. The packed density of the zeolite membrane was controlled by the hydrothermal time and temperature. The sample packed at 100 °C was densely packed with ZSM-5 seeds on the top of the alumina substrate. The

prepared zeolite membranes were characterized with SEM and thin membrane XRD. The hydrogen permeance and selectivity toward carbon oxide gas were 0.6×10^{-6} mol/m²sPa and 3.16, respectively. The hydrogen selective zeolite membranes show promising applications in hydrogen separation from coal gasification such as Integrated Gasification Combined Cycle (IGCC).

Welk and Nenoff [82] studied the permeance and selectivity of both ZSM-5 and silicate-1 zeolite membranes under the flow of gas mixtures, two chosen as benchmarks (50/50 mol% H₂/CH₄ and 50/50 mol% H₂/CO₂) and one chosen to simulate the industrial methane reformat stream. Permeation of mixed gases through both ZSM-5 and silicate-1 zeolite membranes had revealed the extraordinary selectivities of these membranes for H₂. The ZSM-5 membrane had the following H₂ selectivities for the 50/50 H₂/CH₄ mixture, the 50/50 H₂/CO₂ mixture and the reformat mixture: 39.4, 60.1 and 58.8, respectively.

Richter et al. [83] coated the ZSM-5 zeolite membrane on the inner surface of ceramic tubes and capillaries to get useful membrane shapes with a high membrane area/module volume ratio for industrial application. On flat discs and by a two-step-crystallization, ZSM-5 membranes of 20 μ m thickness, a very low H₂ permeance of only 30 l/(m² h bar) and a high H₂/SF₆ single gas permselectivity of 51 were achieved (see Figure 10).

Most of the coated membranes were tested by H₂ and SF₆ single gas permeation at 110 °C. The results are given in Table 3.

From Table 3, all tubular membranes had a much higher H₂ permeance and a lower H₂/SF₆ permselectivity compared with flat discs because of the simpler one-step crystallization. The preparation in a resting synthesis solution causes very low H₂/SF₆ permselectivities of 10-14. By using nanosized MFI seeds and by pumping the synthesis solution through the support tubes, homogeneous ZSM-5 membranes of 30 μ m thickness and a high permeance of 4500 l/(m² h bar) and a H₂/SF₆ single gas permselectivity above the Knudsen factor were achieved.

Bernal et al. [36] have grown zeolite MFI membranes (thickness 15-20 μ m) on the surface of macroporous α -alumina and stainless steel support tubes (pore size 200 and 500 nm, respectively) by the secondary (seeded) growth technique. The tubular supports were dipped vertically in an aqueous suspension of colloidal silicate-1 seed crystals (particle size 100 nm) and withdrawn at a speed of 1-2 cm/h to allow the uniform formation of seed layers on the outer (for stainless steel) or inner (for α -alumina) cylindrical surface of the support tubes. The seeded tubes were treated hydrothermally with a clear solution of different composition given in Table 4.

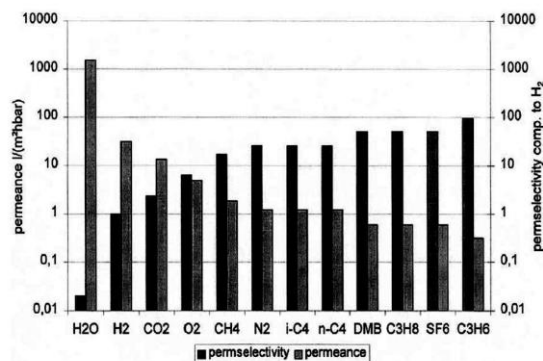


Fig. 10. Single gas permeance of ZSM-5 membrane on flat support at 105 °C, prepared by two-step-crystallization [83].

Table 3
Single gas permeation of ZSM-5 membranes at 110 °C [83].

Support	Seeding	H ₂ permeance (l/m ² h bar)	SF ₆ permeance (l/m ² h bar)	H ₂ /SF ₆ permselectivity
<i>Two-step-crystallization, resting synthesis solution</i>				
Flat disc	MFI powder	30 ^a	0.6 ^a	51 ^a
<i>One-step-crystallization, resting synthesis solution</i>				
Tube	MFI powder	6300	460	14
Small tube	MFI powder	-	-	-
Capillary	MFI powder	-	-	-
Tube	Nano seeds	18040	1520	12
Small tube	Nano seeds	8580	610	14
Capillary	Nanoseeds	3140	660	5
<i>One step-crystallization, moved synthesis solution</i>				
Tube	Nano seeds	9540	480	20
Small tube	Nano seeds	5310	170	31
Capillary	Nano seeds	4550	210	22

^a Measurement at 105 °C

Table 4
Molar compositions of clear solutions for secondary growth [36].

Code	KOH	TPABr	TPAOH	SiO ₂	H ₂ O
A ^a	1.0	1.0	-	4.5	1000
B ^a	-	-	3.0	25	1500
C ^a	1.0	1.0	-	9.0	1000
D ^b	1.6	2.0	-	40	1000

^a Silica source is TEOS.

^b Silica source is Ludox AS-40.

For the best preparations, the binary n-butane/iso-butane permeation rate ratios at 22 °C were as high as 28 and 53 for stainless steel and α -alumina tubes respectively, while the n-butane permeation flux varied in the range of 0.8–3.8 m mol m⁻²s⁻¹.Pa⁻¹.

Kazemimoghadam and Mohammadi [28] explored the possibility of using MFI zeolite membranes to remove ions from aqueous solutions by reverse osmosis (RO). RO desalination by zeolite membranes may offer an alternative for some difficult water treatment processes such as concentration of low level radioactive waste water and desalination of high concentration organic water produced in oil and gas operations where conventional technologies, including polymeric RO membranes, are either inapplicable or inefficient. MFI zeolite has an effective intracrystal nanopore diameter of 0.51 nm which is smaller than the sizes of hydrated ions involved. As a result, complete rejection of hydrated ions is possible by using MFI zeolite membranes.

Aoki et al. [84] hydrothermally synthesized ZSM-5 zeolite (Si/Al = 2525 and 600). These membranes were ion exchanged with H⁺, Na⁺, K⁺, Cs⁺, Ca²⁺ and Ba²⁺. Their gas permeation properties were measured over the temperature range of 323–523 K. Both the Si/Al ratio and the exchanged ion size affected the separation performance. For the membrane with a Si/Al ratio of 600, ion exchange only changed the single gas permeation of i-C₄H₁₀, as the number of exchange sites was small. For the membrane with Si/Al = 25, single gas permeances increased for the exchanged forms in the order: K⁺<Ba²⁺<Ca²⁺<Cs⁺<Na⁺~H⁺, which coincides with the decrease in ion size and only the Cs ion does not fit this trend. From their observation, it was concluded that zeolite membranes can be ion exchanged without irreversibly damaging the membrane performance.

Tuan et al. [85] prepared boron substituted ZSM-5 membranes on porous stainless-steel and α -alumina support. These membranes had higher n-C₄H₁₀/i-C₄H₁₀ separation selectivities, and effectively separated these isomer mixtures at higher temperatures than membranes with aluminum substituted into the framework. Membranes were prepared with Si/B ratios as low as 12, and the best membranes were prepared from alkali-free gels. The highest n-C₄H₁₀/i-C₄H₁₀ permselectivity at 473 K was 60, and the highest at 527 K was 24. It was also reported by them that the B-ZSM-5 membrane preparation was reproducible and the membranes were stable at elevated temperature.

4.5. AIPOs membranes

Microporous aluminophosphate (AIPO_s) are a class of zeolites with a framework structure built of AlO₄ and PO₄ tetrahedral building units. AIPO-18 is an appealing zeolite composition for membrane formation. The AIPO_s framework topology of this aluminophosphate is characterized by a three dimensional framework possessing eight membered intersecting channels with a diameter of 3.8 Å [24]. Thus, the pore size of this aluminophosphate makes it particularly attractive for the separation of CO₂ (kinetic diameter 3.3 Å) from CH₄ (kinetic diameter 3.8 Å).

Carreon et al. [24] used the porous stainless steel tubes as support to grow the AIPO-18 membranes and used for the separation of equimolar CO₂/CH₄ gas mixtures. The AIPO-18 membrane displayed CO₂ permeance as high as ~6.6×10⁻⁸ mol m⁻²s⁻¹.Pa⁻¹ with CO₂/CH₄ selectivities of ~ 52–60 ranging at 295 K and 138 kPa.

4.6. Zeolitic imidazolate frameworks (ZIFs)

Zeolitic imidazolate frameworks (ZIFs) are three dimensional structures consisting of rigid MN₄ tetrahedra (M = metal ions) linked through bridging imidazolate (Im) C₃H₃N₂⁻ anions. Its topology is similar as observed in zeolites and in some aluminophosphates, and thus the family of metal-organic frameworks (MOFs) is of primary importance because of their nanoporous properties and thermal stability. The high specific gas sorption capacities of some ZIFs have led to proposed applications in the fields of gas sorption and separations. Bennett et al. [86] reported for the first time, a reversible pressure-induced amorphization of a zeolitic imidazolate framework (ZIF-4, [Zn(Im)₂]). This occurs irrespective of pore occupancy and takes place via a novel high pressure phase (ZIF-4-I) when solvent molecules are present in the pores. A

significant reduction in bulk modules upon framework evacuation was also noted for both ZIF-4 and ZIF-4-I.

Zeolitic imidazolate frameworks (ZIF) are one kind of metal organic frameworks' subsidiaries which could be used to keep industrial emissions of carbon dioxide out of the atmosphere. One liter of the crystals could store about 83 liters of CO₂. The crystals are non-toxic and require little energy to create, making them an attractive possibility for carbon capture and storage. "The porous structures can be heated to high temperatures without decomposing and can be boiled in water or solvents for a week and remain stable, making them suitable for use in hot, energy-producing environments like power plants" (<http://www.cbc.ca/technology/story/2008/02/15/tech-carbon-capture.html>).

Zeolite imidazolate framework (ZIFs), a subclass of metal organic frameworks (MOFs), has emerged as a novel type of crystalline porous material which combines highly desirable properties from both zeolites and MOFs, such as microporosity, high surface area, and exceptional thermal and chemical stability, making ideal candidates for gas separation applications. In ZIFs metal atoms such as Zn, Co, and Cu are linked through N atoms by ditopic imidazolate (Im) or functionalized Im links to form neutral frameworks and to provide tunable nanosized pores (0.2 to 1.5 nm) formed by four, six, eight, and twelve numbered ring ZnN₄, CoN₄, and CuN₄ tetrahedral clusters. The framework of ZIF compounds closely resembles the framework of zeolites; i.e., the T-O-T bridges (T = Si, Al, P) in zeolite are replaced by M-Lm-M bridges (M = Zn, Co, Cu) and coincidentally, their bond angles in both structures are 145° [22,87].

ZIF-7 possesses an open-framework structure with SOD (cubic symmetry, SOD topology) in hexagonal symmetry, formed by bridging benzimidazolate (bim) anions and zinc cations. The pore size of ZIF-7 is about 0.3 nm, which is just in between the size of H₂ (0.29 nm) and CO₂ (0.33 nm). Therefore, ZIF-7 membranes are expected to achieve high selectivity of H₂ over CO₂ through the molecular sieving effect. This was experimentally proven by Li et al. [88]. Li et al. deposited seeds of ZIF-7 on an alumina disc and used H₂ separation abilities at 220 °C. Figure 11 shows the single and mixed gas (from equimolar binary mixtures) permeances of the ZIF-7 membrane at 220 °C as a function of molecular kinetic diameters of the gas molecule.

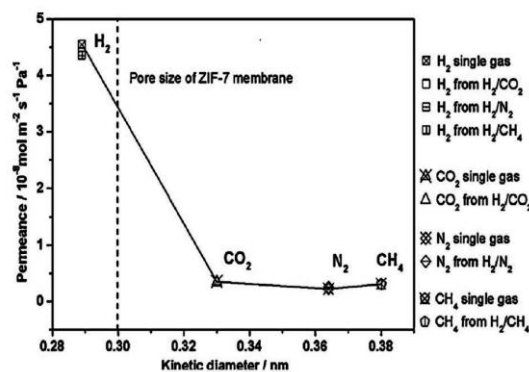


Fig. 11. Permeance of single gases (circles) and from 1:1 mixtures (square: H₂/CO₂ mixture, rhombuses: H₂/N₂ mixture, triangles: H₂/CH₄ mixture) of the ZIF-7 membrane at 200 °C as a function of molecular kinetic diameters [88].

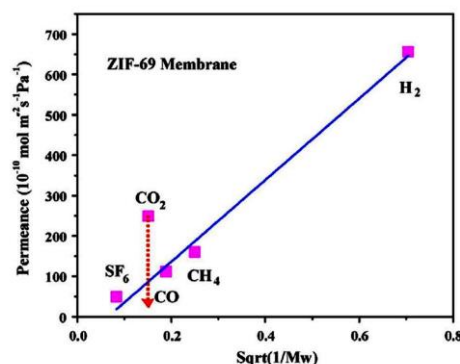


Fig. 12. Single-component gas permeation results through ZIF-69 membrane under 1 bar [29].

Liu et al. [29] were successful in developing an in situ solvothermal synthesis procedure to prepare the first ZIF-69 membrane on porous α -alumina

support. Single gas permeation experiments through ZIF-69 membranes were carried out by a vacuum method at room temperature using H₂, CH₄, CO, CO₂ and SF₆, respectively. The permeances were in the order H₂>CO₂>CH₄>CO>SF₆. The permselectivity of CO₂/CO was 3.5 ± 0.1 with CO₂ permeance of 3.6 ± 0.3 × 10⁻⁸ mol m⁻²s⁻¹Pa⁻¹ at room temperature. All studied gases except CO₂ follow the Knudsen diffusion mechanism, while CO₂ was dominated by surface diffusion due to the adsorption affinity of ZIF-69 (see Figure 12).

The ZIF-7 membrane exhibited promising H₂ separation abilities. At 220°C, the H₂ permeation was ~4.5 × 10⁻¹⁸ mol m⁻²s⁻¹Pa⁻¹ and the mixture separation factors for H₂/CO₂, H₂/N₂, and H₂/CH₄ were 13.6, 18.0, and 14.0, respectively. This confirmed the molecular sieving mechanism. The ZIF-7 membrane also showed excellent hydrothermal stability in the presence of steam.

Bux et al. [89] crystallized a zeolitic framework (ZIF-8) as a thin porous layer on an asymmetric ceramic support. ZIF-8 is not only highly stable, but also shows adsorption affinity toward hydrogen and methane. As ZIF-8 has the narrow size of six-membered-ring pores (~3.4 Å), it was anticipated that a ZIF-8 membrane might be able to separate H₂ (kinetic diameter ~ 2.9 Å) from a larger molecule. Another important feature of ZIF-8 is that it is hydrophobic in behavior, whereas ultra-microporous zeolites are usually hydrophilic. This gives ZIF-8 an advantage over zeolites in the separation of hydrogen from a mixture of steam. The permeances of the single gases, H₂, CO₂, O₂, N₂ and CH₄ and that of a 50:50 mixture of H₂ and CH₄ calculated from the volumetric flow rates through the ZIF-8 membrane are presented in Figure 13.

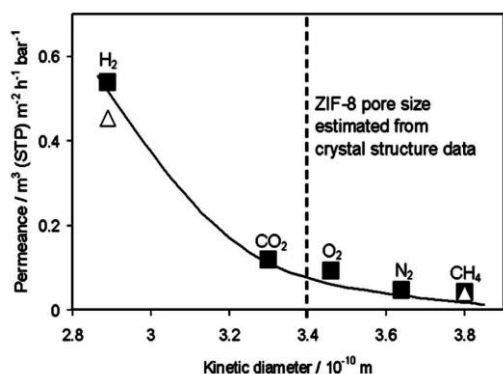


Fig. 13. Single (squares) and mixed (triangles) gas permeances for a ZIF-8 membrane vs. kinetic diameters [89].

From Figure 13, it can be seen that permeances clearly depend on the molecular size of gases. The separation factor between H₂ and CH₄ (H₂:CH₄ was 1:1) was reported 11.2 at 298 K and 1 bar which considerably exceeds the Knudsen separation factor for H₂/CH₄ (~2.8).

Song et al. [90] studied a specific surface around 100-1600 m²/g into a model polymer matrix (Matrimid® 2518) by solution mixing. It was observed that pure gas (H₂, CO₂, O₂, N₂ and CH₄) permeability increased in MMMs. The gas transport of the composite membranes were well predicted by a Maxwell model whilst the processing strategy reported can be extended to fabricate other nanocomposite membranes intended for a wide range of energy application.

Venna et al. [22] synthesized ZIF-8 by in-situ crystallization on a tubular porous α -alumina support. The hydrothermally synthesized seeds provided nucleation sites of membrane growth. CO₂/CH₄ separation performance of alumina supported ZIF-8 membranes is given in the following Table 5. All membranes were coated with two layers except Z4, which was coated with eight layers.

From Table 5, it is clear that the membrane displayed unprecedented CO₂ permeance as high as ~2.4 × 10⁻⁵ mol/m².s.Pa with CO₂/CH₄ separation selectivities of ~ 4 to 7 and separation indexes in the ~6.5 to 10 range at 295 K and a feed pressure of 139 KPa.

Table 5

CO₂/CH₄ separation properties of ZIF-8 membranes at a permeate pressure of 99.5 kPa and pressure drop of 40 kPa [22].

Membrane IDs	P _{CO₂} , mol. m ⁻² s ⁻¹ Pa ⁻¹ (×10 ⁵)	P _{CH₄} , mol. m ⁻² s ⁻¹ Pa ⁻¹ (×10 ⁵)	CO ₂ /CH ₄ selectivity	Separation index (π) ^b
Z1	2.43	4.72	5.1	9.9
Z2	2.19	4.63	4.7	8.0
Z3	2.11	5.17	4.1	6.5
Z4	1.69	2.42	7.0	10.0

^a Z1-Z3 are two layered membranes; Z4 is 8 layered membrane.

^b $\pi = (P_{CO_2} \times (\text{selectivity} - 1)) \times \text{permeate pressure}$.

Koros group fabricated a high-performance gas separation membrane from ZIF-90 crystals as MOF material with three different poly(imide)s as polymer matrices. SEM images of these membranes revealed excellent adhesion of ZIF-90 crystals with the poly(imide)s without any surface-compatibilization procedures. Interfacial voids were absent, and the MOF crystals were well dispersed [91]. Figure 14 shows the pure-component CO₂ and CH₄ gas-transport properties of mixed-matrix membranes containing 15 wt% of ZIF-90 crystal. Ultem and Matrimid mixed-matrix membranes showed significantly enhanced CO₂ permeability without the loss of CO₂/CH₄ selectivity. The mixed-matrix membranes made with 6FDA-DAM (a highly permeable polymer) showed substantial enhancements in both CO₂ permeability and CO₂/CH₄ selectivity, indicating that the membrane is defect free. Both ZIF-90A and ZIF-90B enhanced the separation significantly, but slightly better results were obtained from membranes containing smaller particles (ZIF-90A). The performance of ZIF-90/6FDA-DAM mixed-matrix membranes clearly transcend the polymer upper bound for polymeric membrane performance drawn in 1991, and reaches the technologically attractive region. Table 6 shows the data for mixed-gas (binary) permeation properties.

The enhanced gas-separation performance of the ZIF-90A/6FDA-DAM membrane is clearly seen. The CO₂/CH₄ mixed gas selectivity of the ZIF-90 mixed matrix membrane was even higher than the ideal selectivity measured by the selective sorption and diffusion of CO₂ in the ZIF-90 crystal. It was demonstrated by the Koros group [91] that membranes ZIF-90, especially ZIF-90/6FDA-DAM membranes had unprecedented high performance for CO₂/CH₄ separation and promising CO₂/N₂ separation properties.

Besides gas separation by using MOF membranes, pervaporation studies were also done by using MOF membranes. Diestel et al. [92] studied pervaporation of n-hexane, benzene, mesitylene and their mixtures on zeolitic imidazolate framework-8 membranes.

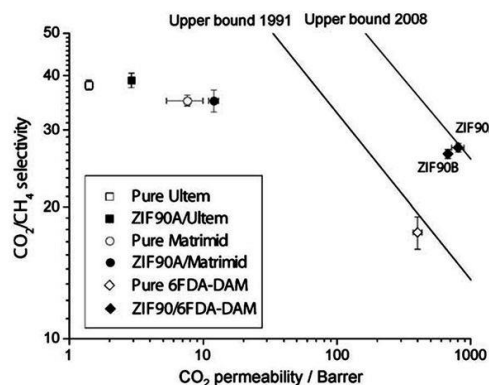


Fig. 14. Gas-permeation properties of mixed-matrix membranes containing 15 wt% of ZIF-90 crystals measured with pure gases. Measurements were performed at 358 °C and 4.5 atm upstream pressures for Ultem and Matrimid membranes, and at 258 °C and 2 atm upstream pressures for 6FDA-DAM membranes. The data for pure Ultem and Matrimid are averaged values from the literature. The upperbounds for polymer membrane performance as defined in 1991 and 2008 are shown [91].

Table 6

Mixed gas permeation properties of membranes at 25 °C and 2 atm, total feed pressure with a 1:1 CO₂/CH₄ mixture [91].

Membranes	CO ₂ permeability	CO ₂ /CH ₄ selectivity
Pure 6FDA-DAM	390	24
15 wt% ZIF-90A/6FDA-DAM	720	37
15 wt% ZIF-90B/6FDA-DAM	590	34

4.7. Zeolite T membranes

In zeolite T, the Si/Al ratio is between 3 to 4 and less hydrophilic than zeolite Y with a Si/Al ratio of less than 3. Zeolite T is an intergrowth-type zeolite of erionite and offertite, of which the pore sizes are 0.36 nm × 0.51 nm and 0.67 nm × 0.68 nm, respectively [93]. A new seeding method, namely, varying-temperature hot-dip coating (VTHDC), was synthesized by Chen et al. [94] for the preparation of the zeolite-T membrane for the dehydration of organics. The resulting zeolite T membrane exhibited high pervaporation performance with the flux reaching 2.12 and 2.52 kg/m² h for the dehydration of 90 wt% EtOH/H₂O and IPA (iso-propyl alcohol/H₂O mixture respectively, at 348 K. The corresponding separation factor was up to 1301 and 10,000, respectively.

Zhang et al. [95] studied the influence of synthesis parameters such as molar ratios of SiO₂/Al₂O₃ and H₂O/SiO₂, alkalinity, synthesis temperature,

and crystallization time on membrane growth and permeation performance of the zeolite-T synthesized by the secondary growth method. It was found that these parameters strongly affect the zeolite T growth and pervaporation performance of the membrane. Under the optimized synthesis conditions of $1\text{SiO}_2:0.015\text{Al}_2\text{O}_3:0.41(\text{Na}_2\text{O}+\text{K}_2\text{O}):30\text{H}_2\text{O}$, the crystalline time was shortened to 6 h at 423 K and a continuous and dense T-type zeolite layer as thin as 5 μm formed on the surface of the support. It significantly improved the membrane density and permselective properties. A permeation flux and separation factor of 4.20 $\text{kg}/(\text{m}^2\text{h})$ and 7800, respectively, were obtained with the as-synthesized membrane for 10 wt% water-90 wt% i-propanol mixtures at 348 K. Furthermore, it also exhibited a very good PV performance for water/ethanol mixtures separation.

Mirfendereski et al. [96] studied the effects of synthesis parameters (synthesis temperature and time) and feed pressure on CO_2 and CH_4 gas permeances through zeolite T membranes. Maximum gas permeances (minimum ideal selectivity) were obtained at a synthesis temperature of 100 $^\circ\text{C}$ and synthesis time of 15 h. Increasing feed pressure causes gas permeances to increase, while CO_2/CH_4 ideal selectivity decreases. Maximum ideal selectivity (70.8) was achieved at 120 $^\circ\text{C}$ synthesis temperatures, 30 h synthesis time and 1 bar feed pressure. The permeance data obtained for CO_2 through the synthesized zeolite membranes was in the range of 10^{-9} to 10^{-6} $\text{mol}\cdot\text{m}^{-2}\cdot\text{s}^{-1}\cdot\text{Pa}^{-1}$.

Zeolite T membranes were prepared by Cui et al. [93] via hydrothermal synthesis on porous mullite tubes seeded with zeolite T crystals using aluminosilicate gel with a molar composition of $\text{SiO}_2:\text{Al}_2\text{O}_3:\text{Na}_2\text{O}:\text{K}_2\text{O}:\text{H}_2\text{O}=1:0.05:0.26:0.09:14$. A zeolite T crystal layer of about 20 μm in thickness was formed on the outer surface of the support after the synthesis at 373 K for 30 h. Single gas and mixed-gas permeation studies through zeolite T membranes were carried out by the vacuum method at a 303–473 K range using He , H_2 , CO_2 , O_2 , N_2 , CH_4 , C_2H_6 and C_3H_8 single component gases and CO_2/N_2 , CO_2/CH_4 and other CO_2 /hydrocarbon mixtures, respectively. In single-gas permeation experiments, with increasing the kinetic diameter from 0.33 nm for CO_2 to 0.43 nm for C_3H_8 , the gas permeance decreased by four orders in magnitude, indicating a kind of molecular sieving behavior for the T type zeolite membranes. Permeance of CO_2 was much higher than those of N_2 and CH_4 and the ideal selectivities for CO_2/N_2 and CO_2/CH_4 were 31 and 266 at 343, respectively. In mixed-gas permeation experiments, zeolite T membranes showed high selectivities for CO_2/N_2 and CO_2/CH_4 pairs of 107 and 400, respectively, at 308 K. The selectivity α decreased with an increase in temperature, but was still in a high level of 20 and 52 for CO_2/N_2 and CO_2/CH_4 respectively. This was due to the synergetic effects of competitive adsorption of CO_2 and molecular sieving of zeolite pores. Because of the increasing effect of single file diffusion, the selectivities for $\text{CO}_2/\text{C}_2\text{H}_6$ ($\alpha=61$) and $\text{CO}_2/\text{C}_3\text{H}_8$ ($\alpha=17$) were rather low.

4.8. SUZ-4- Zeolite

A new SUZ-4 zeolite membrane with tetraethylammonium (TEOH) hydroxide as the template was introduced by Worathanakul and Kongkachuichay [13]. It was fabricated on mullite tube via hydrothermal sol-gel synthesis in a rotating autoclave reactor. Jaroonvechuchattam et al. [97] used rice husk ash as a raw material to synthesize SUZ-4 zeolite via a hydrothermal process in the presence of tetraethyl ammonium hydroxide as the template.

The SUZ-4 possessed a high BET surface area of 396.4 m^2/g , total pore volume of 2.611 cm^3/g and narrow pore size distribution with 97 nm mean diameter and 760 nm long needle crystal shape. It was claimed by the authors that the new SUZ-4 zeolite membrane has the potential to form unusual shape selective and catalytic properties. However, no data is available for gas separation [26].

4.9. ITQ-29-zeolite

Corma et al. [98] first introduced ITQ-29 as a zeolite with the same topological structure as zeolite A but a much higher Si/Al ratio (up to infinity, i.e. pure silica), using a bulky organic template obtained from the self-assembly of two identical organic cationic moieties through π - π type interactions. Casado-Coterillo et al. [99] prepared ITQ-29 crystals and used ITQ-29/polysulfone mixed-matrix-membranes for gas separation. The molar composition of the synthesis gels was: $(1-x)\text{SiO}_2: x\text{GeO}_2: 0.25\text{ROH}$ (4-methyl-2,3,6,7-tetrahydro-1H,5H-pyridio(3.2.1-ij) quinolium hydroxide): 0.25 TMAOH (tetramethylammonium hydroxide): 0.5 HF: $y\text{H}_2\text{O}$, where $x=0-0.05$ and $y=3-12$. These membranes were used for the gas separation of H_2/CH_4 mixtures and promising results (highest H_2 permeability of 21.9 Barrer and a

separation factor of 118 for the 4 wt% ITQ-29/polysulfone membrane) were obtained.

Pure-silica ITQ-29 is a hydrophobic small pore zeolite, which gives ITQ-29 the possibility of sieving and processing small organic molecules with high precision, even in the presence of water or other polar molecules. Al-free ITQ-29 was tested for N_2 , CH_4 and propane, but the selectivity and the permeability were not very high [100]. ITQ-29 membranes prepared by using Kryptofix 222 as SDA (structure directing agent) and activated *in-situ* in the presence of oxygen at 300 $^\circ\text{C}$, gave a separation factor of 127 for $\text{H}_2/\text{C}_3\text{H}_8$ separation [101].

4.10. UZM zeolites

Moiscoso et al. [102] and Blackwell et al. [103] introduced a new family of crystalline aluminosilicate zeolites, named UZM. These zeolites are represented by the following empirical formula: $M_m^{n+}R_r^{p+}Al_{(1-x)}E_xSi_yO_z$. In this expression, M is an alkali or alkaline earth metal such as lithium and strontium, R is a nitrogen containing organic cation such as tetramethyl ammonium and E is a framework element such as gallium.

Recently, Liu et al. [104] patented two methods for the preparation of a small pore microporous UZM-5 zeolite membrane: 1) *in-situ* crystallization of one or more layers of UZM-5 zeolite crystals on a porous membrane support and 2) a seeding method by *in-situ* crystallization of a continuous second layer of UZM-5 zeolite crystals on a seed layer supported on a porous membrane support. The membrane in the form of disks, tubes, or hollow fibers had superior thermal and chemical stability, good erosion resistance, high CO_2 plasticization resistance and significantly improved selectivity over polymer membranes for gas, vapor, and liquid separation. Liu et al. [104] claimed that the microporous UZM-5 zeolite membranes are useful for liquid separation such as deep desulfurization of gasoline and diesel fuels, ethanol/water separation, and pervaporation dehydration of aqueous/organic mixtures, as well as for a variety of gas and vapor separation such as CO_2/CH_4 , CO_2/N_2 , H_2/CH_4 , O_2/N_2 , olefin/paraffin such as propylene/propane, iso/normal paraffin, polar molecules such as H_2O , H_2S , and NH_3 /mixtures with CH_4 , N_2 , H_2 and other light gases.

4.11. Zeolite L

Zeolite L possesses a one-dimensional large pore system parallel to the c axis of the crystal. The unit cell has hexagonal symmetry (P6/mmm) with $a=1.84$ nm and $c=0.75$ nm. The minimum constricting aperture is defined by a ring of 12 tetrahedral atoms (T atoms, e.g., Si, Al) that forms an opening of 0.71 nm [105].

Mixed matrix membranes composed of zeolite L dispersed in the 6FDA-6FpDA-DABA polyimide matrix were fabricated and characterized for gas separation by Pechar et al. [23]. The interfacial contact between the two phases relied on introducing amine functional groups on the zeolite surface and covalently linking them with carboxylic groups present along the polyimide backbone. The scheme for the preparation of 6FDA-6FpDA-DABA is shown in Figure 15.

At 4.053×10^5 Pa (4 atm), oxygen, nitrogen, and methane permeabilities through the MMM increased in accordance with the observed higher gas solubility in the zeolite L, while those of He and CO_2 dropped with increasing pressure in both the mixed matrix and pure polymer systems, suggesting that the gases were not accessing the zeolite pores. This may be due to a partial blockage of the zeolite pores by the APTES (aminopropyl-triethoxysilane) surfactant; APTES was used in zeolite L for amine functionalization.

Yin et al. [106] prepared thin zeolite L/carbon nanocomposite membranes on porous alumina tubes. The permeation properties of pure H_2 , CO_2 , N_2 and CH_4 , together with CO_2/CH_4 and CO_2/N_2 mixtures through the composite membranes were measured. It was observed that the composite membranes represented higher gas permeances and selectivities of CO_2/CH_4 and CO_2/N_2 than the pure carbon membrane. With the phenomenon of competitive permeance, the equimolar mixed CO_2/CH_4 and CO_2/N_2 permeation experiments showed better separation efficiency than the single gas measurements. At 298 K, CO_2/CH_4 and CO_2/N_2 separation factors reached 43.59 and 27.21, respectively, which were higher than 35.75 and 20.43 in the single gas permeation experiments. It was concluded that the composite membrane could be a promising candidate for separation of the industrial CO_2/CH_4 and CO_2/N_2 mixtures. However, further research work is needed to optimize the preparation conditions and to increase the separation efficiency of the supported zeolite/carbon composite membranes.

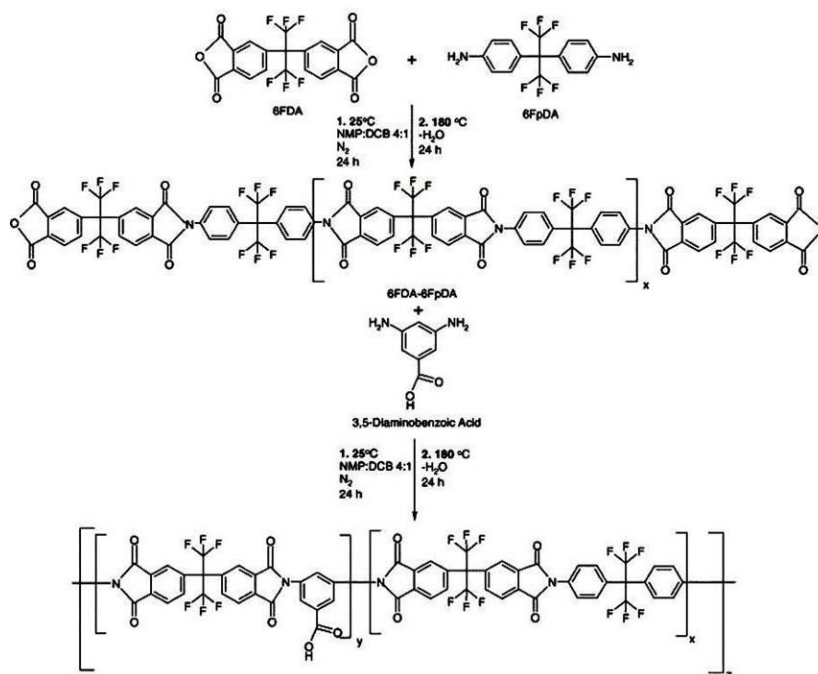


Fig. 15. Synthesis procedure for 6FDA-6FpDA-DABA [23].

4.12. Faujasite (NaX and NaY zeolite) type zeolite membrane

Faujasite is synthesized as other zeolites from alumina sources such as sodium aluminates and silica sources such as sodium silicate. Depending on the silica-to-alumina ratio of their framework, synthetic faujasite zeolites are divided into X and Y zeolite. In X zeolites the ratio is between 2 and 3, while in Y zeolites it is 3 or higher. The FAU-type zeolites, including NaX and NaY have a pore diameter (pd) of ~0.74 nm suitable for separating large molecules. Liu et al. [107] prepared NaA zeolite membranes by secondary growth on the outer surface of tubular mullite support. The support surface was found to have an obvious effect on the quality of as-made zeolite membranes. Three seeding methods, i.e. dip-coating, rubbing, and the combination of rubbing and dip coatings were used and the quality of membranes was compared. The dip-coating treatment could provide well-distributed seeds with poor coverage on dents and pinholes. Rubbing treatment with seed pastes provided seeds into the defects but non-uniform coverage on the flat area. The combined seeding approach was better than the other two seeding methods, which produced high performance membranes with high reproducibility.

Gu et al. [108] prepared FAU (Y-type) zeolite membranes via secondary growth of NaY seed layers on α -alumina supports. The dip-coating seeding technique combined with a repeated short-duration hydrothermal treatment process produced defect-free, pure NaY membranes. At room temperature, the CO₂ selectivity was about 31.2 for the CO₂/N₂ (equimolar) dry gas mixture with a CO₂ permeance of 2.1×10^{-8} mol/m².s.Pa. The presence of water vapor in the feed stream decreased the permeance for both CO₂ and N₂ in a temperature range of 23-200 °C. The presence of water vapor significantly enhanced the CO₂ selectivity at 110-200 °C, but drastically reduced the CO₂ permeance. At 200 °C, with increasing water partial pressure, the CO₂ selectivity increased and then decreased after reaching a maximum of 4.6 at a water partial pressure of 12.3 kPa.

The NaA type zeolite membrane shows excellent performance, but the acid stability is poor. Hasegawa et al. [109] studied the influence of the acid on the permeation properties of polycrystalline NaA type zeolite membranes. Zeolite layers were formed on porous α -Al₂O₃ tubes by a hydrothermal process. When sulfuric acid was added to the feed solution in the pervaporation experiment, the permeation flux of water decreased dramatically immediately after the acid addition (step (I)), then decreased slightly (step (II)), and finally increased significantly (step (III)). The permeation flux of ethanol was also increased significantly in step (II). As a result, the NaA-type zeolite membrane lost its separation ability for an equimolar mixture of water and ethanol at 313 K in 10 min after the addition of 1.0 mL sulfuric acid. This was due to the hydrolysis reaction that occurred mainly in steps (I) and (II). The hydrolysis reaction converted NaA-type zeolite into amorphous compounds, and the amorphous material was dissolved into the ethanol solution in step (III). The destruction process occurred in a shorter period in a solution of lower ethanol concentration and/or higher acid concentration.

Xu et al. [110] successfully synthesized NaA zeolite membranes on a porous support (α -Al₂O₃) from clear solution. Zeolite membrane formation on the support was done on unseeded support and on seeded support. Figure 16 shows the SEM images of the as-synthesized membranes (on unseeded support) with different synthesis time. From the XRD patterns of the as-synthesized membranes, it was revealed that diffraction patterns of NaA zeolite begin to appear after 1 h synthesis. After two hours of synthesis, the intensity of the diffraction patterns of NaA zeolite increases, which means that more NaA zeolite crystals are formed on the support. When the synthesis time was extended to 4-6 h, the diffraction patterns of other types of zeolites, e.g. zeolite X and hydroxyl-sodalite appeared. This indicated that NaA zeolite transformed into other types of zeolite in the alkaline synthesis solution. The transformation of NaA zeolite on the support was confirmed by the SEM images (see Figure 16). When the synthesis time was extended to 3 h, the NaA zeolite on the support surface dissolved and other types of zeolites began to form.

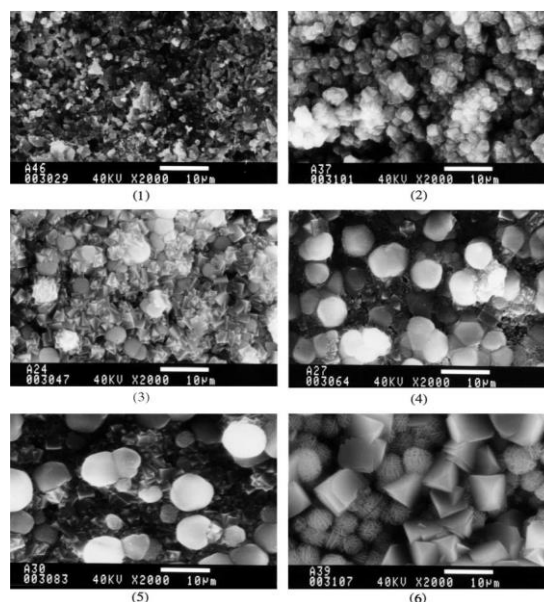


Fig. 16. SEM images of the as-synthesized membranes on the unseeded support with different synthesis time: (1) unseeded support; (2) 1 h; (3) 2 h; (4) 3 h; (5) 4 h; (6) 6 h [110].

In Figure 17, it is seen that there is a crack of 2-3 μ m in size in the membrane after 1 h of synthesis, although the nucleation of NaA zeolite on the support surface was promoted after coating the seeds.

Xu et al. [110] also revealed that the quality of NaA zeolite membranes can be improved by a multi-stage synthesis method. The NaA zeolite membrane with a synthesis time of 2 h after a two-stage synthesis showed the best gas permeation performance. The permeances of H_2 , O_2 , N_2 and $n-C_4H_{10}$ decreased as the molecular kinetic diameters of the gases increased, which showed the molecular sieving effect of the NaA zeolite membrane.

The permselectivity of $H_2/n-C_4H_{10}$ and O_2/N_2 were 19 and 1.8 respectively, which were higher than the corresponding Knudsen diffusion ratios of 5.39 and 0.96.

NaX and NaY zeolite membranes were prepared by Kita et al. [111] hydrothermally on the surface of a porous cylindrical ceramic support. It

preferentially permeated water in the pervaporation of water/alcohol mixtures. The NaY zeolite membrane also showed a high alcohol selectivity in pervaporation or vapor permeation of alcohol/MTBE (methyl ter-butyl ether) etc. and a high benzene selectivity in pervaporation or vapor permeation of benzene/n-hexane or cyclohexane. The high selectivity of the membrane can be attributed to the selective sorption into the membrane. Pervaporation and vapor permeation through NaY zeolite membrane provides an alternative to the conventional industrial purification of organic liquid mixtures such as aliphatic/aromatic hydrocarbons or alcohols/ethers.

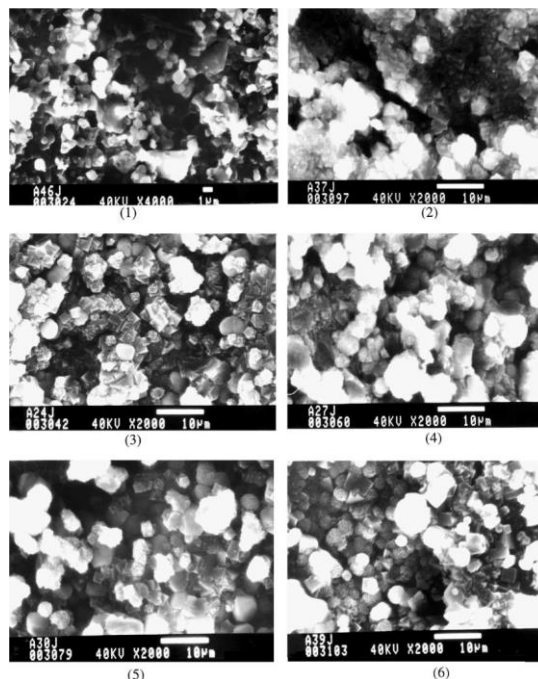


Fig. 17. SEM images of the as-synthesized membranes on the seeded support with different synthesis time: (1) unseeded support; (2) 1 h; (3) 2 h; (4) 3 h; (5) 4h; (6) 6 h [110].

Chen et al. [112] described the preparation of NaA zeolite membranes with high permeance via the microwave heating method under different conditions. The conditions were as follows: i) on a macroporous substrate in gel; ii) on a mesoporous/macroporous (top-mesoporous-layer-modified macroporous) substrate in gel, and iii) on a mesoporous/macroporous substrate in sol. In general, the H_2 permeance of the NaA zeolite membranes by microwave heating in gel was usually at the level of 10^{-6} mol/m².s.Pa, much higher than that by the conventional hydrothermal synthesis. Figure 18 shows the gas permeation properties of the membranes synthesized on the mesoporous top layer of the macroporous substrate in gel after the first growth for 45 min and the secondary growth of 30 min. The results showed that the permeance of the gases decreases with the increase of the molecular kinetic diameter for both membranes, demonstrating the molecular sieving effect of the NaA zeolite layers in both membranes. The gas separation property of the membrane after the second growth was better than that of the membrane after the first growth, with larger permeance (about 2.36×10^{-6} mol/m².s.Pa) along with better permselectivity.

Okamoto et al. [113] prepared NaA zeolite membranes by a one-time-only hydrothermal synthesis with a short reaction time of 3 h at 373 K using a gel with the composition $Al_2O_3:SiO_2:NaO:H_2O=1:2:2:120$ (in moles). A porous α -alumina support tube was used for seeding the zeolite NaA crystals. The completely dried membranes displayed gas permeation behavior attributed to Knudsen diffusion, indicating the presence of interstitial spaces between the zeolite crystal particles, or nonzeolitic pores. The membranes were highly permeable to water vapor but impermeable to every gas unless dried completely. Furthermore, the membranes displayed excellent water-permeable performance (high flux and high selectivity in PV and VP toward water/organic liquid mixtures). The high PV and VP performance was due to the capillary condensation of water in the zeolitic and nonzeolitic pores and the blocking of other molecules from entering the pores. For the water/ethanol/methanol and/dioxane systems, α values were >30000, 5700, and >9000 respectively at 378 K and 10 wt. % of feed water.

Giannakopoulos and Nikolakis [114] separated propylene/propane mixtures using the Fauzsite-type zeolite membrane coated on an α - Al_2O_3

disk. Single-component and binary mixture permeation experiments indicated that the membranes were propylene permselective. The maximum separation factor (13.7 ± 1 at 100 °C) and maximum ideal selectivity (28 at 35 °C) indicated that the membranes had improved performance when compared with the published data. Membrane permselective behavior was maintained over the entire range of feed compositions examined ($P_{total} = 101$ kPa and $P_{propylene} = 12-93$ kPa).

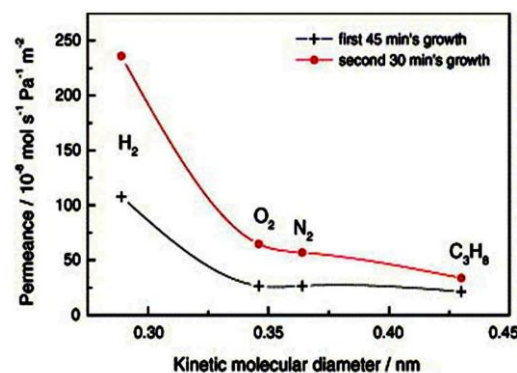


Fig. 18. Gas permeation properties of the NaA zeolite membranes on the mesoporous top layer of the macroporous substrate under microwave heating in gel after first 45 min growth (+) and second 30 min growth (•) as a function of the permeate gas kinetic diameter. Gas permeation experiments were done at room temperature and under 0.10 MPa pressure difference [112].

Jia and Murad [115] examined fauzsite zeolite membranes for gas separation by using the method of molecular dynamics. Two gas pairs, i.e., oxygen/nitrogen and nitrogen/carbon dioxide were used. It was reported that for O_2/N_2 mixtures, the ideal selectivity (pure systems) was higher than the mixture selectivity. On the other hand, for N_2/CO_2 the mixture selectivity was

higher than the ideal selectivity. Their simulation results for both gases and zeolites support the experimental results. By examining the loading of the membranes and the diffusion rates inside the zeolites, they were able to explain such contrasting behavior of N_2/O_2 and $N_2/CO_2/N_2$ mixtures. In the case of O_2/N_2 mixtures, the adsorption and loading of both O_2 and N_2 in the membranes were quite competitive, and thus the drop in the selectivity in the mixture was primarily the result of oxygen slowing the diffusion of nitrogen and nitrogen somewhat increasing the diffusion of oxygen when they pass through the zeolite pores. This is while in the N_2/CO_2 system, CO_2 was rather selectively adsorbed and loaded in the zeolite, leaving very little room for N_2 adsorption. Thus, although N_2 continues to have a higher diffusion rate than CO_2 even in the mixture, there are very few N_2 molecules in the zeolite in mixtures that the selectivity of the mixture increases significantly compared to the ideal (pure system) values. On comparing the simulation results with hydrodynamic theories that classify the permeance of membranes to be either due to surface diffusion, viscous flow, or Knudsen diffusion, results showed that surface diffusion is the dominant mode, except in the case of N_2/CO_2 binary mixtures where Knudsen diffusion also made a contribution to N_2 transport. In another study, Jia and Murad [116] studied the gas separation efficiencies of three zeolites (Faujasite, MFI, and Chabazite) by using the molecular dynamics method. It was noticed that in the mixture components with similar sizes and adsorption characteristics, such as O_2/N_2 , small-pore zeolites are not suited for separation, and this result is explicable at the molecular level. For mixture components with different adsorption behavior, such as CO_2/N_2 , separation is mainly governed by adsorption and small-pore zeolites separate such gases quite efficiently. Further, the loading (adsorption) dominates the separation of gas mixtures in small pore zeolites, such as MFI and Chabazite. For larger-pore zeolites such as Faujasite, diffusion rates do have some effect on gas mixture separation, although adsorption continues to be important. They reported that the molecular simulations could serve as a useful screening tool to determine the suitability of a membrane for potential separation applications.

A high quality NaA zeolite membrane, which shows a $H_2/n-C_4H_{10}$ permselectivity of 106, was synthesized on a seeded $\alpha-Al_2O_3$ support by a multistage synthesis method by Xu et al. [117]. In another study, Xu et al. [118] successfully fabricated the NaA zeolite membrane on a ceramic hollow fiber with an outer diameter of 400 μm , a thickness of 100 μm and an average pore radius of 0.1 μm . A continuous NaA zeolite membrane was formed on hollow fiber support after a three-stage synthesis with a membrane thickness of about 5 μm . Gas permeation properties of He (permeance 1.01×10^{-7} mol/m²sPa) and N_2 (0.276×10^{-7} mol/m²sPa), and the selectivity for He/ N_2 (2.64) were studied. Gas permeation results indicated that only after three-stage synthesis produced NaA zeolite membrane that was formed on the support. Further increasing the synthesis-stage to four stages deteriorated the quality of the NaA zeolite membrane.

Zhou et al. [14] demonstrated that discrete faujasite zeolite crystals with an average size of about 60 nm were attached as a well-defined monolayer on the surface of porous graded alumina support. Ultrathin zeolite X membranes with a total thickness of about 1 μm were grown from the seed monolayers by hydrothermal treatment in clear synthesis solutions. The membranes showed good separation performance for the PV dehydration of ethanol (total flux of 3.37 ± 0.08 kg m⁻²h⁻¹ and a separation factor of 296 ± 4 for dehydration of a 90/10 wt.% ethanol/water mixture by PV at 65 °C). Moreover, the membranes displayed stable performance during PV for 5.5 h operation.

Huang et al. [119] studied the sandwich-structured composite zeolite membranes with enhanced hydrogen selectivity on porous $\alpha-Al_2O_3$ supports by using 3-aminopropyltriethoxysilane (APTES) as an interlayer. Figure 19 shows the schematic diagram for stepwise synthesis of a sandwich structured zeolite LTA-FAU composite membrane by using APTES as an interlayer. Attributing to the covalent linkages with the surface hydroxyl groups, APTES worked as a molecular binder for attracting and anchoring the zeolite precursors onto the support surface to promote nucleation and growth. In addition, the presence of APTES can provide a protective barrier to avoid the degradation of the as-made zeolite layer during the following hydrothermal synthesis. Thus, it is helpful for the formation of well intergrown sandwich-structured composite membranes. The composite membranes display higher separation selectivities than the corresponding single phase zeolite membranes. For LTA-FAU composite membranes at 100 °C and 1 bar, the single gas separation factors of H_2/CO_2 , H_2/N_2 , H_2/CH_4 and H_2/C_3H_8 were 10.6, 8.6, 7.1, and 24.3, respectively, which were higher than those from the corresponding Knudsen coefficients.

X-type zeolite has the Faujasite (FAU) structure and its typical chemical composition is $Na_2O \cdot Al_2O_3 \cdot 2.5SiO_2 \cdot 6H_2O$. It is usually used as an adsorbent and as a catalyst. Li et al. [120] prepared X-type zeolite membranes by a template free method on porous tubular support. The best membrane was prepared as one zeolite layer on a γ -alumina support and it had a tri-isopropyl/ benzene pervaporation flux of 2.3 g/m²h at 300 K. For the separation

of 1,3-propanediol from glycerol in aqueous mixtures by pervaporation at 308 K, the total flux was 2.7 kg/m²h, and 1,3-propanediol/glycerol selectivity was 41. In another study, Li et al. [121] synthesized seven types of zeolite membranes on the inside of alumina and stainless steel support, and used them for the separation of 1,3-propanediol from glycerol and glucose by pervaporation. It was observed that the zeolite structure had a significant effect on the pervaporation flux, and the larger pore membranes had higher fluxes.

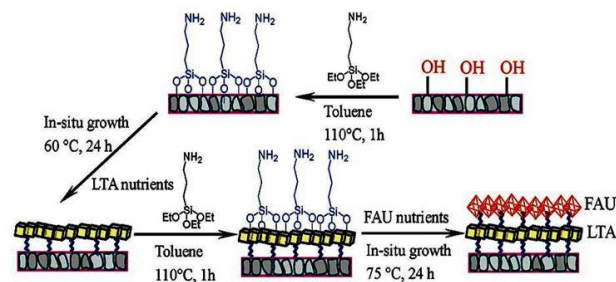


Fig. 19. Schematic diagram for stepwise synthesis of a sandwich structured zeolite LTA-FAU composite membrane by using APTES as an interlayer [119].

Sato and Nakane [122] developed a high-flux NaA zeolite membrane which exhibited higher water flux (5.6 kgm⁻²h⁻¹) by a pervaporation experiment in a mixture of water and ethanol (1:9 wt.%) at 348 K compared with those previously reported for the comparable water/ethanol separation factor, α (103-104). Vapor permeation (VP) experiments on saturated vapor with the above mixture up to 418 K and 930 kPa showed a high performance of flux 31 kgm⁻²h⁻¹ with $\alpha > 104$ that can be applied practically to a hybrid system of distillation-vapor permeation.

Zeolite NaA membranes were prepared hydrothermally by a secondary crystallization process at different temperatures (55 °C – 75 °C) on porous α -alumina-based support tubes (inner side) precoated with a poly(ethyleneimine) (PEI) buffer layer and NaA seed particles. The NaA seed crystals synthesized at 65 °C/2 h in the size range of 100–200 nm having BET surface area of 71.57 m²g⁻¹ were used for secondary crystallization of the membranes. The secondary crystallization at 65 °C for (4 + 4) h (double-stage) showed highly dense NaA grains in the microstructure of the membrane with a thickness of 5 μm . It rendered the permeance values of 50.6×10^{-8} , 2.47×10^{-8} , and 0.55×10^{-8} molm⁻²s⁻¹Pa⁻¹ for H_2 , N_2 , and CO_2 , respectively, with their permselectivity of 20.48 (H_2/N_2), 92 (H_2/CO_2), and 4.49 (N_2/CO_2). A tentative mechanism was illustrated for the interaction of PEI with the support substrate and NaA seed crystals [123].

A modified version of the adsorption-diffusion model derived from the Maxwell-Stefan theory developed by Pera-Titus et al. [124] has discussed the dehydration behavior of zeolite NaA membranes for the PV of ethanol/water mixtures by Pera-Titus et al. [125]. It was concluded that the grain boundaries might behave as fast diffusion paths or nanoscopic shortcuts due to anisotropy of zeolite layers, resulting in apparent water surface diffusivities and lower activation energies for surface diffusion.

4.12. W-Type zeolite

W-type zeolite is a synthetic zeolite that has the same framework topology as the mineral merlinoite (MER). It has an eight membered ring (8MR); and the channel dimensions are 0.31 nm × 0.35 nm, 0.27 nm × 0.36 nm, and 0.51 × 0.34 nm [16]. Membranes consisting of W-type zeolite have a unique nanopore structure which is stable at low pH. Mohammadi and Maghsoodloord [126] fabricated W-type zeolite membranes on the surface of α -alumina (porous) via hydrothermal growth with a maximum pore size of about 4 μm . Studies showed that maximum gas permeates (minimum ideal selectivity for O_2/SF_6 gas separation) were obtained for single layer membranes synthesized at 200 °C for 6 h. With changing synthesis temperature, synthesis time and number of layers and keeping other effective parameters constant, maximum ideal selectivity of 20.1 for O_2/SF_6 gas separation was achieved using a double layer zeolite membrane synthesized via the $Al_2O_3:SiO_2:K_2O:H_2O = 1.0:6.4:5.6:164.6$ gel formula over the flat support at 185 °C for 18 h.

4.13. Hierarchical zeolites

Hierarchical zeolites are a class of microporous catalysts and adsorbents that also contain mesopores, which allow for fast transport of bulky molecules and thereby enable improved performance in petrochemical and biomass processing. Zhang et al. [127] used repetitive branching during one-step hydrothermal crystal growth to synthesize a new hierarchical zeolite made of

orthogonally connected microporous nanosheets. These membranes had a permanent network of 2 to 7 nanometer mesopores, high external surface area and reduced diffusion length which accounts for higher reaction rates for bulky molecules in comparison with other mesoporous and conventional MFI zeolites.

4.14. Hydroxysodalite zeolite (HS zeolite)

Hydroxy-sodalite has the same framework structure as sodalite and consists of the cubic array of β -cages. Hydroxysodalite has a six-membered ring aperture with a pore size of 2.8 Å. The pore size of (hydroxyl-) sodalite is smaller than that of the zeolites with an eight-membered ring aperture, e.g., NaA zeolite, which makes them interesting materials for the separation of small molecules like H₂ or He from various gas or liquid mixtures [128]. The HS zeolite is hydrophilic in nature. Kazemimoghadam [129] fabricated the HS membrane hydrothermally on the surface of porous tubular support. It was reported by him that the HS zeolite membrane has great potential for application in RO desalination of complex mixtures. The zeolite membrane showed high water fluxes. Increasing pressure, feed rate and temperature increases the flux linearly.

5. Other zeolitic type or ceramic/inorganic membranes

Sandström et al. [130] used an MFI membrane comprised of an approximately 0.7 μm silicate-membrane on a fully open and graded porous alumina support to separate CO₂/H₂, CO₂/CO/H₂ and CO₂/CH₄ mixtures at high pressures. The CO₂ fluxes up to 657 kg /m²h was observed, which was many times larger than that previously reported for any zeolite membrane. The very high flux was a result of low membrane thickness, open support, and high pressure, relatively high diffusivity, molecular weight and pressure drop. The maximum CO₂/H₂ separation was 32.1, and was observed at 1000 kPa feed pressure, a permeate pressure of 200 kPa and a temperature of 275 K. The highest measured CO₂ permeance for the binary CO₂/H₂ mixture was $93 \times 10^{-7} \text{ mol m}^{-2} \text{ s}^{-1} \text{ Pa}^{-1}$. The membrane was also CO₂ selective for a CO₂/CO/H₂ mixture. However, both the CO₂ flux and the CO₂/H₂ separation factor were reduced slightly in the presence of CO, probably as a result of competing adsorption between CO and CO₂. The highest measured CO₂/CH₄ separation factor was 4.5.

Nair et al. [131] discussed the results on the separation of close boiling hydrocarbon mixtures by means of zeolite membranes. In the case of silicate membranes (MFI), the selectivity is found to depend on the microstructure. Permeation of xylene isomers through the silicate membranes occurs through both zeolitic and non-zeolitic (intercrystalline) nanopores. The faujasite membranes are found to have high selectivities (40-150) in the separation of binary mixtures containing one aromatic component, and modest selectivities (4-9) for the separation of unsaturated from saturated low-molecular-weight hydrocarbons.

Choi et al. [132] synthesized composites of polybenzimidazole (PBI) with proton-exchanged AMH-3 (a silicate with three dimensional microporous layers) and Swollen AMH-3. Proton-exchanged AMH-3 was prepared under mild conditions by the ion exchange of Sr and Na cations in the original AMH-3 using aqueous solution of dl-histidine. Swollen AMH-3 was prepared by sequential intercalation of dodecylamine following the ion exchange in the presence of dl-histidine. Both silicate materials were introduced into a continuous phase of PBI as a selective phase. Mixed matrix nano-composite membranes, prepared under certain casting conditions, with only 3 wt% of swollen AMH-3 present a substantial increase of hydrogen/carbon dioxide ideal selectivity at 35 °C, i.e., by a factor of more than 2 compared to pure PBI membranes (40 vs. 15). Similar ideal selectivity was observed using higher loadings (e.g., 14%) of proton-exchanged AMH-3 particles suggesting that the transport of hydrogen is faster than carbon dioxide in AMH-3-derived silicates. However, the ideal selectivity of MMMs approaches that of a pure polymer as the operating temperature increases to 100 °C and 200 °C.

By using the stepwise deposition method, Bétard et al. [54] fabricated membranes from MOF 1 and 2, using macroporous alumina and titania as supports. SEM images (see Figure 20) reveal that the MOF crystallites have grown on the support surface and also up to 30 μm deep inside the support pores, where they form a foam-like, lamellar structure.

Figure 21 shows permeances from MOF 1 in the range of $10^{-8} \text{ mol/m}^2 \cdot \text{s} \cdot \text{Pa}$ for both CO₂ and CH₄ which moderately increase with increasing pressure. Particularly at lower pressure, there is an obvious reduction of mixed gas permeances compared to the pure gas ones.

The CO₂ and CH₄ permeance of membrane 2 (see Figure 22) are of the same order of magnitude as the permeances of membrane 1.

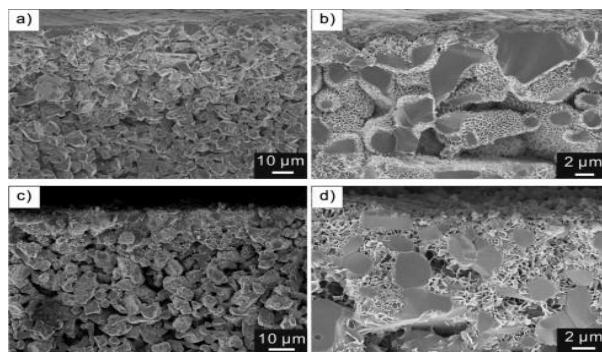


Fig. 20. Representative examples of SEM micrographs of the cross-sections of [Cu₂(ndc)₂(dabco)]_n (1) on alumina (a and b) and [Cu₂(BME-bdc)₂(dabco)]_n (2) on titania substrates (c and d) at different magnifications. The morphology of the resulting MOF crystals seems to be independent of the support type [54].

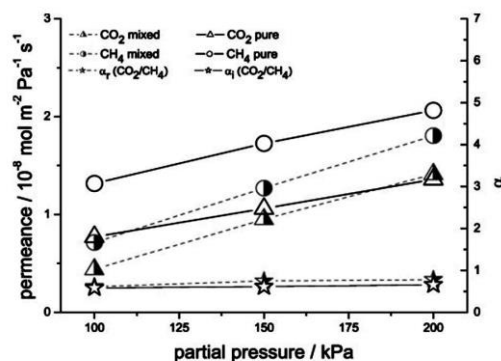


Fig. 21. Permeances of pure and equimolar mixed CO₂ and CH₄ measured for the [Cu₂(ndc)₂(dabco)]_n (1) membrane at room temperature (T = 298 K) as function of pressures at the feed side (total pressures for pure gases, partial pressures for the gas mixture). The ideal and mixed gas separation factor α_i and α_m were calculated from the corresponding ratio of the CO₂/CH₄ permeances [54].

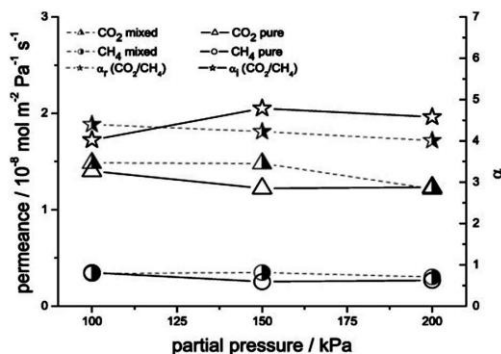


Fig. 22. Permeances of pure and equimolar mixed CO₂ and CH₄ measured for the [Cu₂(BME-bdc)₂(dabco)]_n (2) membrane at room temperature (T = 298 K) as function of pressures at the feed side (total pressures for pure gases, partial pressures for the gas mixture). The ideal and mixed gas separation factor α_i and α_m were calculated from the corresponding ratio of the CO₂/CH₄ permeances [54].

Bohrman and Carreon [133] used metal-adeninate biometal organic frameworks (Bio-MOFs) for the separation of CO₂/CH₄ mixture. Bio-MOFs were introduced by Rosi's group [134,135]. Bio-MOFs have permanent microporosity, high surface areas, chemical stability, and exceptional CO₂ adsorption capacities due to the presence of basic bio-molecule building units. In particular, Zn₈(ad)₄(BPDC)₆O₂Me₂NH₂ (where ad = adeninate, BPDC = biphenyldicarboxylate, denoted as Bio-MOF-1), a three dimensional metal organic framework with infinite-adeninate columnar secondary building units (SBUs) which are interconnected via biphenyldicarboxylate linkers, is an attractive material with great potential for CO₂ separation if prepared in membrane form. These membranes displayed high CO₂ permeances and separation ability for CO₂/CH₄ gas mixtures. The observed CO₂/CH₄ selectivities above the Knudsen selectivity indicated that the separation was promoted by preferential CO₂ adsorption over CH₄. The preferential CO₂ adsorption was attributed to the presence of adeninate amino basic sites

present in the Bio-MOF-1 structure. However, selectivity was slightly below the Robeson plot for CO₂/CH₄ mixtures [73]. Table 7 shows the CO₂/CH₄ separation performance of the stainless supported Bio-MOF-1 membranes.

Xomeritakis et al. [136] demonstrated a novel and efficient method for molecular engineering of the pore size and porosity of microporous sol-gel silica membranes. Adding a suitable organic template (e.g. tetraethyl- or tetrapropylammonium bromide) in polymeric silica sols resulted in pores in the range of 5-6 Å. In general, without any modification, the pore size of the synthetic zeolites will be in the range of 3-4 Å. With a pore size of 5-6 Å sol-gel, silica membranes are useful for hydrocarbon isomer separations. The templated membranes exhibited as high as 10⁻⁷ to 10⁻⁶ mol/m².s.Pa for molecules with dk<4.0 Å (e.. CO₂, N₂, CH₄), coupled with single-component selectivities of 100-1800 for N₂/SF₆, 20-40 for n-butane/iso-butane, and 10-20 for para-xylene/ortho-xylene. The unique features of this new approach include simple, fast and scaleable processing under ambient conditions, and the possibility to tune membrane pore size and porosity by proper choice of the type and amount of template.

Table 7
CO₂/CH₄ separation performance of Bio-MOF-1 membranes at a pressure drop of 138 kPa and 298 K [121].

Membrane ^a	Permeance mol m ⁻² .s Pa (x10 ⁻⁷)		
	CO ₂	CH ₄	CO ₂ /CH ₄ selectivity
M1 (3)	11.5	4.6	2.5
M2 (3)	11.9	4.6	2.1
M3 (4)	10.5	4.8	2.6
M4 (7)	5.8	4.7	-

^a Number in parentheses indicate number of layers.

Dual-layer polyethersulfone (PES)-zeolite beta/BTDA-TDI/MDI copolyimide (P84) composite hollow fibers, was applied to fabricate the dual layer nanocomposite hollow fiber membranes through pyrolysis by Li and Chung [137]. After pyrolysis at 800 °C, these nanocomposite hollow fibers exhibited a significantly enhanced O₂/N₂ and CO₂/CH₄ selectivity of 11.3 and 152, respectively in the pure gas measurement. A comparable CO₂/CH₄ selectivity of 140 was also observed in the mixed gas measurement. The authors claimed that these dual-layer hollow fibers are a type of potential and excellent membrane material for oxygen enrichment and natural gas separation in industrial applications.

Zeolite membranes were synthesized by the dry gel method, using a tubular support of stainless steel by Alfaro and Valenzuela [138]. The composition of precursor gel was 0.22Na₂O:10SiO₂:280H₂O:0.5TPABr (tetrapropylammonium bromide). It was observed that the amount of each hydrocarbon permeated from the mixture of hydrocarbons was as follows: n-C₄H₁₀>1-C₄H₁₀>C₃H₈>C₂H₆>CH₄. The separation factor measured for the N₂/SF₆ ratio was 5 times higher than the theoretical one. This improved selectivity to N₂ was explained in terms of the properties such as the pore size of the membrane, controlling Knudsen-type diffusion. In the hydrocarbon separation of natural gas, n-butane showed the higher concentration in the permeated side of the membrane.

Kuznicki [139] synthesized a new class of molecular sieve materials, which is generally denoted as Engelhard titano-silicates (ETS). Unlike zeolites, their frameworks are built by corner sharing SiO₄ tetrahedra and TiO₆ octahedra resulting in new structures, which cannot be built by connecting only tetrahedral units, the framework units of zeolites. The ETS materials contain a channel system like zeolites which, in principle, enables them to be used in a similar molecular sieve and/or adsorptive separations. Membranes consisting of a thin intergrown layer of Na-ETS-4 on porous titania supports were highly water permselective with selectivities as high as 400 and a corresponding water flux of 0.01 mol/m².s in room temperature pervaporation experiments using 1:1 water/ethanol mixtures. With increasing water content in the feed solution (in the range of 10-90 %) the water flux was increasing linearly, while the selectivity did not vary significantly. The selectivity of the ETS-4 membranes was similar to the highest reported for Na-X and Na-Y membranes. These Na-ETS-4 membranes may find applications in pervaporation as well as separation of permanent gases.

Stoeger et al. [140] fabricated highly c-oriented, intergrown, continuous crystalline aluminophosphate AlPO₄-5 and CoAlPO₄-5 (both of the AFI framework type) membranes which were grown on porous α- alumina by the seeded method. The membrane quality was inspected through pervaporation measurements consisting of a liquid hydrocarbon feed of n-heptane and 1,3,5-triisopropylbenzene. It was observed that the separation factor was 2.8 with a corresponding flux of 1.2 kgm⁻².h⁻¹. However, further investigation is needed focusing on growth, calcination, and microstructure optimization.

Recently, UK researchers have developed a porous material named NOTT-202 that can soak up CO₂ from the atmosphere. NOTT-202 is a "metal-organic frame work" that works like a sponge, absorbing a number of gases at high pressures. But as the pressure is reduced, CO₂ is retained as

other gases are released [141]. Solvothermal reaction of H4L (biphenyl-3,3'.5,5'-tetra(phenyl-4-carboxylic acid)) (see Figure 23) with In(NO₃)₃ in an acidic (HNO₃) mixture of CH₃CN/DMF(dimethylformamide) (v/v=1:2) at 90°C affords the solvated framework complex Me₂NH₂⁺1.75[In(L)]1.75(DMF)12(H₂O)₁₀ (NOTT-202). The counter-cation Me₂NH₂⁺ is generated by in situ decomposition of the DMF solvent during the reaction.

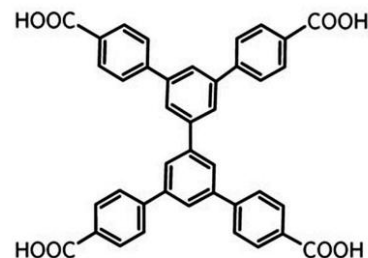


Fig. 23. Chemical structure of H4L (This ligand has approximate dimensions of 14.6x114.7 Å) [141].

The unique partially interpenetrated metal-organic framework (MOF) NOTT-202 represents a new class of dynamic material that undergoes pronounced framework phase transition on desolvation. NOTT-202 consists of two MOF networks attached to a central indium metal atom and overlaid in such a way as to leave gaps where the carbon dioxide is stored. This discovery holds promise for carbon dioxides capture and storage, or even for removing CO₂ from the exhaust gases of power plants and factories. However, there are some drawbacks to the material, i.e. its stability in the presence of high-temperature water vapor is questionable. Large scale production of this type of material has long been considered a major challenge (<http://www.bbc.co.uk/news/science-environment-18396655>).

MER type zeolite was investigated by Nagase et al. [142]. The micropore structure of the MER-type zeolite comprises double-eight rings and γ-cage, and pore diameter is 0.27-0.51 nm. The MER (merlinoite) zeolite membranes are relatively acid tolerant in the low-silica 8MR zeolite group, and low-SAR type. The MER membrane exhibited high water selectivity for 90% acetic acid solution. The separation factor of the membrane was as high as that of the LTA-type zeolite membrane (more than 5000). However, the dehydration performance and permeation mechanism of the membrane are not clear. Hasegawa et al. [33] determined the stabilities and dehydration performances of MER-type zeolite membranes prepared on porous α-alumina tubes by the secondary growth of seed crystals (SiO₂/Al₂O₃ = 4.7). The membranes showed relatively high stability, permeability, and separation performances. The permeation flux and separation factors were 1.9 kgm⁻².h⁻¹ and 9300, respectively, for an equimolar mixture of ethanol and water at 350 K. Membranes were also used for the dehydration of several organic solvents (methanol, n-propanol, i-propanol, and acetone) containing water. It was noticed that the separation factor increased with the molecular diameter of the organic solvents.

Kim et al. [143] investigated the modified MFI-type zeolite membrane as high-temperature water-gas shift (WGS) membrane reactors (MRs) in corporation with a nanocrystalline Fe/Ce WGS catalyst. The effects of the MR operating conditions and the membrane separation performance on the CO conversion (χ_{co}) were studied experimentally and by calculations using ample one-dimensional plug-flow reactor (PFR) model. The model calculations have indicated that the membrane had the potential to achieve high CO conversion of χ_{co} >99% under practically operating conditions. Due to its excellent hydrothermal stability and chemical resistance, the modified MIF-type zeolite membrane are potentially useful for constructing MR for high temperature WGS reaction of coal-derived syngas.

6. MMMs zeolite

Recent work aimed at developing membranes capable of operating above the upper bound has focused on mixed matrix membranes (MMMs). These membranes combine polymer with inorganic filler, usually a zeolite or a molecular sieve. Early attempts were made on rubbery polymers by mixing zeolite to be used for pervaporation. Later work started on glassy polymers by mixing zeolites in polymer to make MMMs suitable for gas separation application [144].

The inclusion of dispersed particles can have three possible effects on the permeability of gases; the discrete particle can act as molecular sieves, altering permeability in relation to molecular size, the particles can disrupt the

polymeric matrix resulting in increased micro cavities and hence increase permeability, or they can act as a barrier to the gas transport and reduce permeability [145]. The mixed matrix membranes provide the opportunity to overcome the individual deficiencies of molecular sieves and polymers, and achieve gas separation performance above the famous Robeson's upper bound.

Traditionally, MMMs are comprised of zeolite particles dispersed in a polymer matrix. Zeolites often exhibit relatively high penetrant sorption capacities and penetrant size-based selectivities compared to polymers due to their large micropore volumes and well defined, rigid structures. There are several drawbacks to the use of zeolites in MMMs which are as follows [53]:

1. Preparation of defect-free zeolite crystals can be difficult, time consuming, and costly.
2. There are a limited number of possible zeolite structures and compositions.
3. Costly surface chemistries are often needed to improve adhesion to polymer matrix.

The main problem in fabricating the MMMs membranes is removing voids at the interface of the particle and polymer. Extensive and intensive work has been carried out to promote adhesion between the rigid polymer chains and molecular sieves. These works include thermal treatment, silane coupling agents, integral chain linkers, and polymer coating on the molecular sieve surface [146,147]. However, it is still a challenge for the researchers with different types of MMMs membrane fabrication.

Mixed matrix membranes (MMMs) of polyimide (PI) (Matrimid® 5218) and zeolite 13X, ZSM-5 and 4A were prepared via a solution casting procedure by Chaidou et al. [148]. The effect of zeolite loading, pore size and hydrophilicity/hydrophobicity of zeolite on the gas separation properties of these MMMs were studied. It was revealed that permeability of He, H₂, CO₂ and N₂ increased with zeolite loading. The effect of zeolite content on gas permeabilities at 25 °C and feed pressure of 10 bars is shown in Figure 24. This figure (Fig. 24) indicates that permeability of all studied gases generally increase with increasing zeolite content. This could be due to the formation of void spaces around the zeolite crystals resulted combination to channel network.

Figure 25 shows the effect of zeolite loading on gas pair selectivity of PI-zeolite MMMs. It indicates that the H₂/N₂ selectivity (Figure 25-a) remains relatively constant for each zeolite up to 20% loading for 13X and 4A as well as 10% for ZSM-5 declining somewhat at higher content. The selectivity of CO₂/N₂ is significantly improved with the incorporation of the three zeolites in the PI membrane.

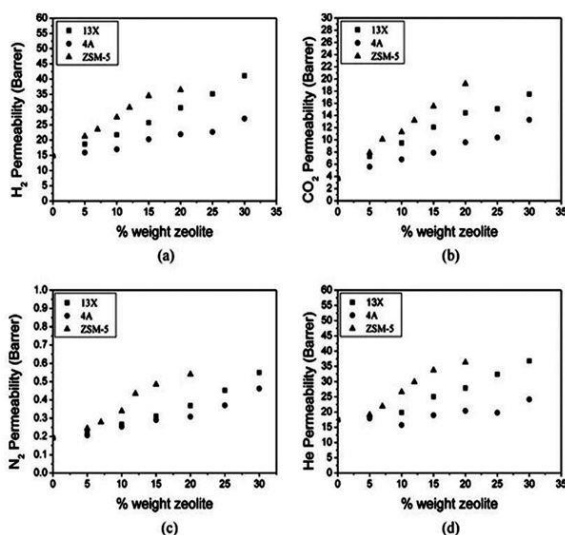


Fig. 24. Effect of zeolites loading on gas permeability of PI-zeolite mixed matrix membranes at $T = 25^{\circ}\text{C}$ and $P_{\text{feed}} = 10$ bar (a) H₂ permeability, (b) CO₂ permeability, (c) N₂ permeability and (d) He permeability [148].

Woo et al. [149] studied the n-butane/i-butane selectivity through poly (1-trimethylsilyl-1-propyne) (PTMSP)/MFI composite membranes. It was revealed that on dispersion of MFI particles in PTMSP gave composite membranes with good butane isomer selectivity. Also, the permeabilities of i-butane and n-butane through the composite were higher than that of the pure polymer membrane. With increasing temperature, permeabilities decreased as mixture selectivity of n-butane/i-butane increased. The highest selectivity was achieved at 150 °C, with the best membrane giving a 56 % increase over the pure polymer coupled with an almost three-fold increase in permeability. The

best results for the separation of n-hexane and 2,2-dimethylbutane was at 200°C, giving more than a 150% increase in permeability and around 40% increase in selectivity over the pure polymer for all the composites.

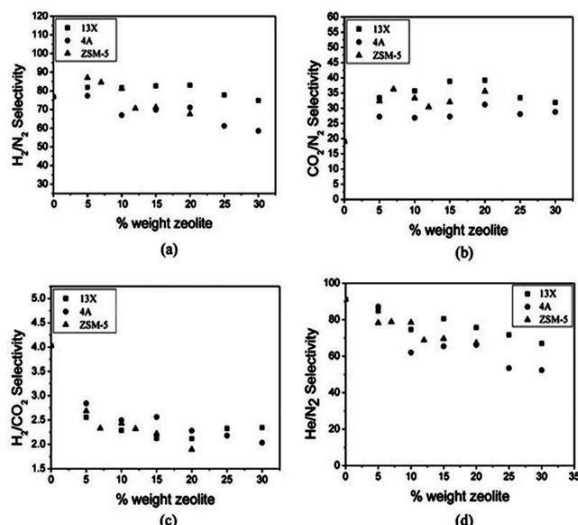


Fig. 25. Effect of zeolite loading on gas pair selectivity of PI-zeolite mixed matrix membranes (a) H₂/N₂ selectivity, (b) CO₂/N₂ selectivity (c) H₂/CO₂ selectivity and (d) He/N₂ selectivity [148].

Hussain and König [150] prepared MMMs by incorporation of zeolite (ZSM-5) filler in a PDMS matrix to separate CO₂ from the gas mixture. MMMs were prepared using the microsieve ZSM-5 and rubbery polymer in different compositions. It was observed that the ideal separation factor for CO₂/N₂ remains constant for all zeolite filled membranes. The permeability of CO₂ and N₂ increased three times in the case of 66% zeolite-filled membrane compared to a pure silicon membrane. At high pressures, high permeance and separation factors were observed for CO₂-N₂ feed gas mixtures. These membranes could be used up to 250 °C.

A ZSM-5 zeolite membrane and a ZSM-5/silicalite bilayer zeolite membrane synthesized on porous alumina supports coated with an yttria stabilized zirconia (YSZ) intermediate barrier layer for membrane stability improvement was fabricated by Wang and Lin [151]. The YSZ intermediate barrier layer was used to prevent diffusion of Al³⁺ from the porous alumina support into the zeolite membrane layer to have a better control of Al³⁺ concentration in MFI zeolite membranes. A thin, high quality ZSM-5 top layer was synthesized on a thick silicalite bottom layer to form a ZSM-5/silicalite bilayer membrane. Both membranes were catalytic cracking deposition (CCD) modified using methyldiethoxysilane (MDES) as the precursor to reduce the zeolitic pore size to improve the H₂/CO₂ separation factor. Compared with the ZSM-5 zeolite membrane, the ZSM-5/silicalite bilayer membrane showed more improvement in H₂/CO₂ separation (from 4.95 to 25.3) and less reduction in H₂ permeance by CCD modification (from 1.85×10^{-7} to 1.28×10^{-7} molm⁻²sPa at 450 °C).

Mixed matrix membranes based on zeolite LTL dispersed in a glassy polyimide, 6FDA-6FpDA, as well as in block copolymers composed of 6FDA-6FpDA and amine terminated polydimethylsiloxane (PDMS) were fabricated by Pechar et al. [23]. Pure gas permeability tests were performed using He, O₂, N₂, CH₄ and CO₂ for each membrane. Permeability was shown to increase for all gases as the siloxane content in the copolymer increased. The addition of zeolite L to the polymer matrix lowered the permeability of all gases regardless of the polymer matrix, and there were no improvements in the ideal selectivity of any gas pairs investigated.

Ismail et al. [152] fabricated MMMs hollow fiber membranes by mixing polyethersulfone (PES) with zeolite 4A, and, by mixing PES with modified zeolite 4A. Modified zeolite 4A was synthesized by treating zeolite 4A with Dynasylan Amino silane coupling agents. The silane coupling agent acts as an interface between an inorganic substrate (zeolite) 4A and an organic material (PES), to bond, or couple these two dissimilar materials. The molecular formula for Dynasylan Amino is H₂N-(CH₂)₃-Si(OC₂H₅)₃.

The silicon in the center is connected to two different functional groups; the organophilic amino group (NH₂) and the ethoxy group (C₂H₅O). Surface treatment of zeolites with the DA silane coupling agent produced silanol groups on the zeolite surface. Scheme 1 (see Figure 26) shows the chemical structure of 3-aminopropyl-triethoxy methyl silane and chemical modification on the zeolite surface.

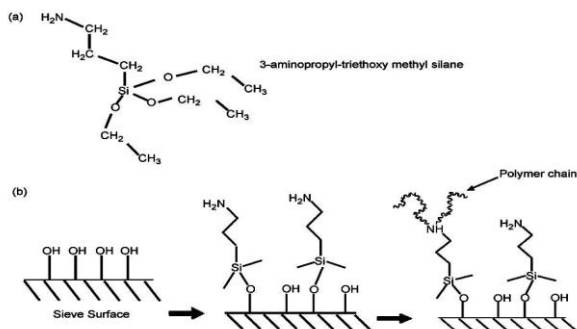


Fig. 26. Scheme 1 (a) Chemical structure of (3-aminopropyl)-triethoxy methyl silane; (b) chemical modification on zeolite surface [152].

The permeabilities of pure gases O₂, N₂, CO₂ and CH₄, and the calculated ideal separation factor for O₂/N₂, CO₂/CH₄ gas pairs for different polymer concentrations of DA silane//PES zeolite MMMs are tabulated in Table 8.

From Table 8, selectivity values for untreated zeolites are very low. This could be due to the presence of severe voids between zeolite particles and agglomeration which was confirmed by SEM. The increase in selectivity with the increase of DA silane was due to the formation of better contact as well as good adhesion between polymer and zeolite phases. Sen et al. [153] enveloped a polycarbonate (PC) zeolite 4A MMMs for the gas separation. Table 9 shows the permeability and selectivity results of dense homogeneous PC membranes and PC-zeolite MMMs.

Table 8
Effect of silane concentration on the gas separation performance of PES-zeolite mixed matrix hollow fiber membranes at room temperature and 10 bar [152].

Membrane	Single gas permeance (GPU)				Selectivity	
	CO ₂	CH ₄	O ₂	N ₂	CO ₂ /CH ₄	O ₂ /N ₂
Untreated	33.77	11.81	8.94	4.19	2.86	2.13
10 wt.% DA silane	20.25	1.32	3.47	1.27	15.43	2.74
10 wt.% DA silane	10.17	0.451	3.03	0.987	22.57	3.07
10 wt.% DA silane	6.67	0.232	2.71	0.567	28.75	4.78

Table 9
Permeability and selectivity results of POC-zeolite 4A MMS (at room temperature) [153].

Zeolite (w/w%)	Permeability (Barrer)				Selectivity			
	N ₂	H ₂	O ₂	CH ₄	CO ₂	H ₂ /N ₂	CO ₂ /N ₂	CO ₂ /CH ₄
0	0.270	15.3	1.80	0.374	8.80	56.7	6.70	32.6
20	0.200	13.4	1.70	0.240	7.80	67.0	8.50	39.0
30	0.179	13.1	1.60	0.186	7.00	73.2	8.90	39.1

Table 9 indicates that, single gas permeabilities through PC-zeolite 4A MMMs are lower than those of pure PC membrane, and the permeability of all studied gases generally decrease with increasing zeolite content. On the other hand, the permeabilities, selectivities of PC-zeolite 4A membranes for H₂, O₂ and CO₂ over N₂, and, CH₄ over CO₂ were higher than the selectivities of pure PC membranes. The permeability and selectivity results of PC-zeolite 4A MMMs indicated an increasing trend toward Robeson's upper bound curve for industrially important gas pairs when compared with the pure PC membrane.

Casado-Coterillo et al. [99] reduced the size of pure ITQ-29 zeolite crystals via varying the seeding, water content and crystallization time and got a good degree of crystallinity. These small particles were dispersed at low loading in commercial polysulfone Udel to form MMMs for gas separation. These membranes showed promising results in the separation of H₂/CH₄ mixtures (highest H₂ permeability 21.9 Barrer and separation factor of 118 for the 4 wt% ITQ-29/polysulfone membrane).

SAPO-5 zeolite was used to modify the structure of polyurethane membranes to improve their properties [18]. The zeolite addition into polyurethane membranes induces an increase in the water flux. The SAPO-5 zeolite acted as a cross-linker on the polyurethane polymer. The SEM study revealed the absence of voids around the zeolites, which suggested that there was a good contact at the interface between the zeolite and polymer.

Adams et al. [53] synthesized a MOF of copper, and terephthalic acid (CuTPA) and made MMMs. CuTPA is the product of the thermal desolvation of CuTPA.DMF (N,N-dimethylformamide). Before desolvation, the carbonyl groups of the DMF molecules associate with the copper atoms of the CuTPA framework as shown in Figure 27.

From synthesized CuTPA, DMF, CuTPA-PVAc (polyvinyl acetate) membrane was prepared. SEM analysis of the cross-section of the membrane (15% CuTPA-PVAc MMM) showed that there was good dispersion and adhesion between the polymer and CuTPA. PVAc is a low Tg polymer and is shown to create defect-free zeolite-polymer MMMs. Figure 28 shows the

average normalized permeabilities of 15% CuTPA-PVAc MMMs for different gases, while Figure 29 shows the averaged normalized gas pair selectivities of 15% CuTPA-PVAc MMMs for different pairs of gases.

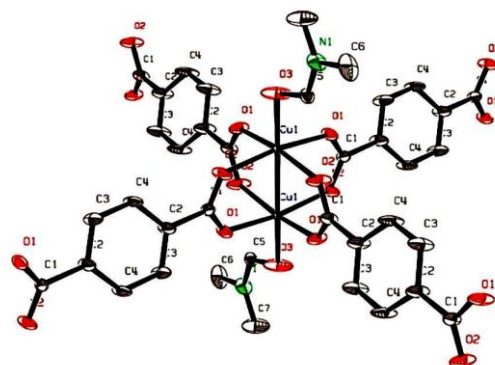


Fig. 27. Stereo-model of CuTPA·DMF [53].

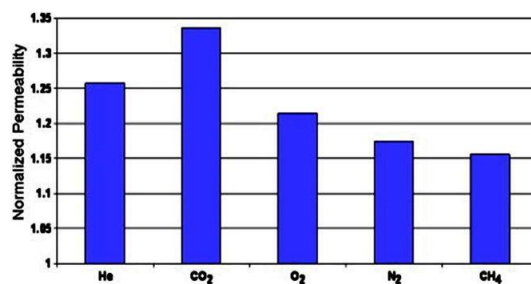


Fig. 28. Averaged normalized permeabilities of 15% CuTPA-PVAc MMMs [53].

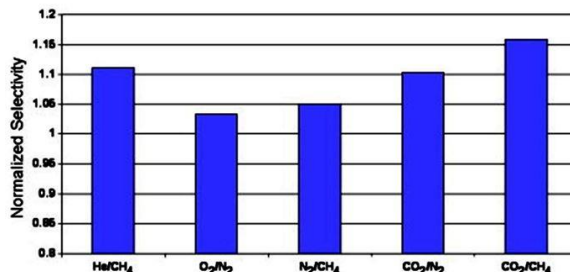


Fig. 29. Averaged normalized gas pair selectivities of 15% CuTPA-PVAc MMMs [53].

Table 10 summarizes the average pure gas permeabilities for pure PVAc and the MMMs, and Table 11 summarizes the selectivities of different pairs of gases.

Pure gas permeabilities and selectivities of 15% CuTPA-PVAc MMMs showed improvements over pure PVAc properties. Careful attention to the permeability trends from gas to gas and the time lag behavior of the MMMs suggested that the MMMs are free of interfacial voids, that the gases have easy access to the CuTPA crystals, and that real mixed matrix effects were noted.

Funk and Lloyd [154] introduced the concept of zeolite-filled microporous mixed matrix membranes named ZeoTIPS. ZeoTIPS membranes, which were formed using the thermally induced phase separation (TIPS) process, consist of zeolite particles supported in a microporous polymer matrix. ZeoTIPS membranes were designed to improve upon the performance of dense mixed matrix membranes for gas and liquid separations and to approach the performance of zeolite membranes while avoiding their drawbacks. They presented a model which can be used to demonstrate the potentiality of these membranes for gas separation applications. Permeation modeling of ZeoTIPS membranes showed the potential for improvement over dense mixed matrix membrane performance when the ZeoTIPS membrane was modeled as a polymer in parallel with zeolite and void in series. The membrane performance was predicted to surpass Robeson's upper bound for gas separation polymers. The greatest improvement was exhibited when the polymer in an ideal ZeoTIPS membrane was impermeable to the species to be separated, in contrast to a mixed matrix membrane, which requires permeability of the polymer. An ideal ZeoTIPS membrane can be predicted to

improve the mixed matrix membrane performance even when the polymer has a higher permeability than the zeolite itself. When the ZeoTIPS membrane structure is non-ideal, as in the case when the polymer coats the zeolite particles, there is a significant increase in selectivity and permeability compared to dense matrix membranes.

New monomers having silica groups as an intermediate for the preparation of siloxane modified poly(imide siloxane)-zeolite 4A and 13X mixed matrix membranes (MMMs) containing amide groups PMDA-[ODA: (DABA/PTMS)] + zeolite (9:1) by using different ratios of zeolite monomers were fabricated by Boroglu and Gurkaynak [155]. The permeation data of gases (O₂ and N₂ through these membranes are given in the following Table 12.

From Table 12, the permeability of all gases for the poly(imide siloxane)-zeolite 4A membranes decreased with an increase in zeolite loading. It was revealed that the zeolites were well distributed throughout the membrane and the zeolites and polymer had good contact at the interface.

Table 10

Averaged gas permeabilities ± 1 standard deviation (in Barrers) of pure PVAc and 15% CuTPA-PVAc MMMs [53].

	P _{He}	P _{O₂}	P _{N₂}	P _{CH₄}	P _{CO₂}
PVAc	15.1 \pm 0.8	0.514 \pm 0.034	0.0783 \pm 0.0064	0.0697 \pm 0.0034	2.44 \pm 0.32
MMMs	19.0 \pm 0.5	0.624 \pm 0.026	0.912 \pm 0.0032	0.0806 \pm 0.0035	3.26 \pm 0.23

The permeation of water vapor, CO, H₂, and CH₄ and their binary mixtures through a thin zeolite-4A membrane was studied by Zhu et al. [156]. It was reported that the zeolite-4A membrane synthesized with pre-treatment of the supporting TiO₂ with UV-photons exhibited a high permeance property and maintains high selectivity for water. The permeance of water vapor in the binary mixtures was almost the same as its unary permeance and only weakly temperature dependent. The permeances of the gaseous components were strongly suppressed by water, resulting in high selectivities for water removal in the presence of these gases. This was due to the high adsorption affinity and capacity of water inside the zeolite 4A cages, preventing the bypassing of the second component through the membrane.

It was demonstrated that a novel p-xylenediamine/methanol soaking method could efficiently remove the polymer-zeolite interface defects of the mixed-matrix structure [131]. The mixed-matrix structure was in the form of an ultrathin (1.5-3 μ m) polysulfone/zeolite beta mixed-matrix layer that was supported by a neat Matrimid[®] layer in a dual-layer composite hollow fiber. The SEM study showed that the particle and polymer phases had a distinct boundary, whereas in p-xylenediamine/methanol treated was none. The ideal selectivities of the mixed-matrix hollow fibers treated with p-xylenediamine/methanol (30 wt % zeolite) for O₂/N₂ and CO₂/CH₄ was about 30 and 50% superior to that of the neat PSf Matrimid[®] hollow fibers, respectively. The selectivity was much greater than that suggested by Knudsen diffusion, which was due to a less defective structure, which might arise from removal of the polymer-particle defects by p-xylenediamine priming.

Table 11

Averaged gas permeabilities ± 1 standard deviation (in Barrers) of pure PVAc and 15% CuTPA-PVAc MMMs [53].

	$\alpha_{\text{He/CH}_4}$	$\alpha_{\text{O}_2/\text{N}_2}$	$\alpha_{\text{N}_2/\text{CH}_4}$	$\alpha_{\text{CO}_2/\text{N}_2}$	$\alpha_{\text{CO}_2/\text{CH}_4}$
PVAc	212 \pm 1.75	6.57 \pm 0.143	1.09 \pm 0.0433	32.1 \pm 1.36	34.9 \pm 2.86
MMMs	237 \pm 11.8	6.79 \pm 0.136	1.14 \pm 0.0191	35.4 \pm 1.68	40.4 \pm 2.45

Table 12

Gas permeation data of poly(imide siloxane)-zeolite mixed matrix membrane (PMDA-[ODA:(DABA/PTMS)] (9:1) = M) [53].

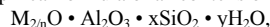
Polyimide membranes	P _{O₂} (Barrer)	P _{N₂} (Barrer)	$\alpha_{\text{O}_2/\text{N}_2}$
M	0.96	0.17	5.64
M + % 5 zeolite 4A	0.93	0.12	7.81
M + % 10 zeolite 4A	0.92	0.12	7.80
M + % 15 zeolite 4	0.85	0.10	8.05
M + % 2 zeolite 13X	2.06	1.74	1.18
M + % 10 zeolite 13X	2.05	1.80	1.14

Ozturk and Demirciyeva [157] introduced zeolite 3A, 4A and 5a within polyimide (PI) and polyetherimide (PEI) to make composite membranes. The effects of annealing temperature, zeolite loadings, feed pressures and mixed gas and biogas feeding on the separation of CO₂-CH₄ by membranes were investigated. It was observed that the MMMs prepared by introducing zeolite 4A into PI were a suitable candidate for CO₂/CH₄ separation and/or methane enrichment from biogas. The results revealed that there is a partial relation between gas permeability and sorption capacity of the membrane used. Biogas separation showed that the CO₂ content in the permeated gas increased as much as 95% at 3 bar feed pressure. The highest CO₂ content in the permeated gas was obtained when PI/4a-MMM was used, and followed by

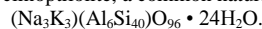
PI/3A, pure PI, PI/5A, PEI/4A and PEI/3A. Table 13 shows few researches of MMMs [158].

7. Ion exchange zeolite membranes

Zeolites are crystalline, hydrated aluminosilicates of alkali and alkaline earth metals, having infinite, three-dimensional atomic structures. They are further characterized by the ability to lose and gain water reversibly and to exchange certain constituent atoms, also without a major change of atomic structure. Along with quartz and feldspar minerals, zeolites are three-dimensional frameworks of silicate (SiO₄) tetrahedra in which all four corner oxygen's of each tetrahedron are shared with adjacent tetrahedra. If each tetrahedron in the framework contains silicon as its central atom, the overall structure is electrically neutral, as is quartz (SiO₂). In zeolite structures, some of the quadric-charged silicon is replaced by triply-charged aluminium, giving rise to a deficiency of positive charge. The charge is balanced by the presence of singly- and doubly-charged atoms, such as sodium (Na⁺), potassium (K⁺), calcium (Ca²⁺), and magnesium (Mg²⁺), elsewhere in the structure. The empirical formula of a zeolite is of the type:



where M is any alkali or alkaline earth atom, n is the charge on that atom, x is a number from 2 to 10, and y is a number from 2 to 7. The chemical formula for clinoptilolite, a common natural zeolite is:



Atoms or cations (i.e., charged metal atoms) within the second set of parentheses are known as structural atoms, because with oxygen they make up the rigid framework of the structure. Those within the first set of parentheses are known as exchangeable ions, because they can be replaced (exchanged) more or less easily with other cations in aqueous solution, without affecting the aluminosilicate framework. This phenomenon is known as ion exchange, or more commonly cation exchange. The exchange process involves replacing one singly-charged exchangeable atom in the zeolite by one singly-charged atom from the solution or replacing two singly-charged exchangeable atoms in the zeolite by one doubly-charged atom from the solution. The magnitude of such cation exchange in a given zeolite is known as its cation-exchange capacity (CEC) and is commonly measured in terms of moles of exchangeable cation per gram (or 100 grams) of zeolite or in terms of equivalents of exchangeable cations per gram (or 100 grams) of zeolite.

Very high affinity for polar molecules. The effects of metal balancing cation in zeolite structure on gas adsorption depend primarily on the size and shape of the gas molecules, the size of cation and its location in the channel, and its interaction with the gas molecules. Zeolite modification such as the cation exchanged technique is used to determine the effect of different cation on gas adsorption characteristics.

Zhu et al. [159] studied the structural response of MFI, FAU, and LTA type zeolite powders to the presence of cations commonly found in sea salts including Na⁺, K⁺, Ca²⁺, and Mg²⁺. The results obtained from ion adsorption testing and X-ray powder diffraction showed that the zeolites interacted with monovalent and divalent cations, and these interactions altered the crystal dimensions of the zeolites. The changes in structure could possibly affect diffusion properties of these materials when used as membranes for desalination.

LTA and MFI membranes were also studied for desalination via pervaporation [160]. Membranes were hydrothermally grown on the surface of an α -alumina porous support. The synthesized membranes were used for removal of cationic and anionic species from aqueous solutions by the pervaporation method. The separation factors obtained were 7081 and 105 for NaA and ZSM-5 membranes, respectively. Both membranes effectively removed (more than 99 wt %) I⁻, CS⁺ and Sr²⁺ from their single salt solutions (0.001 mol dm³) over a temperature range of 298-338 K. Malekpour et al. [160] suggested that this method has the ability to desalinate harsh environment solutions involving strong solvent and radioactive components.

H-SAPO-34 crystals and membranes were ion exchanged with various cations (Li⁺, Na⁺, K⁺, NH₄⁺, Cu²⁺) in anhydrous solutions without damaging the crystal structure or membrane integrity [161]. For SAPO-34 crystals, ion exchange decreased the pore volume when some ions were exchanged and changed adsorption properties. The H₂, CO₂, and CH₄ permeances decreased through SAPO-34 membranes after exchange, and H₂/CH₄ and CO₂/CH₄ ideal and separation selectivities increased because of changes in adsorption and diffusion properties. The decrease in gas permeances was larger for exchange with the largest cations, K⁺ and NH₄⁺.

Hasegawa et al. [162] separated the CO₂-CH₄ and CO₂-N₂ system by using ion exchanged FAU-type zeolite membranes with different Si/Al ratios. They prepared FAU-type zeolite membranes with different Si/Al ratios on the outer surface of α -Al₂O₃ support tubes by means of a hydrothermal synthesis.

Table 13
Few researches of MMMs [158].

Mixed matrix membrane		
Organic	Zeolite	Observation
PDMS	Silicate-1 13X	Enhanced the separation performance of poorly selective rubbery membrane for the CO ₂ /CH ₄ .
EPDM	KY	Zeolite-5A showed no change in gas selectivity with decrease permeability due to impermeable characteristic towards CO ₂ .
CA	zeolite -5A Silicalite	Did in fact reverse the selectivity of CA membrane from H ₂ to CO ₂ for CO ₂ /H ₂ separation
	NaX AgX	
Polyvinyl acetate	4A	Formation of chemical bonds has good adhesion, but there is still nonselective: leakage ^o from the existence of nanometric region.
PES	4A	Due to low mobility of polymer chain in glassy polymer such as to prevent them to complete cover the zeolite surface which resulted in void interface
PI, Polycarbonate	13X 4A	

Table 14
Recent studies on different zeolites/zeolitic membranes (mainly for gas separation).

Zeolite membranes embrates	Used for	Ref.
Zeolite X	Pervaporation	[14]
Zeolite nanosheets of the MWW and MFI structure type	Separation of xylene isomers, He/H ₂ , He/N ₂	[18]
SAPO-44	H ₂ /N ₂ , H ₂ /CO	[19]
Amino-functionalized SAPO-34	CO ₂ /CH ₄ , CO ₂ /N ₂	[22]
ZIF-8	CO ₂ /CH ₄	[22]
Zeolite L MMMs	He, CO ₂ , CH ₄ , O ₂ , N ₂	[23]
Ion-exchanged SAPO-34	Light gas separation	[24]
H-SAPO-34		
AIPO-18	CO ₂ /CH ₄	[24]
Zeolite A imidazolate frameworks	Capture of CO ₂ from binary mixtures with CH ₄ , N ₂ , O ₂	[25]
Ion-exchanged FAU	CO ₂ /CH ₄ , CO ₂ /N ₂	[27]
MFI	Desalination	[28]
ZIF-69	CO ₂ /CO mixture	[29]
MER	Dehydration	[33]
LTA	H ₂ , H ₂ /N ₂ , H ₂ /C ₃ H ₈	[34]
MFI	Butane isomers separation	[36]
NaA	H ₂ , N ₂ , O ₂ , C ₃ H ₈	[41]
Natural zeolite	H ₂ , CO ₂	[61]
DDR	He, H ₂ , CO ₂ , CO, CO ₂ /CH ₄	[30, 31, 66, 68]
ZSM-5	H ₂ /CO ₂ , H ₂ /SF ₆	[81, 83]
Ion-exchanged ZSM-5	CO ₂ , He, H ₂ , SF ₆ , <i>n</i> -C ₄ H ₁₀ , <i>i</i> -C ₄ H ₁₀	[84]
ZIF-7	H ₂ /CO ₂ , H ₂ /N ₂ , H ₂ /CH ₄	[87]
T	H ₂ , CO ₂ , O ₂ , N ₂ , CH ₄ , C ₂ H ₆ , C ₃ H ₈ , CO ₂ /N ₂ , CO ₂ /CH ₄	[93]
UZM-5	Liquid separation such as deep desulfurization of gasoline and diesel fuels, ethanol/water separation, and pervaporation dehydration of aqueous/organic mixtures, as well as for a variety of gas and vapor separation	[104]
FAU	CO ₂ /N ₂	[108]
Faujasite (FAU)	Simulation of O ₂ /N ₂	[115, 116]
LTA-FAU composite	H ₂ , CO ₂ , N ₂ , CH ₄ , C ₃ H ₈	[119]
W	O ₂ /SF ₆	[126]
Hydroxysodalite	RO, waste water treatment. H ₂ / <i>n</i> -C ₄ H ₁₀	[128, 129]
Bio-MOF-1	CO ₂ /CH ₄	[133]
Zeolite β MMMs	O ₂ /N ₂ , CO ₂ /CH ₄	[147]
Ag and Cu ion exchanged faujasites	H ₂ S adsorption	[163, 164]
MFI	H ₂ /CO ₂ , H ₂ /CO ₂ /H ₂ O (ternary mixtures)	[169]
MFI	CO ₂ /CH ₄ , H ₂ /CO ₂	[170, 171]
SAPO-34	CO ₂ /H ₂ , H ₂ /CH ₄ , CO ₂ /CH ₄ , <i>i</i> -C ₄ H ₁₀	[75, 76, 172, 173, 174, 175]
Na A	Single gas permeation, pervaporation, vapor permeation,	[113, 176]
4A zeolite filled sodium alginate membrane	Pervaporation	[177]
Ion-exchanged faujasite-type zeolite	CO ₂ /N ₂	[178]
Beta zeolite	Adsorption separation of N ₂ , O ₂ , CO ₂ , CH ₄	[179]
HSSZ-13 MMMs	O ₂ /N ₂ , He/N ₂ , CO ₂ /CH ₄	[180]
ZIF-7-MMCMs	CO ₂ , N ₂ , CH ₄	[181]
MOF-5	H ₂ , N ₂ , CH ₄ , CO ₂ , SF ₆	[27, 182]
ZSM-5	Organic vapor separation	[183]
Zeolite Y filled PDMS	Sorption and pervaporation of aroma compounds	[184]

The membranes were ion-exchanged with Rb⁺ and K⁺ ions, and the permeation properties were investigated by using equimolar mixtures of CO₂-CH₄ and CO₂-N₂ at 308 K. Permeances for single-component systems at a temperature of 308 K were in the order of CO₂>N₂>CH₄, and decreased with decreasing Si/Al ratio. Permeances and selectivities of CO₂ for the CO₂-CH₄ system were approximately half the values obtained for the CO₂-N₂ system. The NaX(1)-type zeolite membrane showed the maximum CO₂ selectivities, which were 28 for the CO-CH₄ system and 78 for the CO₂-N₂ system. In an attempt to increase the CO₂ selectivity, the incorporated Na⁺ ions were exchanged with Rb⁺. The effect of the ion-exchange was the highest for the NaY-type zeolite membrane. The CO separation ability of the NaY-type zeolite membrane was further improved by ion exchange with K⁺. The CO₂/CH₄ selectivity of the KY-type zeolite membrane was in the range of 20-40 and the CO₂ permeance was in the range of (7.5-90)×10⁻⁷ mol.m⁻².s⁻¹.Pa⁻¹.

Tsapatsis group [163] studied the H₂S adsorption from dilute streams containing He, N₂, CO₂, CO and H₂O by using Ag and Cu ion exchanged faujasites and zeolite X and Y in sodium form. Ag and Cu exchanged zeolites demonstrated very high H₂S adsorption capacities at room temperature and 150 °C in H₂S/He mixtures. The Ag form of zeolite X and Y were able to remove H₂S in the presence of all gases. CuX and CuY were efficient in removing H₂S in the presence of N₂, CO₂ and water vapor at 150 °C but failed to remove H₂S in the presence of 2% CO. It was concluded that AgY is the most promising adsorbent for H₂S.

Kamarudin et al. [164] modified the zeolite by the cation exchanged technique and studied the effect of different cations on gas adsorption characteristics. It was observed that at very low concentration of adsorbed gas, the type of cation influences the adsorption characteristics, where divalent cations adsorb more gas than monovalent cations exchanged zeolite. At higher concentration of adsorbed gas, the effect of cation is insignificant.

However, different gases adsorb differently depending on the adsorbate-adsorbent interactions.

Liu and Cen [165] fabricated two types of zeolite with different wetting properties, the hydrophilic FAU and hydrophobic MFI as the RO membrane. Both can reach nearly 100% rejection of salt ions and when the membrane thickness is smaller than 3.5 nm, then the permeability was about 2×10^{-9} m/Pa.s which was two orders higher than the commercial state-of-the-art. For both FAU and MFI zeolites, few sodium ions can enter the nanopores whereas the chloride ions cannot. This effectively blocks salt ions from entering the clean water region, and maintaining high permeability to water molecules. The pressure drop was inversely proportional to water molecules. The pressure drop was linearly dependent on the thickness of the zeolite membrane.

8. Large size experiment

Despite 25 years of intense R&D on the development of zeolite membranes, there are only few pilot plants in operation, mainly dewatering of bio-ethanol and i-propanol using hydrophilic LTA membranes.

The first large-scale pervaporation plant, which produces 530 l/h of solvents (EtOH, IPA, MeOH, etc.) at less than 0.2 wt.% of water from 90 wt.% solvent at 120 °C, has been put into industrial operation in 2000 by Mitsui Engineering and Shipbuilding Co. Ltd. [166]. The plant is equipped with 16 modules, each of which consists of 125 pieces of NaA zeolite membrane tubes. However, the excellent water separation is based on the strong hydrophilic nature of the LTA membrane and not on molecular sieving [167].

Jiuyu High Tech Co. of China claims that they have sold more than 100 systems based on zeolite membranes for solvent dehydration. The company has 60% of the membrane market for such applications in China (ICOM 2014, Suzhou, China) [168].

9. Summary

Zeolites have unique properties such as thermal and chemical stability, shape selective separation, etc. The disadvantages associated with zeolite membranes are their cost and complex fabrication procedure. Thin and compact zeolite membranes without support invasion should offer high flux and selectivity simultaneously, which is necessary in industrial applications. But the thinness increases zeolite membrane fragility, which hinders potential incorporation into a module, which is a big challenge.

Despite much progress in the development of zeolite molecular sieve membranes, there is no industrial gas separation by zeolite membranes, with the exception of the de-watering of bio-phenol by steam permeation using LTA membranes [11]. In the last ten years, a study on the MOF (metal organic framework) for gas separation revealed that MOF membranes show improved performance in comparison with the pure polymer membranes. MOFs possess a combination of organic and inorganic building blocks that give them enormous flexibility in pore size, shape, and structure when compared with zeolite. The porosity of MOFs is 90% higher than in zeolites and research has shown that some of them are thermally stable, even in the presence of steam, up to 400 °C [31]. As different forms of zeolites are organic-inorganic material, the MOF nanoparticles can be easily embedded into organic polymers and can be applied in industries. In pervaporation, the zeolite membrane has been more successful in dehydrating organic compounds than in removing organic compounds from water. This is mainly due to the high hydrophilicity of A-type zeolite membranes.

In recent years, there has been much development in the areas of zeolite membranes, and its use in industrial-scale development is still not predicted for the near future. However, the only industrial application of the zeolite membrane is in solvent dehydration, which is a decade old.

Membranes made from zeolites, crystalline materials with precisely defined pores in the size range of molecules (angstroms to nanometers) are a promising material which achieves highly selective separations based on molecular recognition by the membrane pores. However, small-pore hydrophilic zeolite membranes for the dehydration of solvents and biofuels can be found in several small to medium scale industrial plants. Zeolite membranes have been too expensive to replace competing technology for many other applications.

The molecular simulations could serve as a useful screening tool to determine the suitability of a membrane for potential separation applications. Table 14 shows recent studies on different zeolites/zeolitic membranes, mainly for gas separation.

10. Future works

More studies on the economic feasibility of zeolite membrane processes, long-term stability of membranes and up scaling are needed. Further improvements especially in cost reduction and membrane reliability should still be endeavored to facilitate the wide introduction of zeolite-based membrane for separation into industrial practice. Researchers will focus their work on developing thinner zeolite membranes (membranes) with a hierarchical approach, in which nanoscale zeolite crystals or fragments of these structures are assembled into larger porous networks to compete with the present technology. In addition, the relatively high price of membrane units, the difficulty of controlling the membrane thickness, permeance, high-temperature sealing, reproducibility and the dilemma of up scaling can be addressed in the future.

Polymeric membranes were one of the fastest growing fields of membrane technology, but they could not meet the separation performances required especially in higher operating pressures due to deficiencies problem. Mixed matrix membranes (MMMs) which comprises polymeric and inorganic membranes presents an interesting approach for enhancing the separation performance. MMMs is yet to be commercialized as the material combinations are still in the research stage. Material selection and method of preparation are the most important part in fabricating a membrane. The main problem in fabricating the MMMs membranes is removing voids at the interface of the particle and polymer. Extensive and intensive work has been carried out to promote adhesion between the rigid polymer chains and molecular sieves. These works include thermal treatment, silane coupling agents, integral chain linkers, and polymer coating on the molecular sieve surface. However, it is still a challenge for the researchers with different types of MMMs membrane fabrication.

References

- [1] E. Roland, P. Kleinschmit, Zeolites, Ullmann's Encyclopedia of Industrial Chemistry, Wiley-VCH Verlag GmbH & Co. Weinheim, Germany 2012.
- [2] R. M. Barrer, Chemical nomenclature and formulation of compositions of synthetic and natural zeolites Pure Appl. Chem. 51 (1979) 1091-1100.
- [3] C. Baerlocher, L. McCusker, D. H. Olson, Atlas of Zeolite Framework Types, 6th Revised edn, Elsevier, Amsterdam, and previous editions 2007.
- [4] W. M. Meier, D.H. Olson, Atlas of Zeolite Structure Types, 2nd Revised edn, Butterworth and Co Ltd, University Press, Cambridge, UK, 1988.
- [5] D. S. Coombs, A. Alberti, T. Armbruster, G. Artioli, C. Colella, E. Galli, J.D. Grice, F. Liebau, J. A. Mandarino, H. Minato, E. H. Nickel, E. Passaglia, D. R. Peacor, S. Quartieri, R. Rinaldi, M. Ross, R. A. Sheppard, E. Tillmanns, G. Vezzalini, Recommended nomenclature for zeolite minerals: Report of the subcommittee on zeolites of the International Mineralogical Association, Commission on new minerals and mineral names. Can. Mineral. 35 (1997) 1571-1606.
- [6] Nanoporous Materials Gordon Research Conference (2008), June 15-20, Colby College, Waterville, ME.
- [7] B. A. Tavolaro, E. Drioli, Zeolite membranes, Adv. Mater. 11 (1999) 975-996.
- [8] J. A. Ritter, A. D. Ebner, State-of-the-art adsorption and membrane separation processes for hydrogen production in the chemical and petrochemical industries. Separation Science & Technology, 42 (2007) 1123-1193.
- [9] M. Nomura, T. Yamaguchi, S. Nakao, Silicalite membranes modified by counterdiffusion CVD technique, Ind. Eng. Chem. Res. 36 (1997) 4217-4223.
- [10] B. Topuz, M. Çiftçioglu, Permeation of pure gases through silica membranes with controlled pore structures, Desalination 200 (2006) 80-82.
- [11] M.P. Pina, R. Mallada, M. Arruebo, M. Urbiztondo, N. Navascués, O. J. de la Iglesia, J. Santamaría, Zeolite films and membranes. Emerging applications, Microp. Mesop. Mater. 144 (2011) 19-27.
- [12] J. Caro, Are MOF membranes better in gas separation than those made of zeolites? Current Opinion in Chemical Engineering, 1(1) (2011) 77-83.
- [13] P. Worathanakul, P. Kongkachuichay, World Academy of Science, Engineering and Technology 47 (2008) 90-93.
- [14] H. Zhou, D. Korelskiy, T. Leppäjärvi, M. Grahn, J. Tanskanen, J. Hedlund, Ultrathin zeolite X membrane for pervaporation dehydration of ethanol, J. Membr. Sci. 399-400 (2012) 106-111.
- [15] M.M.H. Htun, M.M. Htay, M. Z. Lwin, Preparation of zeolite NaX, (Faujasite) from pure silica and alumina sources. Int. Con. Chem. Envir. Issues. Iccel, 2012, July 15-16, Singapore, 2012.
- [16] H. Maghsodloord, S.Y. Mirfendereski, T. Mohammadi, A. Pak, Effects of gel parameters on the synthesis and characteristics of W-type zeolite nanoparticles, Clays and Clay Minerals 59 (2011) 328-335.
- [17] V.A. Tuan, L.L. Weber, J. L. Falconer, R. D. Noble, Synthesis of B-substituted β -zeolite membranes, Ind. Eng. Chem. Res. 42 (2003) 3019-3021.
- [18] G. Ciobanu, G. Carja, O. Ciobanu, Structure of mixed matrix membranes made of polyurethane matrix, Micro. Meso. Mater. 115 (2008) 61-66.
- [19] Z. Liu, Z. Lin, L. Cheng, Synthesis and separating performance of SAPO-44 zeolite membrane, Chinese Chemical Lett. 16 (2005) 413-415.
- [20] S. Li, J.L. Falconer, R.D. Noble, Improved SAPO-34 membranes for CO₂/CH₄ separation, Adv. Mater. 18 (2006) 2601-2603.
- [21] L. Yue, M. Zhu, H. Su, X. You, C. Deng, X. Lv, Effects of synthesis parameters on hydrothermal of NaA zeolite, Adv. Mat. Res. 148-149 (2011) 144-148.

- [22] R.S. Venna, A. Carreon, Highly permeable zeolite framework-8 membranes for CO₂/CH₄ separation, *J. Am. Chem. Soc.* 132 (2010) 76-78.
- [23] T.W. Pechar, S. Kim, B. Vaughan, E. Marand, M. Tsapatsis, H. K. Jeong, C. J. Cornelius, Fabrication and characterization of polyimide-zeolite L mixed matrix membranes for gas separations, *J. Membr. Sci.* 277 (2006) 195-202.
- [24] M.L. Carreon, S. Li, M.A. Carreon, AlPO-18 membranes for CO₂/CH₄ separation, *Chem. Commun.* 48 (2012) 2310-2312.
- [25] R. Banerjee, H. Furukawa, D. Britt, C. Knobler, M. O'Keeffe, O. M. Yaghi, Control of pore size and functionality in isorecticular zeolitic imidazolate frameworks and their carbon dioxide selective capture properties, *J. Am. Chem. Soc.* 131 (2009) 3877-3875.
- [26] P. Worathanakul, P. Kongkachuchay, New SUZ-4 zeolite membrane from sol-gel technique, *World Academy of Science, Engineering and Technology* 2 (2008) 11-21.
- [27] Y. Liu, Z. Ng, E. A. Khan, H. K. Jeong, C-b. Ching, Z. Lai, Synthesis of continuous MOF-5 membranes on α -alumina substrate, *Micro. Meso. Mater.* 118 (2009) 296-301.
- [28] M. Kazemimoghdam, T. Mohmmadi, Synthesis of MFI zeolite membrane for water desalination, *Desalination* 206 (2007) 547-553.
- [29] Y. Liu, E. Hu, E.A. Khan, Z. Lai, Synthesis and characterization of ZIF-69 membranes and separation, *J. Membr. Sci.* 353 (2010) 36-40.
- [30] T. Tomita, K. Nakayama, H. Sakai, Gas separation characteristics of DDR type zeolite membrane, *Micro. Meso. Mater.* 68 (2004) 71-75.
- [31] S. Himeno, T. Tomita, K. Suzuki, K. Nakayama, K. Yajima, S. Yoshida, Synthesis and permeation properties of DDR-Type zeolite membrane for separation CO₂/CH₄ gas mixture, *Ind. Eng. Chem. Res.* 46 (2007) 6989-6997.
- [32] H. Van. Koningsveld, H. Gies, Similarities between the clathrasils DOH, DDR, MEP and MTN, *Z. Kristallogr.* 219 (2004) 637-643.
- [33] Y. Hasegawa, T. Nagase, Y. Kiyozumi, F. Mizukami., Preparation, characterization, and dehydration of MER-type zeolite membranes, *Sep. Purif. Tech.* 73 (2010) 25-31.
- [34] Y. Li, H. Chen, J. Liu, W. Yang, Microwave synthesis of LTA zeolite membranes without seeding, *J. Membr. Sci.*, 277 (2006) 230-239.
- [35] K. Horri, K. Tanaka, K. Kita, K. Okamoto, *Proc. 26th Autumn Meeting of Soc. Chem. Eng. Japan*, 1994 pp. 99.
- [36] M. P. Bernal, G. Xomeritakis, M. Tsapatsis, Tubular MFI zeolite membranes made by secondary (seeded) growth, *Catalysis Today*, 67 (2001) 101-107.
- [37] J. Caro, M. Noack, Zeolite membranes – Recent developments and progress, *Micro. Meso. Mat.* 115 (2008) 215-233.
- [38] G.A. Tompsett, W.C. Conner, K. S. Yngvesson Microwave synthesis of nanoporous materials, *ChemPhyChem.* 7 (2006) 296-319.
- [39] Y. Li, W. Yang, Microwave synthesis of zeolite membranes: A review, *J. Membr. Sci.* 316 (2008) 3-17.
- [40] C.S. Cundy, Microwave techniques in the synthesis and modification of zeolite catalysts, *A Review, Collect. Czech. Chem. Commun.* 63 (1998) 1699-1723.
- [41] Z. L. Cheng, Z. Liu, H. L. Wan, Microwave-heating synthesis and gas separation performance of NaA zeolite membrane, *Chinese J. Chem.* 23 (2005) 28-31.
- [42] J. Choi, H. K. Jeong, M.A. Snyder, J. A. Stoeger, R.I. Masel, M. Tsapatsis, Grain boundary defect elimination in a zeolite membrane by rapid thermal processing, *Science* 325(5940) (2009) 590-593.
- [43] M.K. Naskar, D. Kundu, M. Chatterjee, Silicalite-1 zeolite membranes on unmodified and modified surfaces of ceramic supports: A comparative study, *Bull. Mater. Sci.* 32(5) (2009) 537-541.
- [44] L.T.Y. Au, W.Y. Mui, P.S. Lau, C. Tellez, K.L. Yeung, Engineering the shape of zeolite crystal grain in MFI membrane and their effects on the gas permeation properties, *Micro. Meso. Mater.* 47 (2001) 203-216.
- [45] W.C. Wong, L.T.Y. Au, C.T. Ariso, K.L. Yeung, Effects of synthesis parameters on the zeolite membrane growth, *J. Membr. Sci.* 191 (2001) 143-163.
- [46] J.L.H. Chau, C. Tellez, K. L. Yeung, K. Ho, The role of surface chemistry in zeolite membrane formation, *J. Membr. Sci.* 164 (2000) 257-275.
- [47] K. Varoon, X. Zhang, B. Elyassi, D. B. Brewer, M. Gettel, S. Kumar, J. A. Lee, S. Maheshwari, A. Mittal, C. Y. Sung, M. Cococcioni, L. F. Francis, A. V. McCormick, A. Mkhoyan, M. Tsapatsis, Dispersible exfoliated zeolite nanosheets and their application as a selective membrane, *Science* 334 (2011) 72-75.
- [48] L. Liu, M. Cheng, D. Ma, G. Hu, X. Pan, X. Bao, Synthesis, characterization, and catalytic properties of MWW zeolite with variable Si/Al ratios, *Micro. Meso. Mater.* 94 (2006) 304-312.
- [49] K. Aoki, K. Kusakabe, S. Morooka, Separation of gases with an A-type zeolite membrane, *Ind. Eng. Chem. Res.* 39 (2000) 2245-2251.
- [50] K. Shqau, J. C. White, P. K. Dutta, H. Verweij, Modified zeolite Y membranes for high-performance CO₂ separation, *US 20110247492*, 2011.
- [51] E.L. First, C.E. Gounaris, J. Wei, C. A. Floudas, Computational characterization of zeolite porous networks: an automated approach, *Phys. Chem. Chem. Phys.* 13 (2011) 17339-17358.
- [52] M.O. Daramola, E.F. Aransiola, T.V. Ojumu, Potential applications of zeolite membranes in reaction coupling separation processes, *Materials* 5 (2012) 2101-2136.
- [53] R. Adams, C. Carson, J. Ward, R. Tannenbaum, W. Koros, Metal organic framework mixed matrix membranes for gas separations, *Micro. Meso. Mater.* 131 (2010) 13-20.
- [54] A. Bétard, H. G. Bux, S. Henke, D. Zacher, J. Caro, R. A. Fischer, Fabrication of a CO₂-selective membrane by stepwise liquid-phase deposition of an alkyl ether functionalized pillared-layered metal-organic framework [Cu₂L₂P]_n on a macroporous support, *Micro. Meso. Mater.* 150 (2012) 76-82.
- [55] W. Y. Jin, D. G. Cheng, F. Q. Chen, X. L. Zhan, Synthesis of MFI-type zeolite membrane encapsulated activated carbon particles using a modified seeded method, *Acta Phys. Chim. Sin.* 29 (2013) 139-143.
- [56] M.W. Ackley, S. U. Rege, H. Saxena, Application of natural zeolites in the purification and separation of gases, *Micro. Meso. Mater.* 61 (2003) 25-42.
- [57] L. B. Sand, F. A. Mumpton, (Eds.) *Natural zeolites: occurrence, properties, use*, Pergamon Press, Oxford, 1978.
- [58] G. V. Tsisitshvili, T. G. Andronikashvili, G. N. Kirov, L. D. Filizova, *Natural Zeolites*, Ellis Horwood, New York, 1992.
- [59] W. An, P. Swenson, L. Wu, T. Walker, A. Ku, S.M. Kuznicki, Selective separation of hydrogen from C₁/C₂ hydrocarbons and CO₂ through dense natural zeolite membranes, *J. Membr. Sci.* 369 (2011) 414-419.
- [60] P. Swenson, B. Tanchuk, A. Gupta, W. An, S. M. Kuznicki, Pervaporative desalination of water using natural zeolite membranes, *Desalination* 285 (2012) 68-72.
- [61] S.A.H. Hejazi, A.M. Avila, T.M. Kuznicki, A. Weizhu, S.M. Kuznicki, Characterization of natural zeolite membranes for H₂/CO₂ separations by single gas permeation, *Ind. Eng. Chem. Res.* 50 (2011) 12717-12726.
- [62] V.P. Moreno, J.J.C. Arellano, H.B. Ramirez, Characterization and preparation of porous membranes with a natural Mexican zeolite, *J. Phys. Condense. Matter* 16 (2004) S2345-S2352.
- [63] E. Ajenifuja, O.O. Akinwunmi, M.K. Bakare, J.A. Ajao, I.F. Adeniyi, E. O.B. Ajay, Remediation of polluted water using natural zeolitic aluminosilicates/lateritic clay ceramic matrix membrane, *ISRN Ceramics* 2012 (2012), Article ID 672601, 11 page.
- [64] H. Gies, Studies on clathrasils IX: Crystal structure of deca-dodecasil 3R, the missing link between zeolites and clathrasils, *Z. Kristallogr.* 175 (1986) 93-104.
- [65] K. Nakayama, K. Suzuki, M. Yoshida, T. Tomita, Gas separation of carbon dioxide gas from a mixed gas, or ethylene and ethane from each gas, oxygen or nitrogen from air; silica main component; filters, separators; permselectivity, high strength, noncracking. *US 7014680 B2*, 2006.
- [66] M. Kanezashi, J. O'Brien-Abraham, Y.S. Lin, K. Suzuki, Gas permeation through DDR-type zeolite membranes at high temperatures, *AIChE. J.* 54 (2008) 1478-1486.
- [67] S. Himeno, K. Takeya, S. Fujita, Development of biogas separation process using DDR-type zeolite membrane, *Kagaku Gokoku Ronbunshu* 36 (2010) 545-551.
- [68] J. van den Bergh, W. Zhu, J.C. Goren, F. Kapteijn, K. Mouljin, K. Yazima, K. Nakayama, T. Tomita, S. Yoshida, Natural gas purification with a DDR zeolite membrane; permeation modelling with Maxwell-Stefan equations, *Stud. Surf. Sci. Catal.* 170 (2007) 1021-1027.
- [69] M. Kanezashi, T. Shioda, T. Gunji, T. Tsuru, Gas permeation properties of silica membranes with uniform pore sizes derived from polyhedral oligomeric silsesquioxane, *AIChE J.* 58 (2012) 1733-1743.
- [70] S. E. Jee, D. S. Sholl, Carbon dioxide and methane transport in DDR zeolite: Insights from molecular simulations into carbon dioxide separations in small pore zeolites, *J. Am. Chem. Soc.* 131 (2009) 7896-7904.
- [71] E.W. Ping, R. Zhou, H.H. Funke, J.L. Falconer, R.D. Noble, Seeded-gel synthesis of SAPO-34 single channel and monolith membranes for CO₂/CH₄ separations, *J. Membr. Sci.* 415-416 (2012) 770-775.
- [72] L. M. Robeson, The upper bound revisited, *J. Membr. Sci.* 320 (2008) 380-400.
- [73] S. Li, J.G. Martinek, J.L. Falconer, R.D. Noble, High-pressure CO₂/CH₄ separation using SAPO-34 Membranes, *Ind. Eng. Chem. Res.* 44 (2005) 3220-3228.
- [74] M.A. Carreon, S. Li, J.L. Falconer, R.D. Noble, Alumina-supported SAPO-34 membranes for CO₂/CH₄ separation, *J. Am. Chem. Soc.* 130 (2008) 5412-5413.
- [75] J.C. Poshusta, V.A. Tuan, E.A. Pape, R.D. Noble, J. Falconer, Separation of light gas mixtures using SAPO-34 membranes, *AIChE J.* 46 (2000) 779-789.
- [76] M. Hong, S.L. John, J.L. Falconer, R. D. Noble, Hydrogen purification using a SAPO-34 membrane, *J. Membr. Sci.* 307 (2008) 277-283.
- [77] J.K. Das, N. Das, S. Bandopadhyay, Effect of PVP intermediate layer on the properties of SAPO-34 membrane, *Adv. Mater. Sci. Eng.* 2012 (2012), Article ID 650217, 7 pages.
- [78] T. L. Chew, A. L. Ahmad, S. Bhatia, Ba-SAPO-34 membrane synthesized from microwave heating and its performance for CO₂/CH₄ gas separation, *Chem. Eng. J.* 171 (2011) 1053-1059.
- [79] M. Hong, J.L. Falconer, R.D. Noble, Modification of zeolite membranes for H₂ separation by catalytic cracking of methyl diethoxysilane, *Ind. Eng. Chem. Res.* 44 (2005) 4035-4041.
- [80] Y. Takata, T. Tsuru, T. Yoshioka, M. Asaeda, Gas permeation properties of MFI zeolite membranes prepared by the secondary growth of colloidal silicalite and application to the methylation of toluene, *Micro. Meso. Mater.* 54 (2002) 257-268.
- [81] W.T. Kwon, S.R. Kim, E.W.B. Kim, S.Y. Bae, Y. Kim, H₂/CO₂ gas separation characteristic of zeolite membrane at high temperature, *Adv. Mater. Res.* 26-28 (2007) 267-270.
- [82] M.E. Welk, T.M. Nenoff, H₂ separation through zeolite thin film membranes, *Prep. Pap.-Am. Chem. Soc. Div. Fuel Chem.* 40 (2004) 889-890.
- [83] H. Richter, I. Voigt, G. Fischer, P. Puhlfürb, Preparation of zeolite membrane on the inner surface of ceramic tubes and capillaries, *Sep. Purif. Tech.* 32 (2003) 133-138.
- [84] K. Aoki, V. A. Tuan, J.L. Falconer, R.D. Noble, Gas permeation properties of ion-exchanged ZSM-5 zeolite membranes, *Micro. Meso. Mater.* 39 (2000) 485-492.
- [85] V. A. Tuan, J.L. Noble, R.D. Falconer, Boron-substituted ZSM-5 membranes: Preparation and separation performance, *AIChE J.* 46 (2000) 1201-1208.
- [86] T.D. Bennett, P. Simoncic, S.A. Moggach, F. Gozzo, P. Macchi, D.A. Keen, J.C. Tan, A.K. Cheetham, Reversible pressure-induced amorphization of a zeolitic imidazolate framework (ZIF-4), *Chem. Commun.* 47 (2011) 7983-7985.
- [87] Y. Li, F. Liang, H. Bux, W. Yang, J. Caro, Zeolitic imidazolate framework ZIF-7 based molecular sieve membrane for hydrogen separation, *J. Membr. Sci.* 354 (2010) 48-54.
- [88] Y.-S. Li, F.-Y. Liang, H. Bux, A. Feldhoff, W.-S. Yang, J. Caro, Molecular sieve membrane: Supported metal-organic framework with high hydrogen selectivity, *Angew. Chem. Int. Ed.* 59 (2010) 548-551.

- [89] H. Bux, F. Liang, Y. Li, J. Cravillon, M. Wiebcke, J. Caro, Zeolitic imidazolate framework membrane with molecular sieving properties by microwave-assisted solvothermal synthesis, *J. Am. Chem. Soc.* 131 (2009) 16000-16001.
- [90] Q. Song, S. K. Natraj, M. V. Roussanova, J. C. Tan, D. J. Hughes, W. Li, P. Bourgoin, M.A. Alam, A.K. Cheetham, S. A. Al-Muhtaseb, E. Sivaniah, Zeolitic imidazolate framework (ZIF-8) based polymer nanocomposite membranes for gas separation, *Energy Environ. Sci.* 5 (2012) 8359-8369.
- [91] T.H. Bae, J. S. Lee, W. Qiu, W. J. Koros, C. W. Jones, S. Nair, A high-performance gas-separation membrane containing submicrometer-sized metal-organic framework crystals, *Angew. Chem. Int. Ed.* 49 (2010) 9863-9866.
- [92] L. Diestel, H. Bux, D. Wachsmuth, J. Caro, Pervaporation studies of n-hexane, benzene, mesitylene and their mixtures on zeolitic imidazolate framework-8 membranes, *Micro. Meso. Mater.* 164 (2012) 288-293.
- [93] Y. Cui, H. Kita, K. Okamoto, Preparation and gas separation performance of zeolite T membrane, *J. Mater. Chem.* 14 (2004) 24-32.
- [94] X. Chen, J. Wang, D. Yin, J. Yang, J. Lu, Y. Zhang, Y., High-performance zeolite T membrane for dehydration of organics by a new varying temperature hot-dip coating method, *AIChE J.* 59(3) (2013) 936-947.
- [95] X. Zhang, X. Song, L. Qiu, M. Ding, N. Hu, R. Zhou, X. Chen, Synthesis and pervaporation performance of highly reproducible zeolite T membranes from clear solutions, *Chinese J. Catal.* 34 (2013) 542-547.
- [96] S. M. Mirfendereski, T. Mazaheri, M. Sadrzadeh, T. Mohammadi, CO₂ and CH₄ permeation through T-type zeolite membranes: Effect of synthesis parameters and feed pressure. *Sep. Purif. Technol.* 61 (2008) 317-323.
- [97] N. Jaronvechuchitarn, P. Sansuksom, P. Worathanakul, P. Kongkachuichay, SUZ-4 zeolite synthesis derived from rice husk ash, *Chiang. Mai. J. Sci.* 401 (2013) 110-116.
- [98] A. Corma, F. Rey, J. Rius, M. J. Sabater, S. Valencia, Supramolecular self-assembled molecules as organic directing agent for synthesis of zeolites, *Nature* 431 (2004) 287-290.
- [99] C. Casado-Coterillo, J. Sato, M.T. Jimare, S. Valencia, A. Corma, Preparation and characterization of ITQ-29/polysulfone mixed-matrix membranes for gas separation: Effect of zeolite composition and crystal size, *Chem. Eng. Sci.* 73 (2012) 116-122.
- [100] I. Tiscornia, S. Valencia, A. Corma, C. Téllez, J. Coronas, J. Santamaría, Preparation of ITQ-29 (Al-free zeolite A) membranes, *Micro. Meso. Mater.* 110 (2008) 303-309.
- [101] A. Huang, J. Caro, Steam-stable hydrophobic ITQ-29 molecular sieve membrane with H₂ selectivity prepared by secondary growth using Kryptofix 222 as SDA, *Chem. Commun.* 46 (2010) 7748-7750.
- [102] J.G. Moscoso, G.J. Lewis, M.A. Miller, D.Y. Jan, R.L. Patton, L.M. Rohde, UZM-5, UZM-5P and UZM-6: crystalline aluminosilicate zeolites and processes using the same, *US 6613302 B1*, 2003.
- [103] C.S. Blackwell, R. W. Broach, M. G. Gatter, J. S. Holmgren, D. Y. Jan, G. J. Lewis, B. J. Mezza, T. M. Mezza, M. A. Miller, J. G. Moscoso, R. L. Patton L. M. Rohde, M. W. Schoonover, W. Sinkler, B. A. Wilson, S. T. Wilson, Open-framework materials synthesized in the TMA+/TEA+ mixed-template system: The new low Si/Al ratio zeolites UZM-4 and UZM-5, *Angewan. Chem. Int. Edi.* 42 (2003) 1737-1740.
- [104] C. Liu, J. G. Moscoso, S. T. Wilson, Microporous UZM-5 inorganic zeolite membranes for gas, vapor and liquid separation, *US 20120240763*, 2012.
- [105] M. Tsapatsis, M. Lovallo, T. Okubo, M. E. Davis, M. Sadakata, Characterization of zeolite L nanoclusters, *Chem. Mater.* 7 (1995) 1734-1741.
- [106] X. Yin, J. Wang, N. Chu, J. Yang, J. Lu, Y. Zhang, D. Yin, Zeolite L/carbon nanocomposite membranes on the porous alumina tubes and their gas separation properties, *J. Membr. Sci.* 348 (2010) 181-189.
- [107] Y. Liu, Z. Yang, C. Yu, X. Gu, N. Xu, Effect of seeding methods on growth of NaA zeolite membranes, *Micro. Meso. Mat.*, 143 (2011) 348-356.
- [108] X. Gu, J. Dong, T. M. Nenoff, Synthesis of defect-free FAU-type zeolite membranes and separation of dry and moist CO₂/N₂ mixtures, *Ind. Eng. Chem. Res.* 44 (2005) 937-944.
- [109] Y. Hasegawa, T. Nagase, Y. Kiyozumi, T. Hanaoka, F. Mizukami, Influence of acid on the permeation properties of NaA-type zeolite membranes, *J. Membr. Sci.* 349 (2010) 189-194.
- [110] X. Xu, W. Yang, J. Liu, L. Lin, Synthesis of NaA zeolite membranes from clear solution, *Micro. Meso. Mater.* 43 (2001) 299-311.
- [111] H. Kita, K. Fuchida, T. Horita, H. Asamura, K. Okamoto, Preparation of faujasite membranes and their permeation, *Sep. Purif. Technol.* 25 (2001) 261-268.
- [112] X. Chen, W. Yang, J. Liu, L. Lin, Synthesis of zeolite NaA membranes with high permeance under microwave radiation on mesoporous-layer-modified macroporous substrates for gas separation, *J. Membr. Sci.* 255 (2005) 201-211.
- [113] K. Okamoto, H. Kita, K. Hori, K. Tanaka, M. Kondo, Zeolite NaA membrane: preparation, single-gas permeation, and pervaporation and vapor permeation of water/organic liquid mixtures' *Ind. Eng. Chem. Res.* 40 (2001) 163-175.
- [114] I. G. Giannakopoulos, V. Nikolakis, Separation of propylene/propane mixtures using faujasite-type zeolite membranes, *In. Eng. Chem. Res.* 44 (2005) 226-230.
- [115] W. Jia, S. Murad, Molecular dynamics simulations of gas separation using faujasite-type zeolite membranes, *J. Chem. Phys.* 120 (2004) 4877-4885.
- [116] W. Jia, S. Murad, Separation of gas mixtures using a range of zeolite membranes: A molecular-dynamics study, *J. Chem. Phys.* 122 (2005) 234708/1 - 234708/11.
- [117] X. Xu, W. Yang, J. Liu, X. Chen, L. Lin, N. Stroh, H. Brunner, Synthesis and gas permeation properties of an NaA zeolite membrane, *Chem. Commun.* (2000) 603-604.
- [118] X. Xu, W. Yang, J. Liu, L. Lin, N. Stroh, H. Brunner, Synthesis of NaA zeolite membrane on a ceramic hollow fiber, *J. Membr. Sci.*, 229 (2004) 81-85.
- [119] A. Huang, N. Wang, J. Caro, Stepwise synthesis of sandwich-structured composite zeolite membranes with enhanced separation selectivity, *Chem. Commun.* 48 (2012) 3542-3544.
- [120] S. Li, V. A. Tuan, J. L. Falconer, R. D. Noble, X-type zeolite membranes: preparation, characterization, and pervaporation performance, *Micro. Meso. Mat.* 53 (2002) 59-70.
- [121] S. Li, V. A. Tuan, J. L. Falconer, R. D. Noble, Effects of zeolite membrane structure on the separation of 1,3-propanediol from glycerol and glucose by pervaporation, *Chem. Mater.* 213 (2001) 1865-1873.
- [122] K. Sato, T. Nakane, A high reproducible fabrication method for industrial production of high flux NaA zeolite membrane, *J. Membr. Sci.* 301 (2007) 151-161.
- [123] K. P. Dey, D. Kundu, M. Chatterjee, M. K. Naskar, Preparation of NaA zeolite membranes using poly(ethyleneimine) as buffer layer, and study of their permeation behavior, *J. Amer. Ceramic Society* 96 (2013) 68-72.
- [124] M. Pera-Titus, J. Llorens, J. Tejero, F. Cunill, Description of the pervaporation dehydration performance of A-type zeolite membranes: A modeling approach based on the Maxwell-Stefan theory, *Catalysis Today* 118 (2006) 73-84.
- [125] M. Pera-Titus, C. Fité, V. Sebastián, E. Lorente, J. Llorens, F. Cunill, Modeling Pervaporation of ethanol/water Mixtures within 'Real' zeolite NaA membranes, *Ind. Eng. Chem. Res.* 47 (2008) 3213-3224.
- [126] T. Mohammadi, H. Maghsodllood, Synthesis and characterization of ceramic membranes (W-type zeolite membranes), *Int. J. Appl. Ceram. Technol* 3 (2013) 365-375.
- [127] X. Zhang, D. Liu, D. Xu, S. Asahina, K.A. Cychosz, K.V. Agrawal, Y.A. Wahedi, A. Bhan, S.A. Hashimi, O. Terasaki, M. Thommes, M. Tsapatsis, Synthesis of self-pillared zeolite nanosheets by repetitive branching, *Science* 336 (2012) 1684-1687.
- [128] X. Xu, Y. Bao, C. Song, W. Yang, J. Liu, L. Lin, Microwave-assisted hydrothermal synthesis of hydroxy-sodalite zeolite membrane, *Micro. Meso. Mat.* 75 (2004) 173-181.
- [129] M. Kazemimoghadam, Preparation of nanopore HS zeolite membranes for reverse osmosis processes, *Desalination of Water Treatment* 30 (2011) 51-57.
- [130] L. Sandström, E. Sjöberg, J. Hedlund, Very high flux MFI membrane for CO₂ separation, *J. Membr. Sci.* 380 (2011) 232-240.
- [131] S. Nair, Z. Lai, V. Nikolakis, G. Xomeritakis, G. Bonilla, M. Tsapatsis Separation of close-boiling hydrocarbon mixtures by MFI and FAU membranes made by secondary growth, *Micro. Meso. Mater.* 48 (2001) 219-228.
- [132] S. Choi, J. Coronas, Z. Lai, D. Yust, F. Onorato, M. Tsapatsis, Fabrication and gas separation properties of polybenzimidazole (PBI)/nanoporous silicates hybrid membranes, *J. Membr. Sci.* 316 (2008) 145-152.
- [133] J. A. Bohrmann, M. A. Carreon, Synthesis and CO₂/CH₄ separation performance of bio-MOF-1 membranes, *Chem. Commun.* 48 (2012) 5130-5132.
- [134] J. An, R. Fiorella, S. Geib, N. L. Rosi, Synthesis, structure, assembly, and modulation of the CO₂ adsorption properties of a zinc-adeninate macrocycle, *J. Am. Chem. Soc.* 131 (2009) 8401-8403.
- [135] J. An, S. Geib, N.L. Rosi, Cation-triggered drug release from a porous zinc-adeninate metal-organic framework, *J. Am. Chem. Soc.* 131 (2009) 8376-8377.
- [136] G. Xomeritakis, S. Naik, C. M. Braunschweig, C. J. Cornelius, R. Pardey C. J. Brinker, Organic-templated silica membranes: I. Gas and vapor transport properties, *J. Membr. Sci.* 215 (2003) 225-233.
- [137] Y. Li, T. S. Chung, Exploratory development of dual-layer carbon-zeolite nanocomposite hollow fiber membranes with high performance for oxygen enrichment and natural gas separation, *Micro, Meso, Mater.* 113 (2008) 315-324.
- [138] S. Alfaro, M. A. Valenzuela, Zeolite membranes prepared by the dry gel method for gas separation, *A. Zojomo*, 2 (2006) 1-5.
- [139] S. M. Kuznicki, Preparation of small-pored crystalline titanium molecular sieve zeolites, *US4938939*, 1990.
- [140] J. A. Stoeger, C. M. Veziri, M. Palomino, A. Corma, N. K. Kanellopoulos, M. N. Tsapatsis, G. Karanikolos, On stability and performance of highly c-oriented columnar AlPO₄-5 and CoAPO-5 membranes, *Micro. Meso. Mater.* 147 (2012) 286-294.
- [141] S. Yang, X. Lin, W. Lewis, M. Suyetin, E. Bichoutskaia, J.E. Parker, C.C. Tang, D.R. Allan, P.J. Rizkallah, P. Hubbersteyn, N.R. Champness, K. M. Thomas, A. J. Blake, M. Schröder, A partially interpenetrated metal-organic framework for selective hysteretic sorption of carbon dioxide, *Nature Materials* 11 (2012) 710-716.
- [142] T. Nagase, Y. Kiyozumi, Y. Hasegawa, T. Inoue, T. Ikeda, Dehydration of concentrated acetic acid solutions by pervaporation using novel MER zeolite membranes, *Chem. Lett.* 36 (2007) 594-595.
- [143] S. J. Kim, S. Yang, G. K. Reddy, P. Smirniotis, J. Dong, Zeolite membrane reactor for high-temperature water-gas shift reaction: Effects of membrane properties and operating conditions, *Energy Fuels* 27 (2013) 4471-4480.
- [144] R. Mahajan, W. J. Koros, Factors controlling successful formation of mixed-matrix gas separation materials *Ind. Eng. Chem. Res.* 39 (2000) 2692-2696.
- [145] R. Mahajan, W. J. Koros, Mixed matrix membrane materials with glassy polymers. Part 2, *Polym. Eng. Sci.* 42 (2002) 1432-1441.
- [146] C.A. Scholes, S.E. Kentish, G.W. Stevens, Carbon dioxide separation through polymeric membranes systems for flue gas applications, *Recent Patents on Chemical Engineering* 1 (2008) 52-66.
- [147] L. Y. Jiang, T. S. Chung, S. Kulprathipanja, Fabrication of mixed matrix hollow fibers with intimate polymer-zeolite interface for gas separation, *AIChE J.* 52 (2006) 2898-2908.
- [148] C. I. Chaidou, G. Pantoleontos, D. E. Koutsonikolas, S. P. Kaldis, G. P. Sakellariopoulos, Gas separation properties of polyimide-zeolite mixed matrix membrane, *Sep. Purif. Technol.* 47 (2012) 950-962.
- [149] M. Woo, J. Choi, M. Tsapatsis, Poly(1-trimethylsilyl-1-propyne)/MFI composite membranes for butane separations, *Micro. Meso. Mater.* 110 (2008) 330-338.
- [150] M. Hussain, A. König, Mixed-matrix membrane for gas separation: polydimethylsiloxane filled with zeolite, *Chem. Eng. Technol.* 35 (2012) 561-569.
- [151] H. Wang, Y. S. Lin, Synthesis and modification of ZSM-5/silicalite bilayer membrane with improved hydrogen separation performance, *J. Membr. Sci.* 396 (2012) 128-137.

- [152] A.F. Ismail, T. Kusworo, A. Mustafa, Enhanced gas permeation performance of polyethersulfone mixed matrix hollow fiber membranes using novel Dynasylan Amino silane agent, *J. Membr. Sci.* 319 (2008) 306-312.
- [153] D. Sen, H. Kalipcilar, L. Yilmaz, Development of zeolite filled polycarbonate mixed matrix gas separation membranes, *Desalination* 200 (2006) 222-224.
- [154] C. V. Funk, D. R. Lloyd, Zeolite-filled microporous mixed matrix (ZeoTIPS) membranes: Prediction of gas separation performance, *J. Membr. Sci.* 313 (2008) 224-231.
- [155] M.S. Boroglu, M.A. Gurkaynak, Fabrication and characterization of silica modified polyimide-zeolite mixed matrix membranes for gas separation properties, *Polym. Bull.* 66 (2011) 463-478.
- [156] W. Zhu, L. Gora, A.W.C. van den Berg, F. Kapteijn, J.C. Jansen, J.A. Moulijn, Water vapour separation from permanent gases by a zeolite-4A membrane, *J. Membr. Sci.* 253 (2005) 57-66.
- [157] B. Ozturk, F. Demirciyeva, Comparison of biogas upgrading performances of different mixed matrix membranes, *Chem. Eng. J.* 222 (2013) 209-217.
- [158] D. F. Mohshim, H. Mukhtar, Z. Man, R. Nasir, Latest development on membrane fabrication for natural gas purification: A Review, *J. Eng.*, 2013 (2013) Article ID 101746, 7 pages.
- [159] B. Zhu, L. Zou, Y.S. Lin, A. Hill, H. Wang, Y. Huang, M. Duke, The influence of seawater ions on the structural features of MFI, FAU and LTA zeolites, *ICONN 2010 - Proceedings of the 2010 International Conference on Nanoscience and Nanotechnology.* (2010) pp.162-165.
- [160] A. Malekpour, A. Samadi-Maybodi, M. R. Sadati, Desalination of aqueous solutions by LTA and MFI zeolite membranes using pervaporation method, *Braz. J. Chem. Eng.* 28 (2011) 669-677.
- [161] M. Hong, S. Li, H.J. L. Funke, R. D. Falconer, Ion-exchanged SAPO-34 membranes for light gas separations, *Micro. Meso. Mater.* 106 (2007) 140-146.
- [162] Y. Hasegawa, T. Tanaka, K. Watanabe, B. H. Jeong, K. Kusakabe, S. Marooka, Separation of CO₂-CH₄- and CO₂-N₂- systems using ion-exchanged zeolite membranes with different Si/Al ratios, *Korean J. Chem. Eng.* 19 (2002) 309-313.
- [163] P. Kumar, C. Sung, O. Muraza, M. Cococcioni, S.A. Hashimi, A. McCormick, M. Tsapatsis, H₂S adsorption by Ag and Cu ion exchanged faujasites, *Micro. Meso. Mater.* 146 (2011) 127-133.
- [164] K.S.N. Kamarudin, H. Hamdan, H. Mat, Proceeding of the 10th Asian Pacific Confederation of chemical Engineers Congress, Kitakyushi, Japan Oct. 17-21, 2004.
- [165] Y. Liu, X. Cen, High permeability and salt rejection reverse osmosis by a zeolite nano-membrane, *Phys. Chem. Chem. Phys.* 15 (2013) 6817-6824.
- [166] Y. Morigami, M. Kondo, J. Abe, H. Kita, K. Okamoto, The first large-scale pervaporation plant using tubular-type module with zeolite NaA membrane, *Sep. Purif. Technol.* 25 (2001) 251-260.
- [167] H. Kita, in: S. Nakao, M. Matsukata (Eds.), *Proceedings of Post Conference of ICIM5 98-International Workshop on zeolitic membranes and films*, June 28-30, Gifu, Japan, 1998, pp. 43.
- [168] Jiuwu High Tech Co. of China (<http://jiuwu.com>), ICOM, (2014) 20-25 July, Suzhou, China.
- [169] H. Wang, Y.S. Lin, Effects of water vapor on gas permeation and separation properties of MFI zeolite membranes at high temperatures, *AIChE. J.* 58(1) (2012) 153-162.
- [170] J.C. Poshusta, R.D. Noble, J.L. Falconer, Temperature and pressure effect on CO₂ and CH₄ permeation through MFI zeolite membranes, *J. Membr. Sci.* 160 (1999) 115-125.
- [171] Z. Tang, J. Dong, T. M. Nenoff, Internal surface modification of MFI-type zeolite membranes for high selectivity and high flux for hydrogen, *Langmuir* 25 (2009) 4848-4852.
- [172] J.C. Poshusta, R.D. Noble, J.L. Falconer, Characterization of SAPO-34 by water adsorption, *J. Membr. Sci.* 186 (2001) 25-40.
- [173] S. Li, J.L. Falconer, R.D. Noble, SAPO-34 Membranes for CO₂/CH₄ Separation, *J. Membr. Sci.* 241 (2004) 121-135.
- [174] R. Zhou, E.W. Ping, H.H. Funke, J.L. Falconer, R.D. Noble, Improving SAPO-34 membrane synthesis, *J. Membr. Sci.* 444 (2013) 384-393.
- [175] S. Li, M.A. Carreon, Y. Zhang, H.H. Funke, R. D. Noble, J.L. Falconer, Scale-up of SAPO-34 membranes for CO₂/CH₄ separation, *J. Membr. Sci.* 352 (2010) 7-13.
- [176] X. Chen, W. Yang, J. Liu, X. Xu, A. Huang, L. Lin, Synthesis of NaA membranes with high performance, *J. Mater. Sci. Lett.* 21 (2002) 1023-1025.
- [177] H. Sudhakar, C.V. Prasad, K. Sunitha, K.C. Rao, M. C. S. Subha, S. Sridhar, Pervaporation separation of bIPA-water mixtures through 4A zeolite filled sodium alginate membranes, *J. Appl. Polym. Sci.* 121 (2011) 2717-2725.
- [178] K. Kusakabe, T. Kuroda, S. Morooka, Separation of carbon dioxide from nitrogen using ion-exchanged faujasite-type zeolite membranes formed on porous support tubes, *J. Membr. Sci.* 148 (1998) 13-23.
- [179] P. Li, H. Tezel, Adsorption Separation of N₂, O₂, CO₂, CH₄ gases by β zeolite., *Meso. Micro. Mater.* 98 (2007) 94-101.
- [180] S. Husain, W. J. Koros, Mixed matrix hollow fiber membrane made with modified HSSZ-13 zeolite in polyetherimide polymer matrix for gas separation, *J. Membr. Sci.* 288 (2007) 195-207.
- [181] T. Li, Y. Pan, K.V. Peinemann, Z. Lai, Carbon dioxide selective mixed matrix composite membrane containing ZIF-7 nano-fillers, *J. Membr. Sci.* 425-426 (2013) 235-242.
- [182] Y. Yoo, Z. Lai, H.K. Jeong, Fabrication of MOF-5 membranes using microwave-induced rapid seeding and solvothermal secondary growth, *Micro. Meso. Mater.* 123 (2009) 100-106.
- [183] Z. Lai, G. Bonilla, I. Diaz, J.G. Nery, K. Sujaoti, M.A. Amat, E. Kokkoli, O. Terasaki, R.W. Thompson, M. Tsapatsis, D.G. Vlachos, Microstructural optimization of a zeolite membrane for organic vapor separation. *Science* 300 (2003) 456-460.
- [184] I.F.J. Vankelecom, S.D. Beukelaer, J.B. Uytterhoeven, Sorption and pervaporation of aroma compounds using zeolite-filled PDMS Membranes, *J. Phys. Chem.* 101 (26) (1997) 5186-5190.